TOMA, MICHAEL JOHN

THE PURIFICATION AND CHARACTERIZATION OF MYOSIN FROM BOVINE BRAIN

City University of New York PH.D. 1980

PLEASE NOTE:

In all cases this material has been filmed in the best possible way from the available copy. Problems encountered with this document have been identified here with a check mark ✓.

1. Glossy photographs ✓
2. Colored illustrations _____
3. Photographs with dark background ✓
4. Illustrations are poor copy _____
5. Print shows through as there is text on both sides of page _____
6. Indistinct, broken or small print on several pages _____ throughout _____
7. Tightly bound copy with print lost in spine _____
8. Computer printout pages with indistinct print _____
9. Page(s) _____ lacking when material received, and not available from school or author _____
10. Page(s) _____ seem to be missing in numbering only as text follows _____
11. Poor carbon copy _____
12. Not original copy, several pages with blurred type _____
13. Appendix pages are poor copy _____
14. Original copy with light type _____
15. Curling and wrinkled pages _____
16. Other _____

THE PURIFICATION AND CHARACTERIZATION OF MYOSIN FROM BOVINE BRAIN

by

MICHAEL J. TOMA

A dissertation submitted to the Graduate Faculty in Biomedical Sciences in partial fulfillment of the requirements for the degree of Doctor of Philosophy, The City University of New York.

1980

This manuscript has been read and accepted for the Graduate Faculty in Biomedical Sciences in satisfaction of the dissertation requirement for the degree of Doctor of Philosophy.

5/8/80
date

Chairman of Examining Committee

5/8/80
date

Executive Officer

E. W. Breisk

Edward J. Quinn

William J. Nichols

Supervisory Committee

The City University of New York

Abstract

THE PURIFICATION AND CHARACTERIZATION OF

MYOSIN FROM BOVINE BRAIN

by

Michael J. Toma

Adviser: Professor Soll Berl

Myosin is an ATPase and a structural protein involved in the contraction of muscle. The presence of myosin in non-muscle cells and brain has led to the consideration that this protein is involved in contractile events occurring within these non-muscle cells. The possibility that cell motility, transmitter release, and axonal and dendritic outgrowth involve some form of contractile mechanism warrants an investigation into the nature of myosin from brain.

A study was undertaken to investigate the ultrastructure and enzymology of myosin from bovine brain. A procedure utilized for the isolation of myosin from platelets (Pollard et.al., 1974), was modified and extended for the isolation of myosin from bovine brain. Briefly, this procedure involves extraction of bovine brain cortex with a high salt buffer, precipitation of the myosin component by dilution to low ionic strength, ammonium sulfate fractionation and column chromatography. The enzyme is located in column eluted fractions by virtue of its K^+-EDTA

activated ATPase activity and further purified by two cycles of precipitation with a concomitant increase in activity. The preparation was then examined by sodium dodecyl sulfate-polyacrylamide gel electrophoresis and compared to myosins from skeletal and smooth muscle.

The ability of brain myosin to form filaments was compared to that of skeletal muscle and smooth muscle myosins, electron microscopically. A more detailed study of ultrastructure was accomplished by comparing subfragments of the myosin molecule prepared by proteolytic cleavage. The light meromyosin (LMM) subfragments of brain and smooth muscle myosin assemble in a similar fashion, whereas the LMM portion of skeletal muscle myosin assembles in a different fashion. The head portions, obtained by proteolytic cleavage of all three myosins were able to bind to actins from all three tissue sources with a similar periodicity of attachment.

The effect of pH on the substrate saturation kinetics of brain and skeletal muscle myosin was also studied. Both proteins show similar Vmax versus pH curves with a tendency of the Vmax values to increase with increasing pH. Plots of Km versus pH also show a tendency of the Km values for both myosins to increase with increasing pH. Plots of pKm versus pH reveal a possible ionization within the components of the system at/or between pH 7.5-8.0 for brain Ca^{2+}- and K^{+}-EDTA-ATPase, and skeletal muscle K^{+}-EDTA-ATPase. Whereas for skeletal muscle myosin Ca^{2+}-ATPase it appears that there are multiple ionizations occurring over the pH range.

The importance of the similarities and differences of the three myosins studied is discussed in terms of their functioning in a contractile mechanism.

In Memoriam

Dr. C. Mahendran

Teacher, philosopher, scientist and friend

Acknowledgments

I would like to thank my adviser, Dr. Soll Berl for his invaluable help and suggestions throughout my stay in his laboratory.

I would also like to thank Dr. William Nicklas for his helpful ideas during my research as well as his help in the preparation of this manuscript.

I wish to extend special thanks to Dr. D.D. Clarke, for his computer analysis of the kinetic data for this research, according to the Wilkinson procedure, and mostly for his true professorship in guiding me towards an understanding of how enzymes work.

I would also like to thank Ms. Maria Chou for her excellent preparation of the smooth muscle myosin and actins, which were essential for the research in this dissertation.

Thanks to Ray Nunez for teaching me much of the technique involved in protein chemistry when I first began this research, and for his friendship.

Thank you also to Dr. Jerome Schwartz for his teaching me how to use the electron microscope in more than just a technical fashion, and to Ms. Eva Nagy for teaching me how to use a darkroom, also in more than just a technical fashion.

Last but not least, to my parents and my sister, who throughout the years gave me the support that was necessary to grow beyond mere academia. Also, my dear friend Mirilee Pearl for her emotional support and truly scientific

and enlightening discussions. And to Rita Margolies whose friendship and scientific insight, I was privileged to share.

TABLE OF CONTENTS

LIST OF TABLES

LIST OF FIGURES

x

INTRODUCTION

Myosin is an enzyme that plays an important role in the contraction of muscle. The myosin molecule contains the catalytic site that can hydrolyze the terminal phosphate group of adenosine triphosphate (ATP). It is also a structural protein in that it is able to assemble into thick filaments. It is the physical interaction of the thick myosin filaments with the thin actin filaments in muscle, driven by the hydrolysis of ATP, that causes the contraction of muscle.

Actin-like and myosin-like proteins have been found in a number of non-muscle cells, such as platelets, amoeba, macrophages, slime mold plasmodia, brain, and other cell types (Pollard and Weihing, 1974). The unique involvement of actin and myosin in the contraction of muscle, implicates their participation in processes occuring in these cells which may be related to some form of contractility. Much study has been directed towards non-muscle actins (Tilney, 1975; Korn, 1978; Vanderkerckhove and Weber, 1978), yet the chemistry and structure of non-muscle myosins have received little attention. Although it has been shown that myosin isolated from chick brain can form filaments in vitro, and can hydrolyze ATP (Bray and Thomas, 1975; Kuczmarski and Rosenbaum, 1978), detailed investigation into the structure and enzymology of the molecule has not been accomplished. It is the intent of this dissertation, therefore, to further investigate the enzymology and structure of brain myosin.

Many years of study on striated muscle and its proteins has led to a correlation of the structure and function of its contractile proteins.

With this in mind, it seems best to first understand the skeletal muscle system in order to appreciate the involvement of the contractile proteins in non-muscle cells, especially brain.

The sarcomere is the repeating structural unit in striated (skeletal) muscle to which all morphologic events of contraction are referred (Figure 1). It is the segment between two successive Z-lines. The thin actin filaments extend in either direction from the Z-lines where they occupy the interstices between hexagonally packed thick filaments (Bloom and Fawcett, 1975). Myosin is the major component of the thick filaments found in the sarcomere. A model of the myosin molecule may be seen in Figure 2. It may be seen that myosin consists of two "heavy" polypeptide chains of about 200,000 daltons each, and usually two kinds of "light" polypeptide chains of about 16,000-21,000 daltons, contained in the head region of the "heavy" chain. The light chains are essential for both the enzymatic activity and the actin binding ability of the myosin. The head region of the "heavy" chains is formed by folding into globular structures, whereas, the tail region of the "heavy" chain is in α-helical conformation. The head and tail portions can be cleaved by enzymes and further studied. Brief treatment with trypsin cleaves myosin to yield heavy and light fragments called heavy meromyosin (HMM) which contains the head portion of the molecule and part of the tail and retains the ATPase activity, and light meromyosin (LMM), which consists of the rest of the tail portion. Cleavage by papain treatment yields a single head called subfragment one (SF-1) and the tail portion.

Myosin in skeletal muscle exists in the form of filaments which are believed to contain 400 myosin molecules per filament. The myosin

molecules are oriented with their heads away from the midpoint of the filament, as seen in Figure 3. The myosin filament disassembles into the individual molecules at high ionic strength (0.6M KCl) and can be re-assembled in vitro by reducing the ionic strength (0.1M KCl). It is important to note that the LMM portion of the molecule, which is insoluble at low ionic strength, forms the core of the filament, and the head portion of the molecule which is soluble at low ionic strength projects out from the filament thus enabling it to interact with actin and ATP.

The ATPase activity of myosin, as well as the ability to bind actin, resides entirely in the head portion and is stimulated in the presence of K^+-EDTA or Ca^{2+} and inhibited by Mg^{2+}. The actomyosin complex also involves other proteins, troponin and tropomyosin, which serve a regulatory function involving Ca^{2+}. This is one of the important physiologic features of this contractile system. Free Ca^{2+} binds to troponin which causes a configurational change that allows the myosin head to bind to actin, forming a cross bridge which in the presence of Mg^{2+} and ATP causes the actin filament to move across the thick filament resulting in contraction of the muscle. Relaxation is brought about by a reuptake of free Ca^{2+} in the cell and the replacement of the ADP formed in the enzyme reaction with ATP.

A light chain component of skeletal muscle myosin has been shown to be phosphorylated by a Ca^{2+}-requiring light chain kinase found in skeletal muscle, although no physiologic role for the phosphorylation has been established (Szent Gyorgyi, 1951; Huxley, 1963; Needham, 1971; Weber and Murray, 1973; Pires et.al., 1977; Pepe and Drucker, 1979).

A model for the involvement of myosin and actin in the contraction of striated muscle, that has proved valuable with respect to theories concerned with the role of contractile proteins in non-muscle cells, has been proposed by Huxley (1969). The sliding filament model of Huxley is based on the overlapping arrays of actin and myosin filaments which slide past each other when the muscle changes length. The active sliding force is developed by cross bridges in thick myosin filaments, i.e., the biologically active ends of myosin molecules attach to and exert a longitudinal force on the actin filaments. A cross bridge can thus pull in an actin filament a certain distance, release and reattach at another point and pull again. Important points in this theory are that the force generating mechanism is a result of the actomyosin Mg^{2+}-ATPase and is also dependent on Ca^{2+} and the regulatory proteins. Secondly, the structural polarity required in the sliding filament model is of great importance since the direction of relative force experienced by an actin filament when it interacts with an appropriate myosin filament is specified by the structural polarity of the actin filament itself (Mooseker and Tilney, 1975). Indeed, actin filaments are attached on either side of the Z-line with opposite polarity (Huxley, 1963), and myosin is oriented in one sense in half of the length of the filament and in the opposite sense in the other half. "Decoration" of an actin filament can be achieved by treatment of the fiber with heavy meromyosin, which will then attach to the actin filament in a specific structurally oriented "arrowhead" configuration, as seen in the electron microscope by negative staining, (Huxley, 1963) and which in fact, possesses a directionality (Woodrum, et.al., 1975).

The widespread occurrence of a two filament system in striated muscle led to the expectation that all muscle cells would have two kinds of filaments. However, the myofilaments of smooth muscle are less ordered than those of striated muscle. The structure of smooth muscle filaments is difficult to keep intact for microscopic study. One of the components observed in vertebrate smooth muscle are the ribbons, which are believed to consist of a backbone of lentofilaments and a surface lattice of myosin molecules, apparent as projections on the ribbons which are arranged with an axial period of about 140Å (Small and Squire, 1972). In fact, purified smooth muscle myosin has been shown to form, in vitro, ribbon-like filaments with a 140Å period (Bray and Thomas, 1975). Small and Squire (1972) propose that the ribbons possess an opposite polarity on one face with respect to the other, such that thin filaments that interact with one face of a ribbon would slide in the opposite direction to those that interact with the other face. They consider the possibility of many small contractile units in the cell, attached at their ends to the cell membrane.

It has been shown that myosin from smooth muscle requires phosphorylation of a light chain component for actin-induced activation of the myosin-ATPase (Chacko and Conti, 1977; Sobieszek, 1977). This phosphorylation requires a light chain kinase which is dependent on the presence of Ca^{2+} for activation via the calcium dependent regulator calmodulin (Dabrowska et.al., 1977).

As mentioned earlier, the contractile proteins actin and myosin have been found in a number of non-muscle cells such as platelets, amoeba, macrophages, slime mold plasmodia, leucocytes, brain and other cell types.

They are thought to play a part in processes such as amoeboid movement, neuronal outgrowth, endo- and exocytosis and neural transmitter release (Pollard, and Weihing, 1974; Pollard, 1975; Tilney, 1975; Berl, 1975). It has been shown that myosin from platelets (Adelstein and Conti, 1975) also requires phosphorylation of a light chain component for actin-induced activation of the myosin ATPase activity. The phosphorylation requires a light chain kinase which is Ca^{2+}-dependent (Hathaway and Adelstein, 1979).

Huxley (1973) suggested that the more primitive systems share the structural and biochemical features of the sliding filament model for striated muscle. He speculated that these systems, such as the contractile apparatus in amoeba or a fibroblast in tissue culture, as they relate to cytoplasmic streaming and cell movement, operate on an active shearing mechanism - sliding forces developed between polarized actin filaments lying in the cortical gel in a parallel fashion and cytoplasmic myosin in the fluid state propelled along carrying with it other cellular constituents, thus causing cytoplasmic streaming. In tissue culture, a cell would move relative to an attachment site where actin filaments anchor (as in the Z-line of striated muscle) and pass thru the membrane to anchor on the substrate. The front of the cell is pushed forward over the attached filaments due to internal pressure caused by the cytoplasmic stream and fresh attachment of actin filaments provides for advancement. The protein α-actinin could very well be a point of attachment for actin filaments in non-muscle cells. α-Actinin is a component of the Z-line of skeletal muscle tissue, where actin filaments are attached (Stromer and Goll, 1972), is present in non-muscle cells (Craig

and Pardo, 1979; Geiger et.al., 1979), and has been isolated from brain (Schook et.al., 1978).

Bray (1973) set forth a cellular movement model explaining the movement of the growing tips of neurites. It was the relatively constant diameter (0.1 - 0.2 μm) of cytoplasmic extensions, as revealed by electron microscopy and the blocking of protrusion of cytoplasmic flow thru filters with a pore size of 0.15 μm, that led Bray to believe a common mechanism of formation was at work. Since elongated vesicles are seen within such filopodia, often lying parallel to the axis, it was suggested that the contractile proteins are arranged on the membranes of the cell and vesicle within the cytoplasm such that the vesicles can move along and fuse with the growing tip to form extensions of approximately a 0.2 μm diameter. The primary feature of this model is that contractile proteins that are responsible for the movement of the membrane are linked in a polar fashion to membrane surfaces providing for a preferred direction of movement. It is the distribution of this directionality that can cause localized areas of cellular extension. Further discussion on cell movement is taken up by Tilney (1975) and Schroeder (1975).

Pertinent to this discussion is the established presence of actin and myosin in the rat, bovine and cat brain cortex (Puszkin et.al., 1968; Berl, and Puszkin, 1970: Puszkin and Berl, 1972) and synaptosomal fractions (Puszkin et.al., 1972), in the chick embryo brain (Burridge and Bray, 1975; Bray and Thomas, 1976; Kuczmarksi and Rosenbaum, 1979) and chick sympathetic ganglia in tissue culture (Fine and Bray, 1971) as well as the presence of myosin in a rat glial cell line (Ash, 1975). These cells manifest either in the course of development or in the mature state,

axonal and dendritic sprouting and/or cell movement. Modern electron microscopy and autoradiography has led to the concept that the recently closed neural tube includes only one cell type, the neuroepithelial cell, which can divide and differentiate into neuroblasts or glioblasts (Langman, 1969). Neuroblasts derived from this tissue will migrate out and further proliferate until they round up as apolar neuroblasts and differentiate further into bipolar and then multipolar neurons. Actomyosin could very well play a vital role in the migration of neuroblasts with a mechanism comparable to amoeba, macrophage or fibroblast in tissue culture. A mechanism very much like that ascribed to the membrane movements in the neural growth cone, the tip of the growing nerve cell (Bray, 1973; Bunge, 1973), could very well describe the process which occurs in the sprouting of primitive axons and dendrites of the differentiating neuroblast. In fact, ultrastructural analysis of dorsal root ganglion nerve cells undergoing axonal elongation in vitro reveals neurofilaments and a network of interconnecting microfilaments particularly at the growth cone of the axonal tip (Yamoda et.al., 1971). It was also shown that cytochalasin B rounds up growth cones, causes retraction of microspikes and cessation of axon elongation, a process which is reversible after the removal of cytochalasin B.This is important since cytochalasin B, the alkaloid metabolite of a fungus Helminthosporium dematioideum (Carter, 1967), has been shown to decrease acto-HMM-ATPase activity by about 60%, with no effect on myosin alone, (Spudich and Lin, 1972) as well as that of brain actomyosin (Nicklas and Berl, 1974). Further processes sensitive to cytochalasin B, such as cytokinesis, single cell movement (including glial cells), cytoplasmic streaming, blood clot

formation (platelets), smooth muscle contraction, cardiac muscle cell contraction, and calcium induced cortical contraction in eggs, is reviewed by N.K. Wessels et.al. (1971).

Brain actin and myosin have also gained importance due to their possible role in neural transmitter release as proposed by S. Berl, et.al., 1973. The model proposed suggests that actin and myosin are involved in the process of exocytosis by mechanochemical interaction between the pre-synaptic vesicle and membrane. Conformational changes in the interacting membranes lead to the extrusion of vesicle contents. The development of this model was influenced in part by the torsional hypothesis model for the molecular basis of muscle contraction proposed by Driezen and Gershman (1970). This model explains the contractile event at the cross bridge in terms of ATP splitting linked with a quaternary structural change between cross bridge and thin filament sites. Torsional movement generated by cross bridge interaction is accompanied by contraction, a process which is reversible upon loss of Ca^{2+}. The current theory and evidence holding that catecholamines are stored and released from presynaptic vesicles, the importance of Ca^{2+} influx in activating transmitter release, and electron microscopic evidence for fusion of presynaptic vesicles with presynaptic membranes are important to this model (Cf. Berl, S., et.al., 1973, for review). This model came into form with the finding that actomyosin is present in synaptosomal fractions of bovine and rat brain, and not present in mitochondria, microsomal, myelin or supernatant fractions (Puszkin et.al., 1972). It was then hypothesized that following Ca^{2+} influx, due to an action potential, brain actin and myosin, at the site of contact between pre-synaptic vesicles and pre-synaptic membrane,

combine to cause a conformational change in the membranes thus leading to the release of stored transmitter material into the synaptic cleft. Relaxation of this mechanism would occur with the efflux of Ca^{2+}. This mechanism is also applicable to reuptake of neurotransmitter.

This model is supported by other evidence in its favor; viz., the finding of a troponin-tropomyosin like component in the brain (Mahendran and Berl, 1977a,b), the further characterization of actin in synaptosomal preparations by "decoration" with heavy meromyosin, demonstrating an arrowhead configuration like the striated muscle actin counterpart (Schwartz, et.al., 1977), and the inhibition of uptake and release of putative transmitters of K^+-stimulated synaptosomes by vinblastine, colchicine and cytochalasin B and the demonstration of a direct detrimental effect of these drugs on the Mg^{2+}-ATPase of brain actomyosin (Nicklas and Berl, 1974; Nicklas, et.al., 1973). It has also been shown that these drugs added to the incubation medium of guinea pig hypogastric nerve caused an almost complete inhibition of release of dopamine β-hydroxylase and norepinephrine, without modifying the ratio of the two (Thoa, et.al., 1972). This indicated both an exocytotic release of transmitter material and a dependence of this release on both microtubules and microfilaments.

Because of the structural importance of myosin in the sliding filament models just presented, and because of the presence of myosin in the brain, a structural study of the myosin molecule was undertaken. The first step in this study was the isolation of myosin for bovine brain cortex. It should be understood that the process of isolation of brain myosin is much more difficult than that of skeletal myosin. As will be

seen in the Materials and Methods, and Results section of this dissertation, skeletal muscle myosin may be isolated by simple extraction of tissue with high salt, followed by a series of precipitations by dilution to low salt. The brain myosin isolation however, involved a much more complicated extraction medium, ammonium sulfate precipitation, column chromatography, as well as precipitation by dilution to low salt concentration before a fairly clean enzymatically active protein could be obtained. Perhaps, it is the difficulty of this isolation which has prevented many investigators from studying this protein.

The purified protein was studied in terms of its filament formation, electron microscopically, and compared to the much more intensively studied skeletal muscle myosin filaments as well as smooth muscle myosin filaments. Further investigation into its ultrastructure was accomplished by tryptic digestion of the brain myosin molecule and the study of its parts. The LMM portion of brain myosin was studied electron microscopically and compared to the LMM portions prepared from both skeletal muscle and smooth muscle myosins. The head portions of all three myosins were studied by comparing their ability to bind to actin isolated from brain, skeletal muscle and smooth muscle. Enzymologically, a comparison was made between the active sites of brain myosin and skeletal muscle myosin by studying the effect of pH on the substrate saturation kinetics of both proteins, and the determination of the Michealis constants Km and Vmax at each of these pH values. As will be seen in the Results and Discussion section of this dissertation, the Km value, as it relates to pH, is utilized to estimate the pK values of dissociating groups involved in the ATPase activity of the enzyme.

In view of myosins structural and enzymatic relation to the generation of force leading to the contraction of skeletal muscle, and the apparent lack of a well-defined structural arrangement of this protein with actin in brain tissue, a more detailed investigation of both the structure and enzymology of brain myosin is important in order to assess its involvement as a contractile component in neuronal tissue.

Figure 1:

Representation of the interacting thick and thin filaments between two successive Z-lines constituting a sacromere in striated (skeletal) muscle. The actin or thin filaments extend from the Z-lines marked Z, and the thick, or myosin containing filaments lie between the spacing of the thin filaments. This diagram shows the overlap of the thick and thin filaments at different stages of contraction. From Lehninger, (1975).

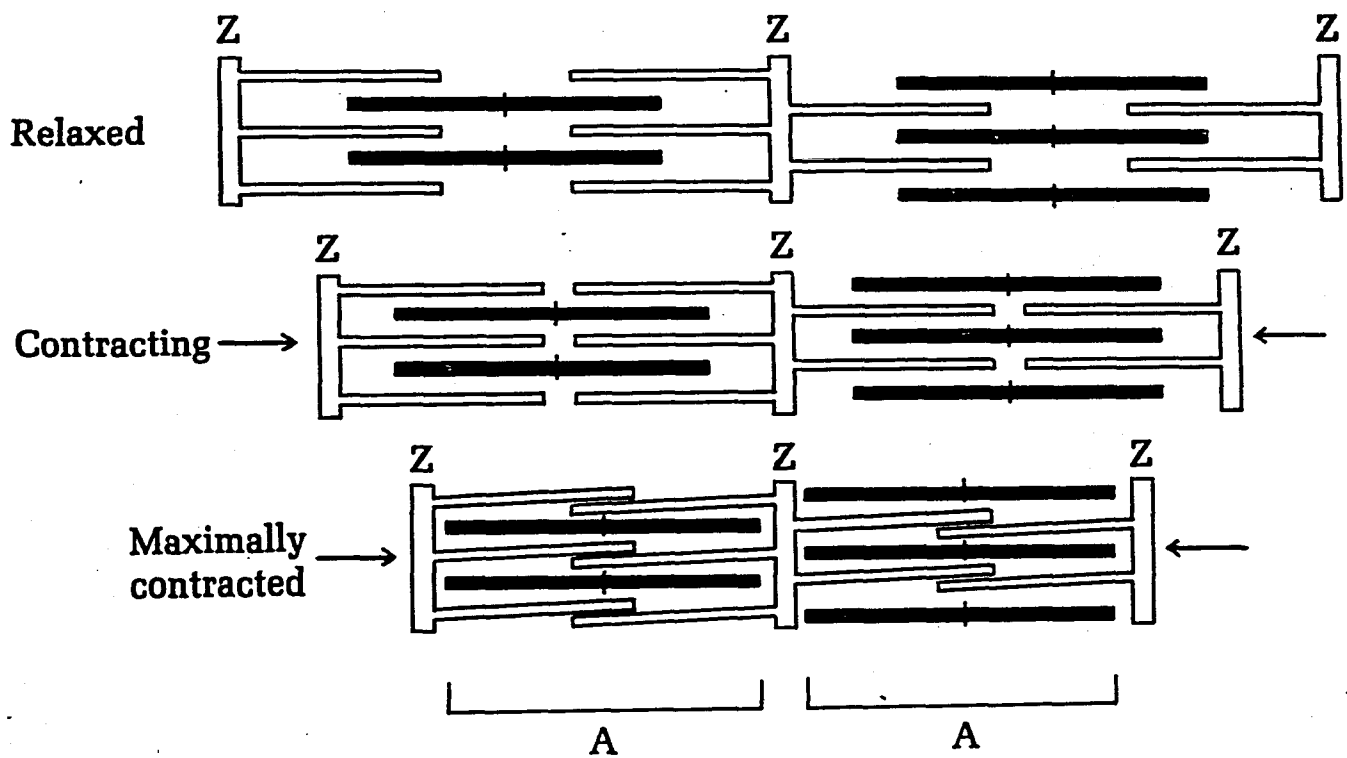

Figure 1

Figure 2:

Diagrammatic representation of a skeletal muscle myosin molecule, from Lehninger (1975), showing the globular double head region and α-helical tail portion, composed of the two heavy chains. Light chains are contained in the head region and approximate proteolytic cleavage points are designated for trypsin and papain. Trypsin cleavage produces two major pieces, the double headed region with part of the tail which is called heavy meromyosin (HMM), and the rest of the tail region which is called light meromyosin (LMM). Cleavage by papain causes the release of the individual heads called subfragment one (SF-1), and the rest of the tail portion.

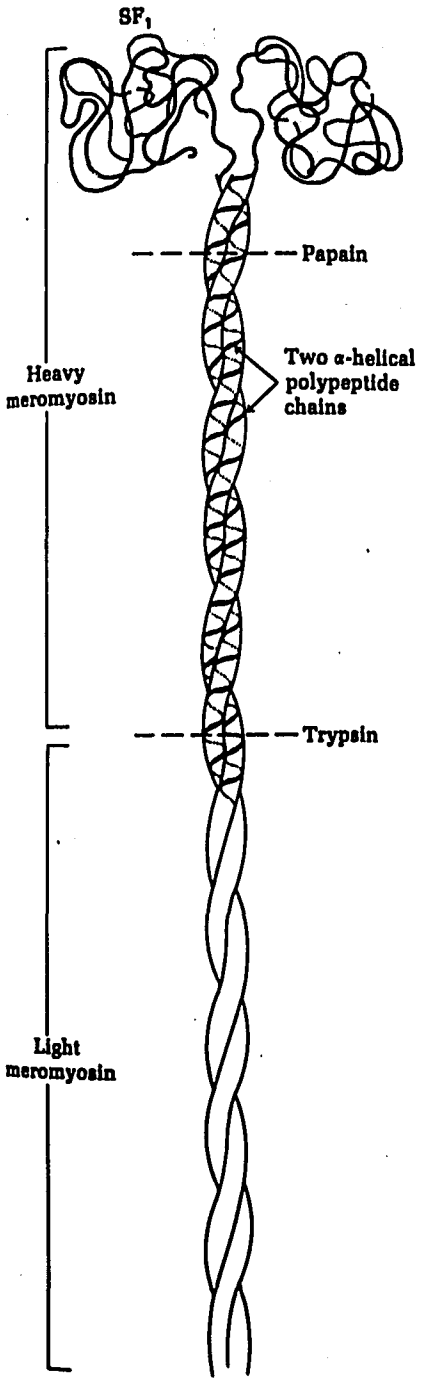
SF_1
Papain
Two α-helical polypeptide chains
Heavy meromyosin
Trypsin
Light meromyosin

Figure 2

Figure 3:

Schematic representation of a myosin thick filament. The filament is seen to consist of a bipolar stacking of the myosin molecules with their tail portions butting end to end and the head regions extending out at opposite directions. From Lehninger (1975).

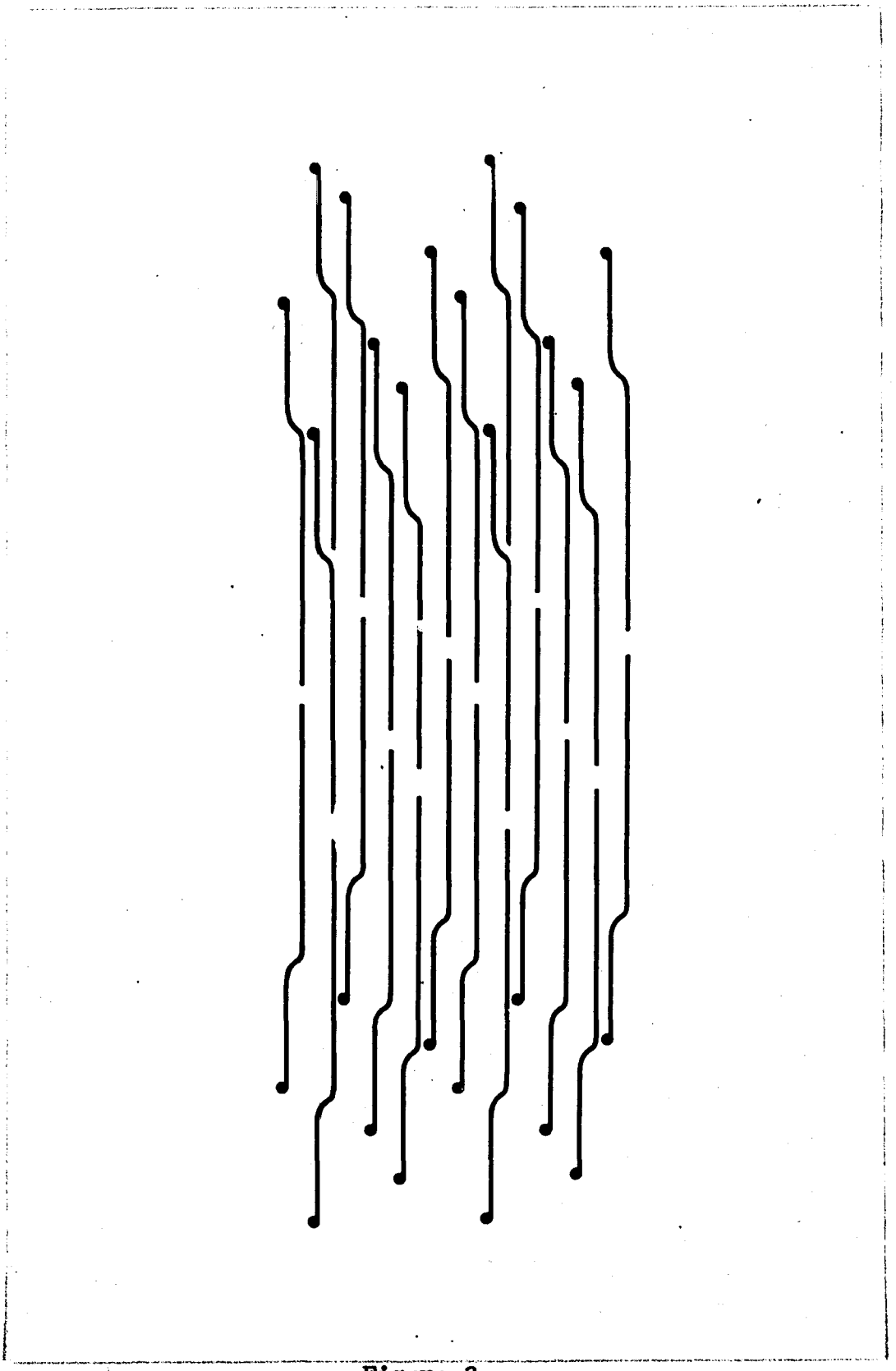

Figure 3

MATERIAL AND METHODS

I. Preparation of proteins.

All procedures are carried out in a cold room at 4°C or on ice, unless otherwise stated.

A. Purification of brain myosin.

1. From bovine brain cortex.

Myosin is prepared from bovine brain cortex after the Pollard et.al. (1974) procedure for the purification of myosin from human blood platelets, with minor modifications (Figure 4). The meninges, blood vessels, brain stem and cerebellum are removed from two bovine brains which are then washed twice in normal saline. The cortex is removed from the white matter by scraping it off with a razor blade. To this tissue is added 3X its volume of extraction buffer: 0.9M KCl, 1.5mM sodium pyrophosphate, pH 7.0, 5mM $MgCl_2$, 1.4mM mercaptoethanol, 30mM imidazole HCl, pH 7.0, and 10^{-5}M phenyl methyl sulfonyl fluoride.

The solution of the protease inhibitor, phenyl methyl sulfonyl fluoride, is prepared immediately before use as a stock solution in methanol. The final concentration of methanol in the extraction buffer is 0.01% (v/v). The bovine brain cortex is given 3 short bursts in a Waring blendor and then homogenized with 3-up and down strokes of a teflon-glass homogenizer. The extract is stirred for 30 min and then centrifuged at 34,800 X g for 30 min. The high ionic strength supernatant containing the myosin is pooled and dialyzed overnight against 15X its volume of: 10mM imidazole HCl, pH 7.0, and 1.4mM mercaptoethanol, in order to precipitate the myosin component by dilution to low

ionic strength. The resulting precipitate is collected by centrifugation at 34,800 X g for 30 min and dissolved using a Dounce type A homogenizer in: 0.6M KI, 5.0mM ATP, 2.8mM mercaptoethanol, 1.0mM $MgCl_2$, and 2.0mM imidazole HCl pH 7.0. The high level of ATP in this buffer is intended to help dissociate myosin complexed with actin, and the KI assists in this separation by depolymerizing the actin, thus freeing the myosin component for subsequent precipitation with $(NH_4)_2SO_4$. The homogenate is brought to 25% saturation in $(NH_4)_2SO_4$ by slow addition of crystalline $(NH_4)_2SO_4$ while stirring, and centrifuged at 34,800 X g for 30 min. The supernatant is brought to 55% saturation in $(NH_4)_2SO_4$ and the resulting precipitate containing myosin is collected by centrifugation at 34,800 X g for 30 min. The pellet is suspended in the above mentioned buffer with KI using a Douce type A homogenizer and centrifuged at 100,000 X g for 30 min to clarify the solution. The supernatant is then applied to a 2.5 X 90 cm column of Biogel A-15m 200/400 mesh (4% Agarose) prepared as follows: the column is first equilibrated with a column buffer composed of: 0.6M KCl, 1.4mM mercaptoethanol, 0.5mM ATP, 0.1mM $MgCl_2$, and 10mM imidazole HCl pH 7.0. Then prior to addition of the sample, 50 ml of the buffer containing KI (Figure 5) is applied. The column is then eluted with the column buffer and collected in 3.5 ml fractions. Protein elution is monitored by absorbance at 280 nm. The protein concentration of each fraction is determined by the method of Lowry et.al., (1951) and the myosin is located by virtue of its ATPase activity in the presence of K^+ and EDTA. K^+-EDTA-ATPase active fractions are pooled and precipitated 2X by repeated dialysis against a 20X volume of: 10.0mM imidazole HCl, pH 7.0, and 1.4mM mercaptoethanol, and homogenization in 0.6M KCl, 10.0mM

imidazole HCl, pH 7.0, and 1.4mM mercaptoethanol. Brain myosin may be stored in 50% glycerol at -20°C (Szent-Gyorgi, 1951). The protein composition of the isolated protein is analyzed by polyacrylamide-gel electrophoresis in the presence of SDS.

2. Isolation of myosin from crude synaptosomal preparation.

Myosin is also isolated from a crude bovine brain synaptosomal preparation prepared after the Puszkin et.al., (1972) modification of the Clarke and Nicklas (1970) method for preparing brain mitochondria. The myosin component is then isolated from the crude mitochondrial-synaptosomal pellet after the procedure of Pollard et.al., (1974), as described above. The meninges and blood vessels are removed from 2 bovine brains, which are then washed in normal saline. The grey matter is suctioned off into a vacuum flask with periodic washings of sucrose, tris, EDTA buffer (STE): 0.25M sucrose, 0.01M tris, pH 7.4, and 0.5mM tris-EDTA to clear the suction tube and wet the cortex. For every 200 ml of STE used to wash the tube, the solution is weighed and the weight of 200 ml of STE alone is subtracted from it. This will give the weight of grey matter obtained. The final mixture is brought up to volume with STE to be 10% bovine brain in STE (w/v). The brain material is homogenized in STE with a teflon-glass homogenizer with a 0.01 inch clearance at slow speed, using 10 up and down strokes. The homogenate is centrifuged at 2,000 X g for 3 min. The supernatant is decanted and put aside. The soft pellet is resuspeded with STE and centrifuged again, the supernatant of which is decanted and pooled with the previous supernatants. The supernatant pool is centrifuged at 13,200 X g for 8 min. The crude mitochondrial pellet which contains synaptosomes, is resuspended again

in STE and centrifuged. The resulting mitochondrial-synaptosomal pellet is measured volumetrically and twice its volume of the extraction buffer mentioned above is added. This is quick frozen in liquid nitrogen and allowed to thaw out overnight in the cold room to rupture the synaptosomes. The extract is centrifuged at 78,000 X g for 30 min. The supernatant is brought to 3X its volume with 2mM $MgCl_2$ slowly with stirring, brought up to pH 6.2 with 0.5M acetic acid and allowed to stand for 20 min, in order to precipitate the myosin component. This is centrifuged at 43,500 X g for 30 min. The pellet is collected and homogenized in the buffer containing KI mentioned above. The rest of the myosin isolation from the crude mitochondrial-synaptosomal pellet is the same as described above for bovine brain cortex.

B. Purification of skeletal muscle myosin.

Myosin is prepared from rabbit skeletal muscle according to a standard isolation procedure of Richards et.al., (1967). This procedure involves the extraction of the back muscles of one white rabbit with a high salt buffer containing 0.37M KCl and 0.4mM ATP. Myosin in the extract is obtained by a series of three cycles of precipitation by dilution of the high salt protein solution to low ionic strength with water.

Skeletal muscle myosin utilized for the kinetic experiments is prepared according to the procedure used for bovine brain cortex described above. Myosin prepared by both of these procedures is stored for future use in 50% glycerol at -20°C.

C. Purification of smooth muscle myosin.

Smooth muscle myosin from chicken gizzards was prepared according to the procedure of Sobieszek and Bremel, 1975.

D. Purification of actins.

Actin from skeletal muscle was prepared from rabbits after the procedure of Carsten and Mommaerts, 1963. Actin was prepared from chicken gizzard smooth muscle after the procedure of Herman and Pollard, 1979, and actin was prepared from bovine brain cortex after the procedure of Bray and Thomas, 1976. Actins to be used for either enzymatic assay or electron microscopy were taken from storage (lyophylized) at -20°C and dissolved in 1mM $MgCl_2$, 0.1M KCl and 10mM imidazole pH 7.0. This buffer causes the polymerization of the actin monomers to form F (filamentous)-actin.

E. Preparation of heavy and light meromyosins.

Heavy and light meromyosins are prepared by proteolytic cleavage of myosins isolated from bovine brain cortex, rabbit skeletal muscle and chicken gizzard smooth muscle after the procedure of Lowey and Cohen (1962).

Myosin is precipitated from 50% glycerol stock solutions kept at -20°C by dialysis overnight against 20X volume of: 10mM imidazole HCl pH 7.0, and 1.4mM mercaptoethanol. The myosin is collected by centrifugation at 12,100 X g for 20 min and homogenized in: 0.5M KCl and 0.1M phosphate buffer pH 7.0. Protein is determined by the procedure of Lowry et.al., (1951) and the protein concentration is adjusted to approximately 10mg/ml. Ten volumes of myosin is mixed with 1 volume of trypsin stock solution at room temperature (approximately 23°C).

The trypsin stock solution is prepared immediately before use; trypsin 0.5mg/ml in 0.001N HCl. The mixture of myosin and trypsin is incubated at room temperature with stirring for 4-5 min, and the reaction terminated by addition of 1 volume of trypsin inhibitor stock solution; soybean trypsin inhibitor 1mg/ml in H_2O previously adjusted to pH 7.4 with NaOH. The tryptic digest is then dialyzed overnight against one liter of; 10mM imidazole HCl pH 7.0, and 1.4mM mercaptoethanol at 4°C. The light meromyosin is pelleted by centrifugation at 100,000 X g for 60 min. The supernatant containing heavy meromyosin is further purified by collecting the fraction precipitating at 40-55% $(NH_4)_2SO_4$ saturation. Collected by centrifugation at 12,100 X g for 20 min, the HMM is homogenized in one ml of; 10mM imidazole HCl pH 7.0, and 1.4mM mercaptoethanol, and dialyzed against 100ml of the same buffer overnight. The light meromyosin is re-precipitated 3X by repeated homogenization in: 0.6M KCl, 10mM imidazole HCl pH 7.0, and 1.4mM mercaptoethanol, and precipitation by dialysis against a 20X volume of: 10mM imidazole HCl pH 7.0, and 1.4mM mercaptoethanol, the first two times, and finally by dialysis against 100X volume of: 0.1M KCl, 10mM imidazole HCl pH 7.0, and 1.4mM mercaptoethanol.

II. Protein determination.

The concentration of protein in a sample is determined by the method of Lowry et.al. (1951), using bovine serum albumin as a standard.

III. ATPase measurements.

A. Assay conditions for the measurement of ATPase activity.

The total volume of each assay mixture is 1.0ml. The concentration of myosin is 5-30μg protein/ml, unless otherwise stated, and in attempts at actin activation of myosin Mg^{2+}-ATPase, polymerized F-actin is added in concentrations 5-fold in excess of myosin. Incubation is in a water bath at the designated temperature with moderate shaking. All time course curves of myosin ATPase are done at a concentration of 1 or 2mM ATP. Measurements of enzyme concentration versus ATPase activity were done with 2mM ATP.

1. Assay conditions for all routine assays at 37°C.

a. For K^{+}-EDTA or Ca^{2+}-ATPase, the incubation mixture consists of: 0.6M KCl, 2mM EDTA or 5mM $CaCl_2$, 50mM imidazole HCl, pH 7.0, and 1mM ATP.

b. For Mg^{2+}-ATPase with or without actin, the incubation mixture consists of: 1mM $MgCl_2$, 50mM imidazole HCl, pH 7.0, 0.1M KCl and 1mM ATP.

2. Assay conditions for kinetic studies at different pH values at 25°C consists of: 0.6M KCl, 2mM EDTA or 5mM $CaCl_2$, and the ATP concentration varied. The desired pH ranges were obtained with the following buffer system; for pH 5.5-6.0, 25mM acetate buffer is used, and prepared by titrating 0.2M acetic acid with 0.2M sodium acetate to the desired pH. For pH 6.5-8.5, 50mM HEPES buffer is used, and prepared by titrating the free acid (N-2-hydroxyethylpiperazine N'-2-ethanesulfonic acid), with the sodium salt, to the desired pH. Glycine buffer is used at pH 9.0; 50mM glycine buffer is used from a 0.1M glycine stock solution titrated to the desired pH with 0.2N KOH.

B. Colorimetric determination of inorganic phosphorus (P_i).

The P_i of ATPase activity of myosin was measured by the Puszkin et.al., (1968) modification of the Marsh procedure (1958) for the colorimetric determination of P_i in the presence of ATP. A standard curve is prepared using $NaH_2PO_4 \cdot H_2O$ as the source of P_i.

IV. Gel electrophoresis.

A. Gradient slab gels.

Protein samples for electrophoretic separation and analysis were run on a slab gel with a linear gradient of polyacrylamide in the presence of sodium dodecyl sulfate (SDS) after the procedure of O'Farrell (1975).

B. Cylindrical gels.

Cylindrical gels for SDS-polyacrylamide gel electrophoresis (SDS-PAGE) were prepared after the method of Weber and Osborn (1969).

V. Electron microscopy.

Protein preparations are examined with a Hitachi HU-11F electron microscope at 75 kV, after negative staining with uranyl acetate. All procedures are carried out at room temperature.

A. Electron microscopy of myosin filaments and light meromyosins (LMM).

Myosin filaments and LMM are prepared by dialyzing 1ml of a 0.3mg/ml solution of myosin or LMM in 0.6M KCl against 100ml of 0.1M KCl, 10mM imidazole HCl, pH 7.0, and 1.4mM mercaptoethanol. One drop is placed on a carbon formvar coated grid and allowed to stand approximately 1 min. The drop is removed by application of filter paper to the side of the grid, 2% uranyl acetate (w/v) is applied after 1-2 min, the uranyl acetate drop is removed with filter paper and the grid is allowed to air dry.

B. Electron microscopy of actin and actin decorated with heavy meromyosin (HMM).

Carbon coated grids are prepared with actin alone or actin with HMM as follows: 1 drop of polymerized actin is placed on grid, allowed to stand for 1 min and washed off with a few drops of polymerizing medium. 1 drop of HMM is applied and allowed to stand for 1 min. This is washed with 1 drop of H_2O which is blotted off (Schwartz et.al., 1977). 1 drop of 0.2% (w/v) tannic acid is applied and allowed to stand for 2 min (Begg et.al., 1978). The drop is removed and 1 drop of uranyl acetate is applied and allowed to stand 1-2 min. The uranyl acetate is removed and the grid is air dried.

Figure 4:

Outline of extraction procedure for the purification of bovine brain myosin adapted after T.D. Pollard et.al., (1974).

EXTRACTION PROCEDURE

Modified after T.D. Pollard, et.al., 1974.

BOVINE BRAIN CORTEX

1. Extraction with 0.6M KCl
   10 mM PP_i
   3 mM $MgCl_2$
   1 mM DTT
   20 mM imidazole HCl pH 7.0

2. Centrifuged
   34,800 X g 30'

Pellet
Discarded

SUPERNATANT

1. Dialyzed vs 10X volume
   1mM DTT
   10mM imidazole HCl pH 7.0

2. Centrifuged
   34,800 X g 30'

PELLET

1. Homogenized in 0.6M KI
   5 mM ATP
   1 mM $MgCl_2$
   2 mM DTT
   20 mM imidazole HCl pH 7.0

2. 25-60% $(NH_4)_2SO_4$ Saturation

3. Centrifuged
   34,800 X g 30'

Supernatant
Discarded

PELLET

1. Homogenized in KI

2. Centrifuged to clarify (100,000 X g 60')

3. APPLIED TO COLUMN

Supernatant
Discarded

Figure 5:

Diagram of 90 X 2.5cm column of agarose-4B showing the discontinuous gradient of the KCl containing buffer comprising 85% of the column volume and the KI containing buffer comprising 15% of the column volume. The 55% $(NH_4)_2SO_4$ fraction is applied to the column in the KI containing buffer. The myosin component of the 55% $(NH_4)_2SO_4$ fraction passes through the KI into and elutes with the KCl containing buffer.

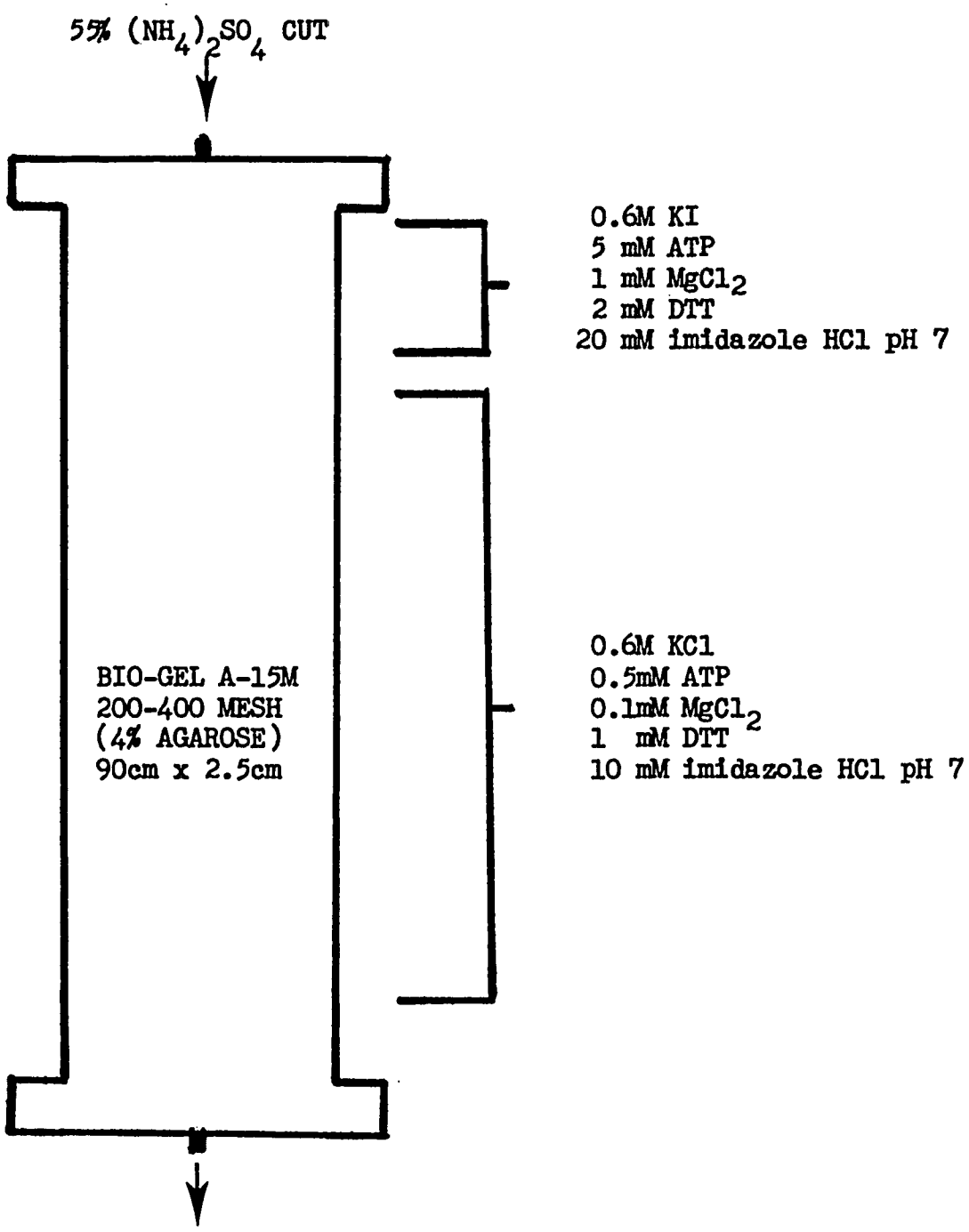
55% $(NH_4)_2SO_4$ CUT
0.6M KI
5 mM ATP
1 mM $MgCl_2$
2 mM DTT
20 mM imidazole HCl pH 7
BIO-GEL A-15M
200-400 MESH
(4% AGAROSE)
90cm x 2.5cm
0.6M KCl
0.5mM ATP
0.1mM $MgCl_2$
1 mM DTT
10 mM imidazole HCl pH 7

RESULTS

Purification of Brain Myosin.

Some minor modification of the Pollard procedure (Pollard et.al., 1974) for the isolation of myosin from platelets were made in adapting this procedure for brain. For the Pollard procedure, the myosin is precipitated from the extracted supernatant by diluting it to 0.15M KCl with 2mM $MgCl_2$ and adjusting the pH to 6.2 with acetic acid. Although this does in fact precipitate myosin from the brain extract supernatant, the volume of material is very large. Therefore, for the sake of convenience, this first precipitation of myosin from the brain extract supernatant was achieved by dilution to 0.06M KCl by dialysis against 10mM imidazole pH 7.0. According to the Pollard procedure the $(NH_4)_2SO_4$ precipitations are done by addition of a saturated solution of $(NH_4)_2SO_4$ to the protein solution until the desired percent saturation in $(NH_4)_2SO_4$ is reached. Again, due to the large volumes dealt with, the protein solution containing brain myosin was brought to the desired saturation level by direct addition of crystalline $(NH_4)_2SO_4$ with monitoring of the pH of the solution. The final stage in the purification of myosin from platelets in the Pollard procedure is elution from the 4% agarose column. Brain myosin, however, is further purified after the column elution, as will be explained.

A typical elution profile of brain myosin using the 4% agarose column is shown in Figure 6. Fractions 40-60, which have K^+-EDTA-ATPase activity are pooled for further purification by re-precipitation as detailed in Methods. The specific activity of the protein increased

with further purification as seen in Table 1. As shown by SDS-PAGE (Figure 7), the pooled fractions contain a high molecular weight contaminant which may be separated from the myosin by a series of precipitations. Myosin is insoluble at low ionic strength, whereas the high molecular weight protein is soluble. The ionic strength is reduced by dialysis as described in the Methods section. Most of the high molecular weight protein remains in the supernatant of the low ionic strength dialysate. The supernatant is free of any myosin and devoid of any detectable ATPase activity. SDS-PAGE of these proteins at different stages of purification is illustrated in Figure 7. From 200g of bovine brain cortex about 20mg of K^+-EDTA-ATPase active protein is obtained after column chromatography, and about 5mg of protein is recovered from this after two cycles of precipitation.

Bovine brain myosin was electrophoresed on 10% and 12% cylindrical SDS-polyacrylamide gels in order to resolve the light chains. 10% polyacrylamide gels sufficiently resolved the 20,000 and 17,000 dalton (Kendrick-Jones, 1973) components of chicken gizzard smooth muscle myosin, but did not clearly resolve the low molecular weight components of the brain myosin preparation (Figure 8). Upon close inspection however, it appears that this rather diffuse band in the 10% gel can be separated into two polypeptides with estimated molecular weights of 18,000 and 16,000 daltons. Electrophoresis of the brain myosin on 12% gels led to a clear separation of the low molecular weight components (Figure 9). Rabbit skeletal muscle myosin electrophoresed on the 12% gel showed the 25,000, 18,000 and 16,000 dalton (Weeds and Lowey, 1971) light chains (Figure 9). Comparatively the brain myosin revealed on the 12% gel, components with apparent molecular weights of 18,000 and 16,000 daltons. No 25,000 dalton component was observed for the brain myosin.

Filament Formation.

Bovine brain myosin forms bipolar filaments, as revealed by the electron microscope, upon dialysis against 0.1M KCl at pH 7.0 and negatively stained with uranyl acetate. The filaments measure end to end 0.350 ± 0.035 μ. The filaments appear dumbell shaped with a bare zone in the middle of the filament, which measures 0.208 ± 0.011 μ. Globular regions are seen at either end of the filaments (Figure 10). The above measurements are within the range reported by Burridge and Bray (1975) of 0.270-0.420 μ for myosin filaments from chick brain with a bare zone of 0.150-0.200 μ. Kuczmarski and Rosenbaum (1979) also report myosin filaments from chicken brain to be 0.300 μ in length with a bare zone of 0.150 μ. As seen in Figures 10 and 11, the brain myosin filaments were observed as a ladder-like assembly of dumbell shaped filaments associated head to head (Figure 10b,c and Figure 11) or in a rather scattered head to head association (Figure 10a). Both these arrangements were observed by Burridge and Bray (1975) and by Kuczmarski and Rosenbaum (1979) for chick brain myosin.

Skeletal muscle myosin upon dialysis against 0.1M KCl at pH 7.0 forms cigar-shaped filaments tapered at either end as described by Huxley (1963). These filaments measure end to end 1.230 ± 0.221 μ which is within the common range of 0.500-1.500 μ reported by Huxley (1963), for skeletal muscle myosin filaments. Two electron micrographs of skeletal muscle myosin filaments are seen in Figure 12a and b, at magnifications of 85,000 and 24,750 respectively.

Smooth muscle myosin, upon dialysis against 0.1M KCl at pH 7.0 revealed rather thickly branched structures of varying length, in the

electron microscope. A typical field showing this effect at 20,500X magnification is seen in Figure 13b. At a higher magnification of 85,000X a periodicity of 140 Å is seen within this branching structure (Figure 13a). A 140 Å periodicity was found by Small and Squire (1972) to be present on the surface of the ribbon-like structures in smooth muscle. This periodicity is believed to represent the spacing of the myosin heads on the surface of the ribbon, which is capable of branching in smooth muscle. Burridge and Bray (1975) also observed, electron microscopically, in vitro formed smooth muscle myosin filaments with a 140 Å periodicity similar to those pictured in this dissertation.

The Light Meromyosins.

As indicated in the Methods section, brain myosin, after brief treatment with trypsin, can be separated into an LMM and HMM portion. An electron micrograph (85,000X) of brain LMM dialyzed against 0.1M KCl at pH 7.0 is seen in Figure 14a. These fibers are seen stacked next to each other forming short filamentous structures with frayed ends.

Skeletal muscle LMM upon dialysis against 0.1M KCl at pH 7.0 assembles into large structures of indefinite length and width. An electron micrograph (85,000X) of skeletal muscle LMM (Figure 14c) is shown next to the brain LMM at the same magnification for comparison. The LMM portion of striated muscle myosin reveals an axial periodicity of 430 Å containing a small band of 100 Å in width. This corresponds to the published observation of a 430 Å axial periodicity containing a small band of 100 Å in width by Huxley (1963).

The LMM portion of smooth muscle myosin at 85,000X magnification may be seen in Figure 14b, next to brain and striated muscle LMMs for

comparison. The short filamentous structures have frayed ends and appear to be composed of thin strands of protein stacked next to one another much like the brain LMM.

Treatment of Actin Filaments with HMM.

Actin filaments from brain, skeletal muscle, and smooth muscle were observed in the electron microscope. Treatment of the actin fibers with the HMM portion of the myosin molecule yields the characteristically decorated fiber originally described by Huxley (1963). Actin filaments from the different sources described above were treated with HMM prepared from brain, skeletal muscle and smooth muscle myosins.

Electron micrographs of undecorated actin fibers prepared from brain, skeletal muscle and smooth muscle may be seen in Figure 15a,b, and c. Treatment of these fibers with brain HMM yields the characteristic arrowhead pattern for brain actin (Figure 16a), skeletal muscle actin (Figure 16b), and smooth muscle actin (Figure 16c). The periodicity of the brain HMM attachment to the actin fibers measures 388 ± 31 Å for brain, 387 ± 23 Å for skeletal muscle, and 436 ± 83 Å for smooth muscle actins. This is in good agreement with the reported value of 366 ± 15 Å for the decoration of skeletal muscle actin with skeletal muscle HMM by Huxley (1963).

The presence of 1mM ATP has been shown to dissociate the skeletal muscle HMM-actin complex (Huxley, 1963). ATP has also been shown to dissociate the complex of synaptosomal actin and skeletal muscle HMM (Schwartz et.al., 1977). Figure 16d shows the dissociation of the brain HMM-brain actin complex after the addition of 1mM ATP, and Figure 16e

shows the dissociation of the brain HMM-skeletal muscle actin complex after the addition of 1mM ATP.

HMM from skeletal muscle myosin also decorated actins from brain, skeletal muscle and smooth muscle (Figure 17a, b, and c). The periodicities of the arrowhead formation measure 398 ± 12 Å for brain actin, 398 ± 31 Å for skeletal muscle actin and 376 ± 29 Å for smooth muscle actin.

HMM prepared from smooth muscle myosin decorates brain, skeletal muscle and smooth muscle actins also (Figure 18a, b, and c). Measurements of the arrowhead periodicities are 358 ± 22 Å for brain actin, 372 ± 29 Å for skeletal muscle actin and 376 ± 29 Å for smooth muscle actin.

Attempt at Actin Activation of Bovine Brain Myosin.

Myosin from bovine brain cortex when assayed alone for Mg^{2+}-stimulated ATPase activity has a specific activity anywhere from 0-0.03 μ moles $P_i \cdot mg^{-1} \cdot min^{-1}$. The addition of polymerized skeletal muscle actin or brain actin does not increase the Mg^{2+}-ATPase activity, if any, of the myosin prepared from brain.

Kinetic Studies.

A comparative study was done on the effect of substrate concentration on the enzyme activity of both brain and skeletal muscle myosins at different pH values. The specific activity of the enzyme is expressed as micromoles of inorganic phosphorus liberated from ATP per milligram of protein per minute (v_o, μ moles $P_i \cdot mg^{-1} \cdot min^{-1}$). Substrate saturation curves were plotted as v_o versus substrate concentration. The values of maximal velocity (Vmax) and the amount of substrate required to yield one-half Vmax (Km) were calculated by the computational method of Wilkinson (1961) with appropriate standard errors.

All assays were carried out at 25°C. The incubation time and concentration of enzyme used for these assays were within a range in which the enzyme activity was linear. Linearity was established with respect to time of incubation for skeletal muscle myosin (Figures 19 and 20) and for brain myosin (Figure 22) at the extreme pH values tested, where the lability of the enzyme was of most concern. The time course curve for skeletal muscle myosin Ca^{2+}-ATPase fits a line with a correlation coefficient value (r^2) for linear regression of 0.997 at pH 5.5 and 0.998 at pH 9.0 (Figure 19). The time course curve for skeletal muscle myosin K^+-EDTA-ATPase has an r^2 of 0.998 at pH 6.5 and 0.996 at pH 9.0 (Figure 20). The time course curve for brain myosin K^+-EDTA-ATPase has an r^2 value of 0.974 at pH 6.5 and 0.992 at pH 9.0 (Figure 22). Therefore, since time usually chosen was within this linear range, the v_o's were indeed initial velocities.

The linearity of ATPase activity of different concentrations of enzyme was established at pH 7.0 for both of these proteins. The enzyme concentration curve for skeletal muscle myosin Ca^{2+}-ATPase has an r^2 value of 0.998 and in the presence of K^+-EDTA the r^2 is 0.995 (Figure 21). The enzyme concentration curve of brain myosin K^+-EDTA-ATPase at pH 7.0 has an r^2 of 0.989 (Figure 23).

The ATP concentration range assayed for the K^+-EDTA-ATPase substrate saturation curve for brain myosin was 0.0125mM-1.0mM, and for striated muscle myosin 0.0125mM-2.0mM. However, saturation with substrate was reached at very low concentrations of ATP for the Ca^{2+}-ATPase. Concentrations of ATP less than 0.0125mM could not provide enough P_i upon hydrolysis of as much as 25% of the substrate to be detected with the assay procedure

utilized. Therefore, the Km values calculated for the Ca^{2+}-ATPase of both brain and skeletal muscle myosin are mostly at or below the lowest ATP concentration used.

The pH range tested at varied substrate concentrations was 6.5-9.0 for the K^{+}-EDTA-ATPase of both brain and muscle myosins, 6.0-9.0 for the Ca^{2+}-ATPase of striated muscle myosin. Above pH 9.0, activity of both myosins was lost. This is most likely due to denaturation of the enzyme, since it has been shown that the light chains of skeletal muscle myosin, which are required for ATPase activity, are liberated from the intact molecule at pH 11.0 (Driezen and Gershman, 1970). Below the lower pH values mentioned above, activity was also lost.

The substrate saturation curves at different pH values for skeletal muscle myosin Ca^{2+}-ATPase are superimposed on Figure 24, and for skeletal muscle myosin K^{+}-EDTA-ATPase on Figure 25. Figure 26 shows the substrate saturation curves at different pH values for the Ca^{2+}-ATPase activity of brain myosin and Figure 27 shows the substrate saturation curves for the K^{+}-EDTA-ATPase of brain myosin. At high ATP concentrations, there is a tendency for a decrease of the ATPase activity at the different pH values with both myosins.

A statistical method (Wilkinson, 1961) was used for estimating the Km and Vmax values of the Michealis-Menten equation with appropriate standard errors from the data obtained by measuring enzyme activity under varied substrate concentrations at different pH values. The Km and Vmax values determined by this procedure are displayed in Table 2 which contains these values for skeletal muscle myosin and Table 3 which contains these values for brain myosin. The negative log of the Km values (pKm) versus

pH were also plotted. This plot reflects dissociating groups of the enzyme, enzyme-substrate complex, or substrate (Dixon and Webb, 1958).

A plot of Vmax versus pH for skeletal muscle myosin K^+-EDTA-ATPase is shown in Figure 28. It can be seen that the Vmax value increases with pH from 6.5-9.0. Below pH 6.5, there is no detectable K^+-EDTA-stimulated ATPase activity, whereas the Ca^{2+}-stimulated (Figure 31) ATPase activity extends further to pH 5.5 with an apparent optimum at pH 6.5. Brain myosin K^+-EDTA-ATPase also shows an increase in Vmax with an increase in pH from 6.5-9.0 (Figure 34). Below pH 6.5, there is also no detectable K^+-EDTA-ATPase activity, whereas the Ca^{2+}-ATPase activity extends further to pH 6.0 (Figure 37).

The plots of Km versus pH for rabbit skeletal muscle K^+-EDTA-ATPase (Figure 29) and Ca^{2+}-ATPase (Figure 32), like brain myosin K^+-EDTA-ATPase (Figure 35) and Ca^{2+}-ATPase (Figure 38) show a tendency of the Km to increase with pH.

A plot of pKm versus pH for skeletal muscle myosin K^+-EDTA-ATPase may be seen in Figure 30. This plot may be consistent with a dissociating group between pH 7.5-8.0. The plot of pKm versus pH for skeletal muscle myosin Ca^{2+}-ATPase (Figure 33) is suggestive of multiple ionizations. For brain myosin K^+-EDTA-ATPase, the plot of pKm versus pH (Figure 36) is consistent with an ionization between pH 7.5 and 8.0. A break in the line for pKm versus pH of brain myosin Ca^{2+}-ATPase (Figure 39) occurs between pH 7.5 and 8.0, which may designate an ionization occurring between these two pH values.

Figure 6:

Elution profile of brain myosin off the agarose-4B column. -x- represents mg of protein per ml of column eluant, and -⊡- represents micromoles of inorganic phosphorus liberated from ATP per ml of eluant for 30 min., in the presence of K^+ and EDTA (y axis), both plotted against fraction number (x axis). Each fraction contains 3.5 ml of eluant.

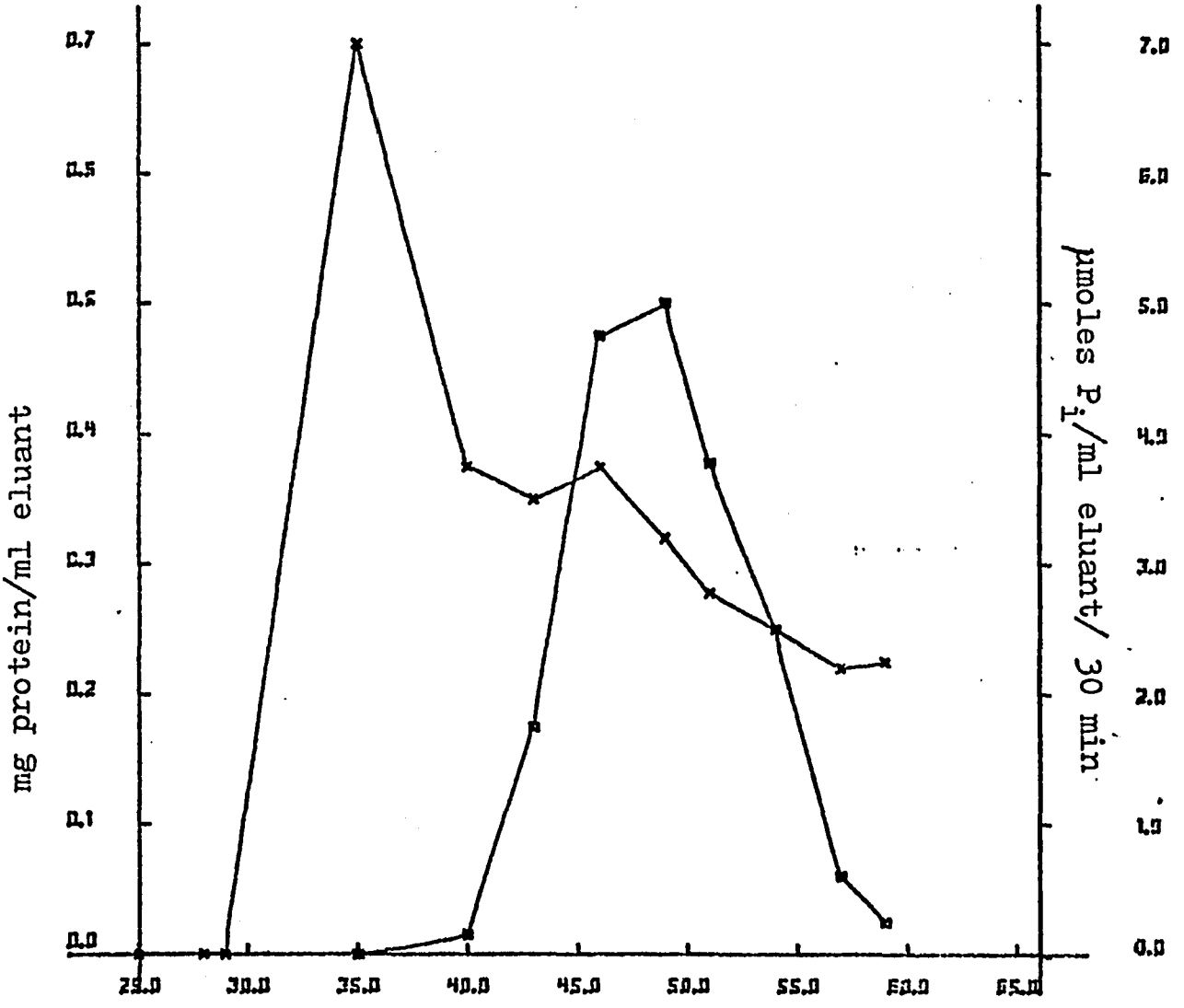
mg protein/ml eluant
μmoles P_i/ml eluant/ 30 min
0.0
0.1
0.2
0.3
0.4
0.5
0.6
0.7
1.0
2.0
3.0
4.0
5.0
6.0
7.0
25.0
30.0
35.0
40.0
45.0
50.0
55.0
60.0
65.0
fraction number

Figure 6

Figure 7:

0-15% polyacrylamide gradient slab gel. Column 1: ribonuclease, molecular weight 15,500 daltons, Column 2: chymotrypsinogen, molecular weight 25,000 daltons, Column 3: skeletal muscle actin, molecular weight 42,000 daltons, Column 4: bovine serum albumin, molecular weight 66,000 daltons, Column 5: phosphorylase-A, molecular weight 95,000 daltons, Column 6: skeletal muscle myosin, Column 7: skeletal muscle myosin, Column 8: supernatant of third precipitation, Column 9: pooled fractions 49-60 after 4 cycles of precipitation, Column 10: pooled fractions 49-60 after three cycles of precipitation, Column 11: pooled fractions 49-60 after two cycles of precipitation, Column 12: pooled fractions 49-60 after one cycle of precipitation, Column 13: supernatant of precipitation one, Column 14: fraction 60, Column 15: fraction 54, and Column 16: fraction 49.

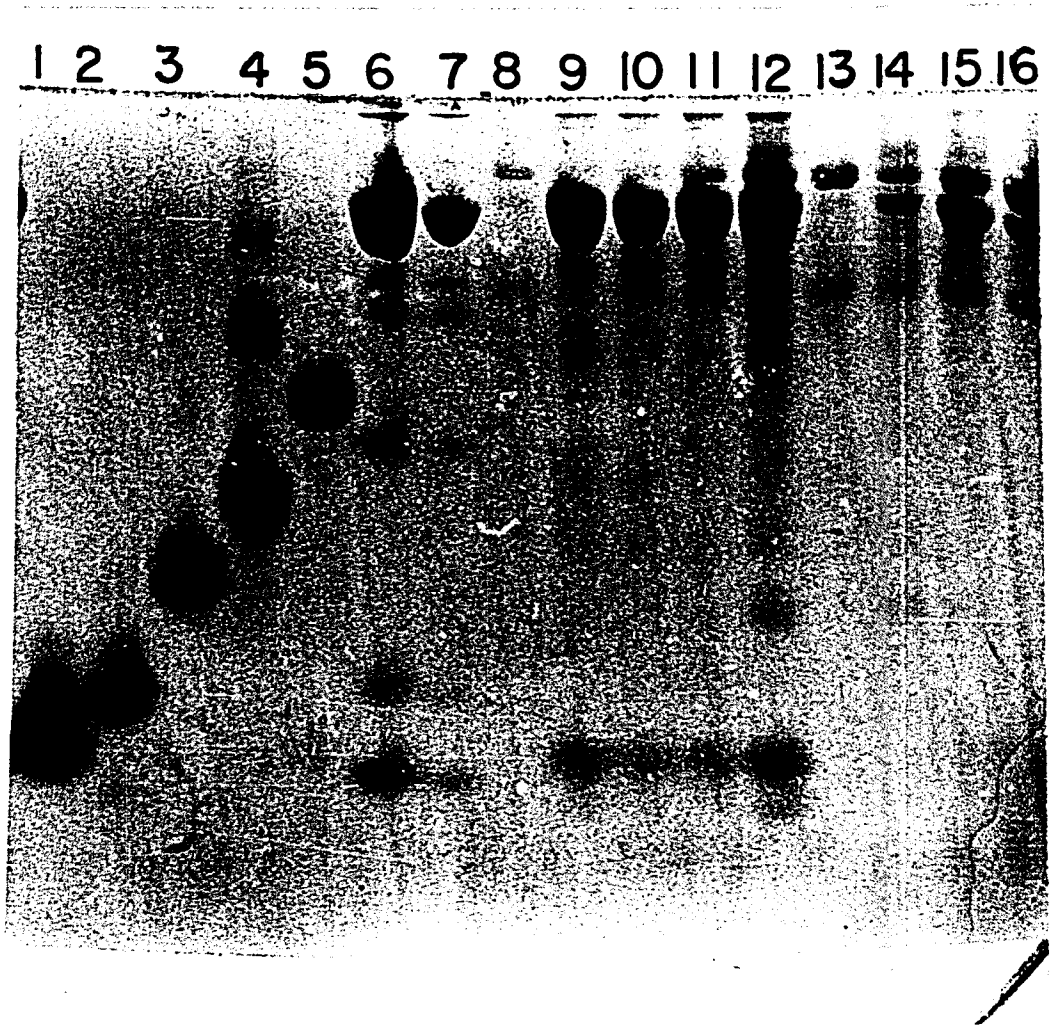

Figure 7

Figure 8:

Cylindrical 10% polyacrylamide gels of smooth muscle myosin and brain myosin.

Figure 8a:

The 20,000 and 17,000 dalton light chain components of smooth muscle myosin are clearly visible at the lower end of the gel.

Figure 8b:

The low molecular weight components of brain myosin are rather diffuse.

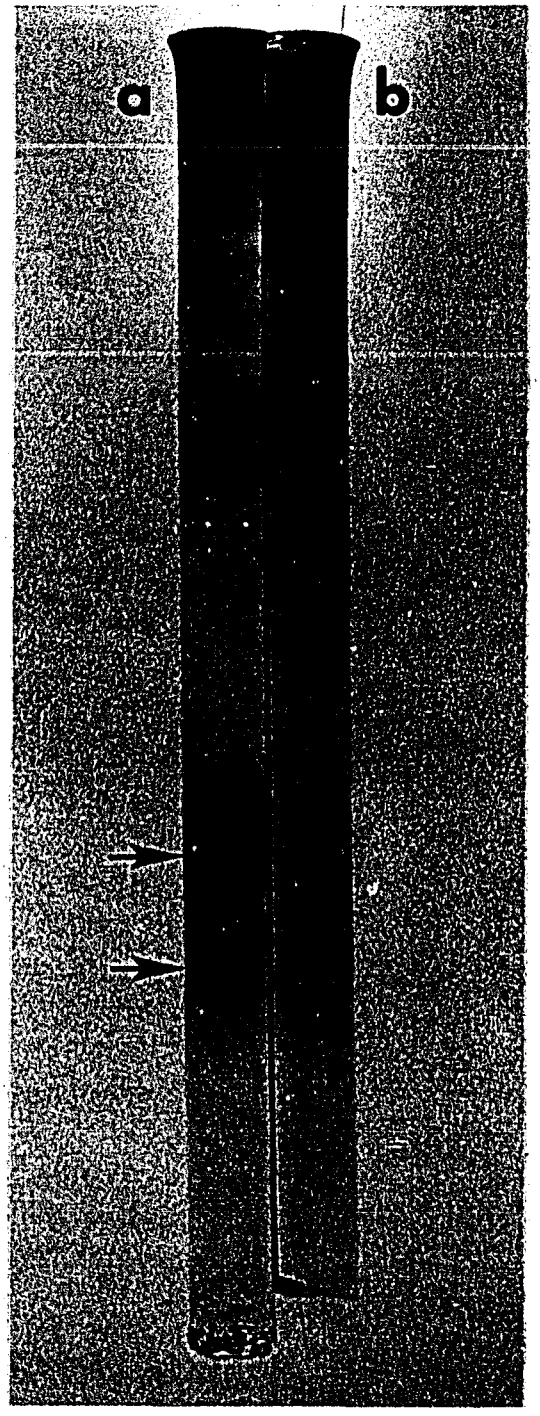

Figure 8

Figure 9:

Cylindrical 12% polyacrylamide gels of skeletal muscle and brain myosins.

Figure 9a:

The light chain componenets of brain myosin are visible at the bottom of the gel within the molecular weight region of approximately 18,000 and 16,000 daltons compared to the skeletal muscle myosin standard.

Figure 9b:

The 25,000, 18,000 and 16,000 dalton light chain components of rabbit skeletal muscle myosin are visible at the bottom of the gel.

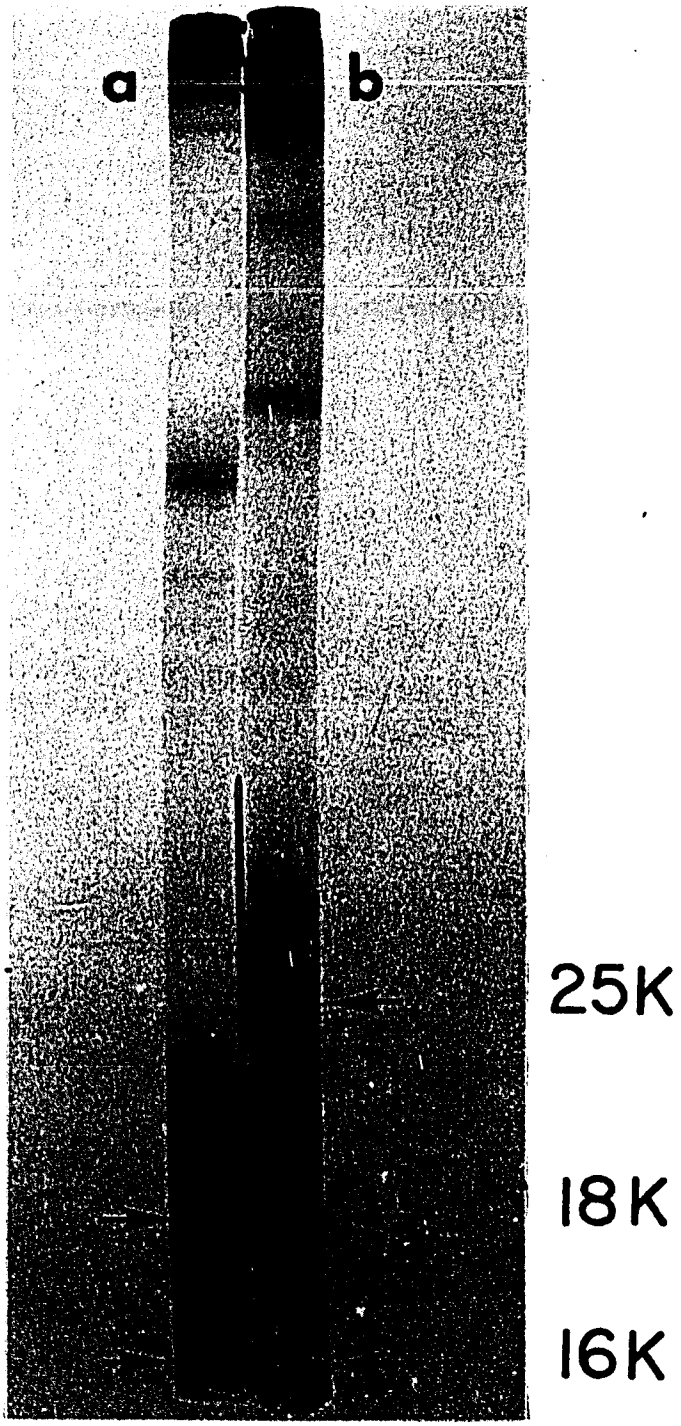

Figure 9

Figure 10:

Electron micrographs of bovine brain myosin filaments.

a) Brain myosin filaments at 85,000X magnification, showing the apx. 0.350 μ dumbell shaped filaments with a bare zone (b) of apx. 0.208 μ. A head to head association is also apparent.

b) Brain myosin filaments at 85,000X magnification showing a ladder-like assembly involving association of the heads.

c) Lower magnification view (35,000X) of the ladder-like structure of the brain myosin filaments.

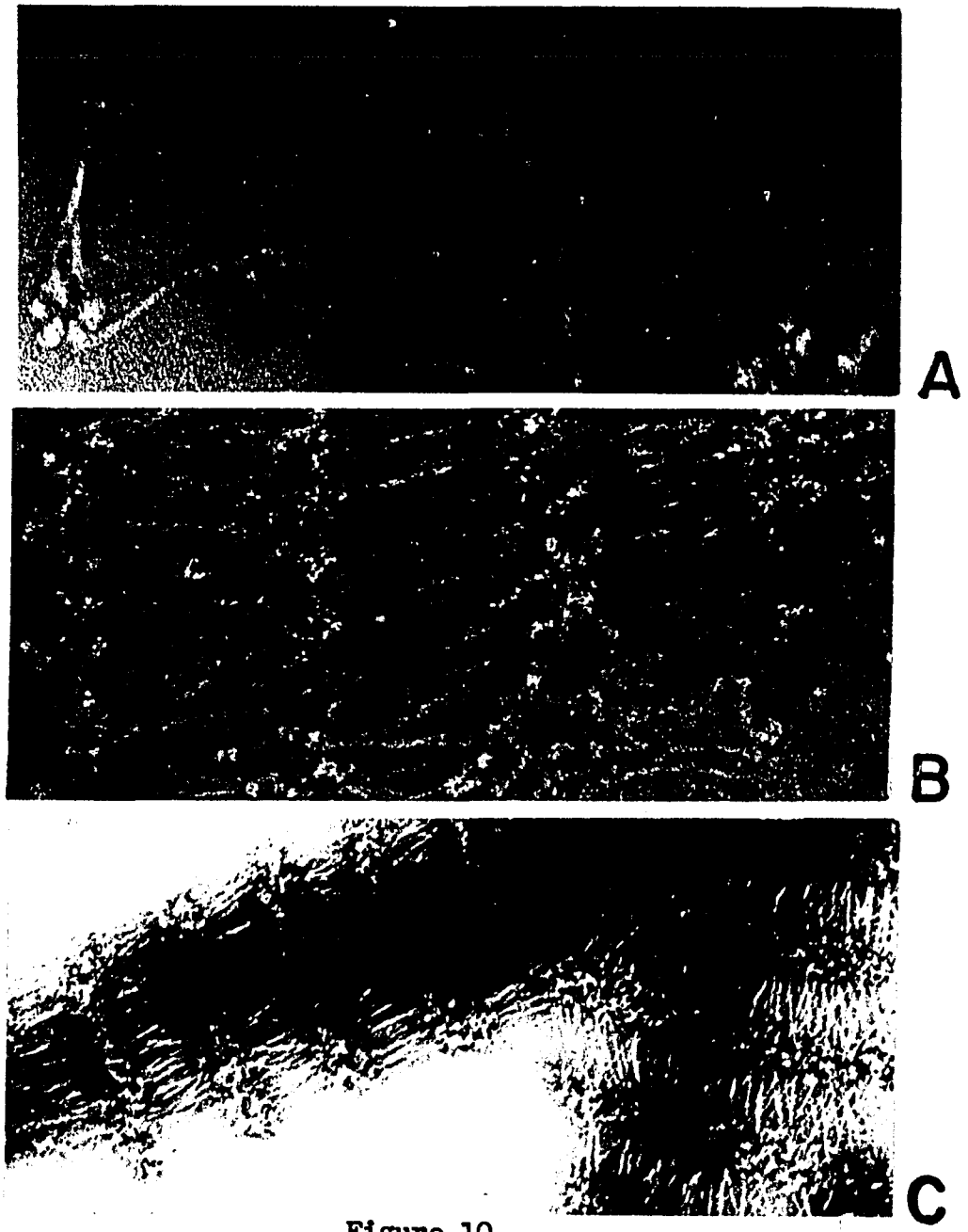

Figure 10

Figure 11:

High magnification view (160,000X) of brain myosin, showing more closely the head to head associations of the dumbell shaped filaments producing a ladder-like assembly.

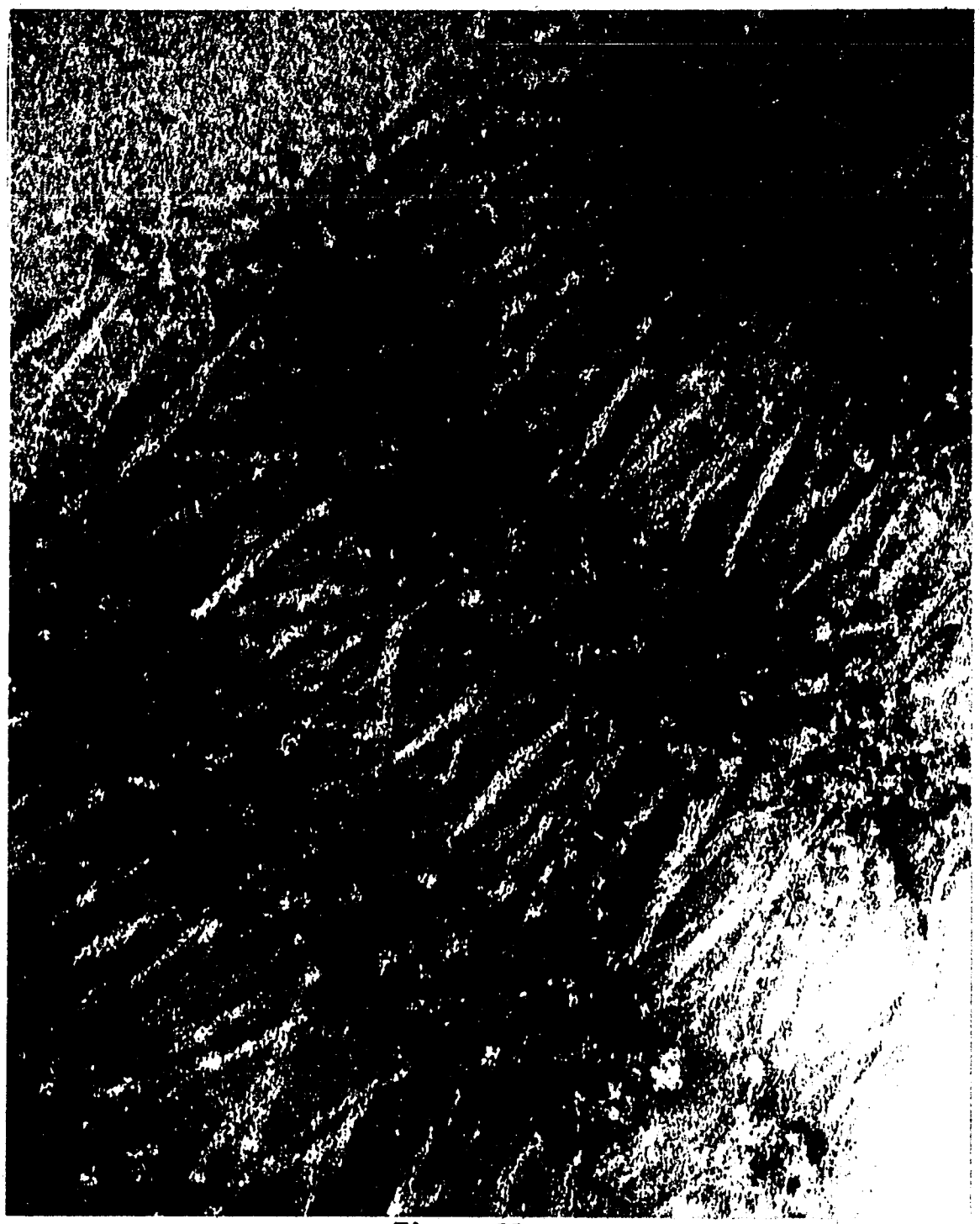

Figure 11

Figure 12:

Electron micrograph of rabbit skeletal muscle myosin filaments.

a) Skeletal muscle filaments at 85,000X magnification, showing the apx. 1.230 μ long cigar-shaped tapered filament.

b) Lower magnification view (24,750X) of the cigar-shaped structure of the skeletal muscle myosin filaments.

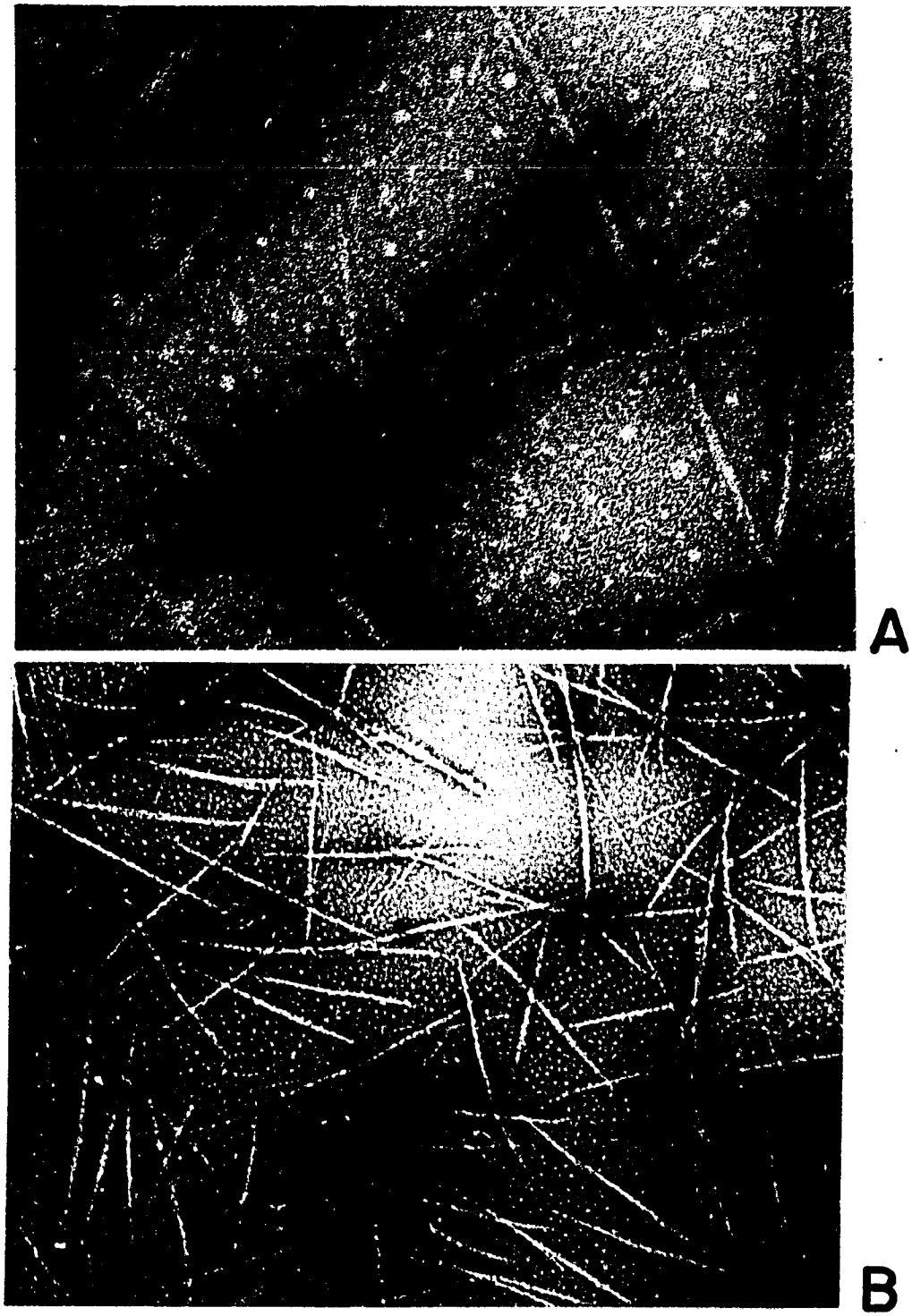

Figure 12

Figure 13:

Electron micrographs of chicken gizzard smooth muscle myosin filaments.

a) Smooth muscle myosin filament at 85,000X magnification, showing a periodicity of apx. 140 Å (arrows).

b) Lower magnification (20,500X) of smooth muscle myosin filament showing a branching point.

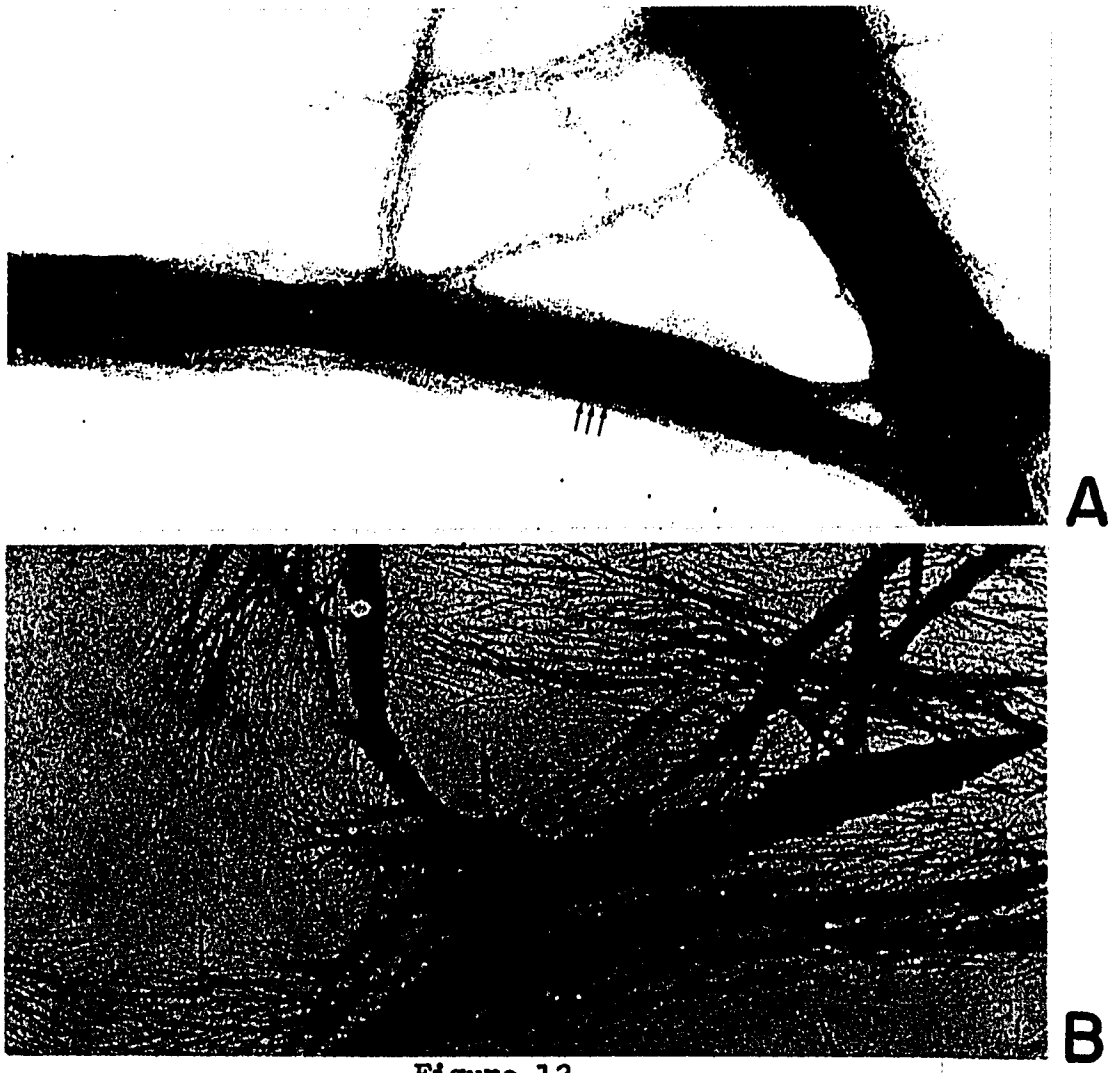

Figure 13

Figure 14:

Electron micrographs of light meromyosins.

a) Brain LMM at 85,000X magnification, showing short filamentous structures of somewhat indefinite length with frayed ends.

b) Smooth muscle LMM at 85,000X magnification with an appearance similar to that of the brain LMM.

c) Skeletal muscle LMM at 85,000X magnification, showing a periodicity of apx. 430 Å.

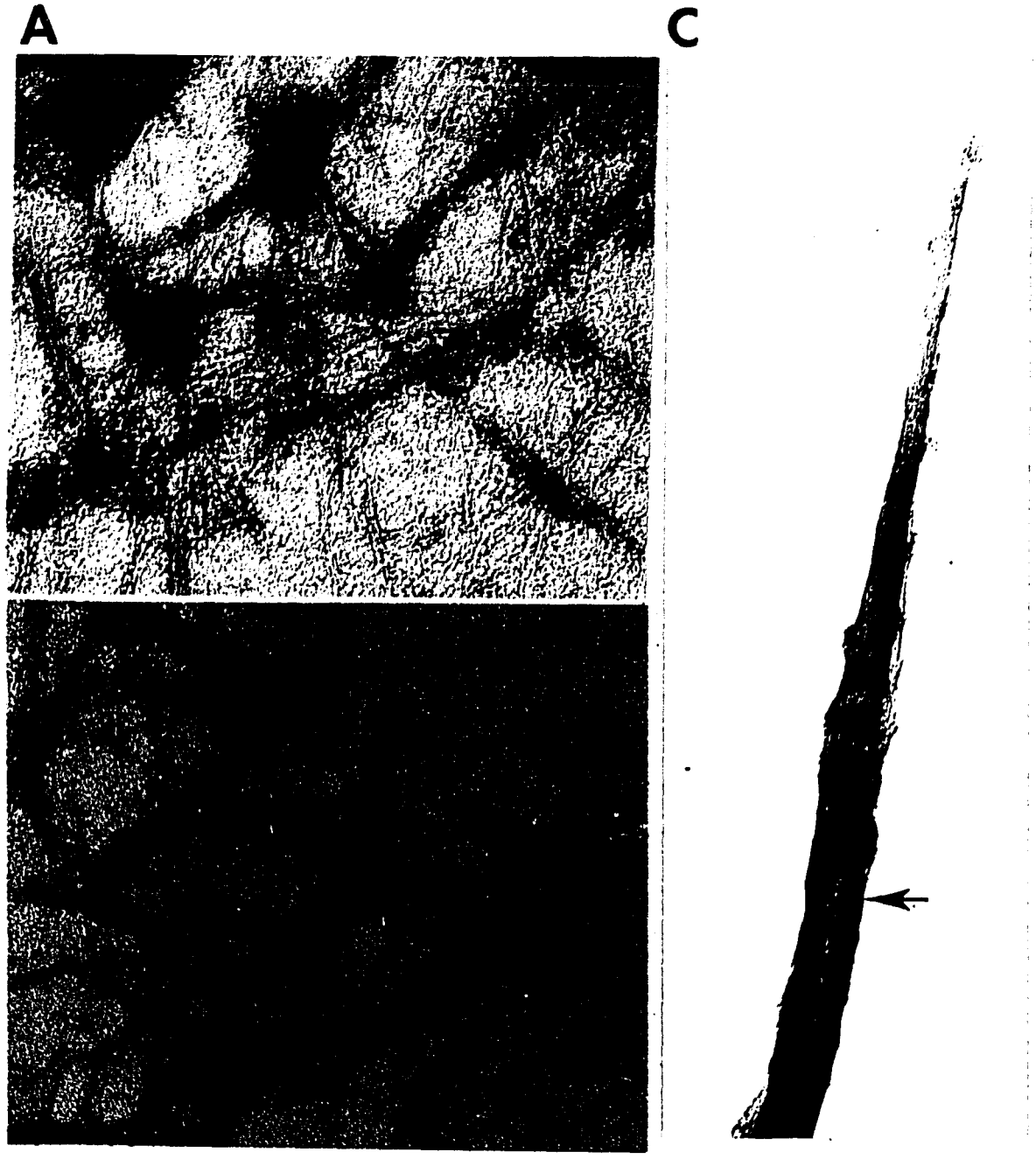

Figure 14

Figure 15:

Electron micrographs of brain, skeletal muscle and smooth muscle actins.

a) Polymerized brain actin at 85,000X magnification showing beaded appearance.

b) Polymerized skeletal muscle actin at 85,000X magnification showing beaded appearance.

c) Polymerized smooth muscle actin at 85,000X magnification showing beaded appearance.

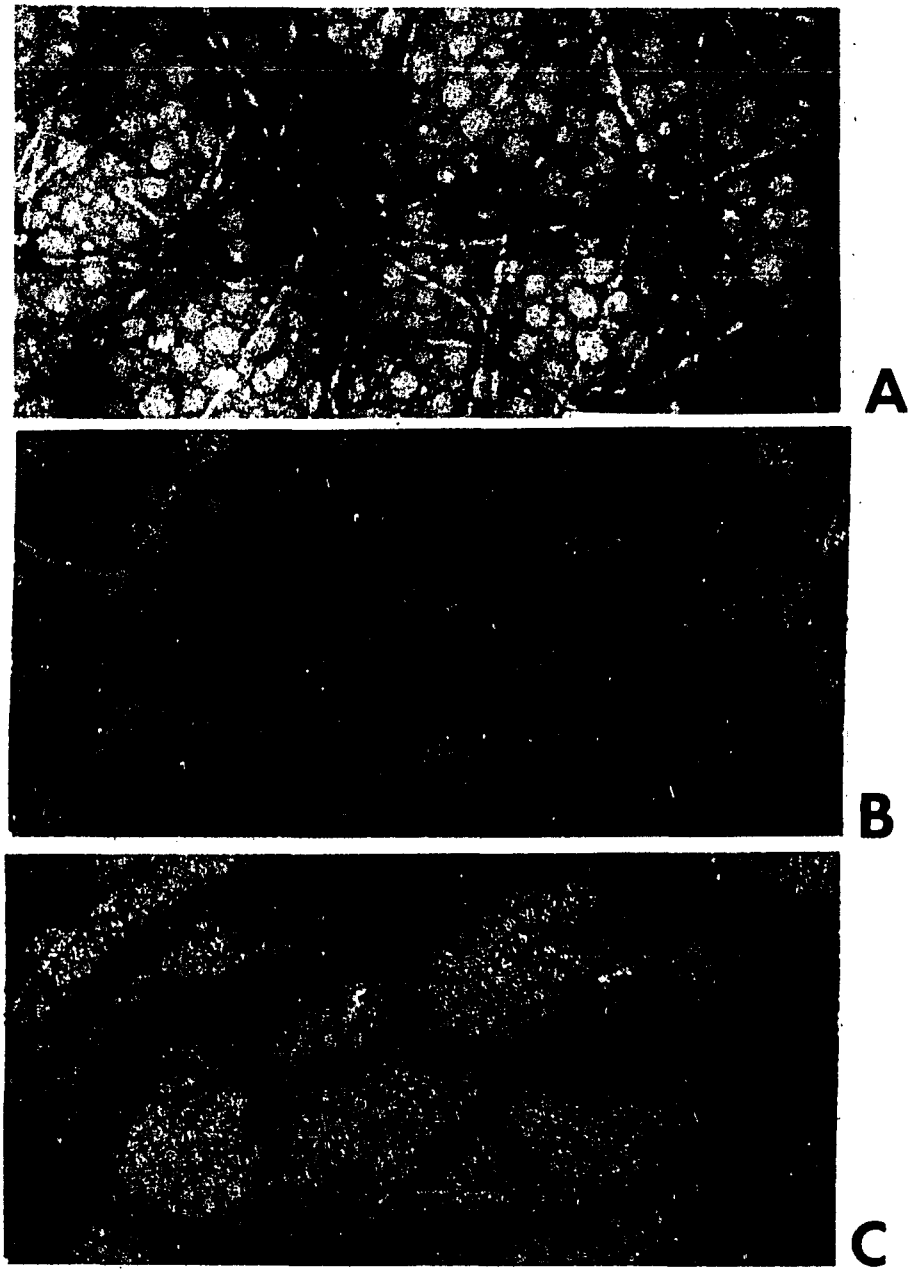

Figure 15

Figure 16:

Electron micrographs of brain HMM decorating actin filaments in the presence and absence of ATP.

a) Brain HMM decorating brain actin filaments at 85,000X magnification showing a 388 ± 31 Å periodicity of attachment. Small arrows mark arrowhead period, long arrow marks direction of arrowhead attachment.

b) Brain HMM decorating skeletal muscle actin filaments at 85,000X magnification showing a 387 ± 23 Å periodicity of attachment.

c) Brain HMM decorating smooth muscle actin filaments at 85,000X magnification showing a 436 ± 83 Å periodicity of attachment.

d) Brain HMM-brain actin complex dissociated by addition of 1mM ATP. Magnification 85,000X.

e) Brain HMM skeletal muscle actin complex dissociated by addition of 1mM ATP. Magnification 85,000X.

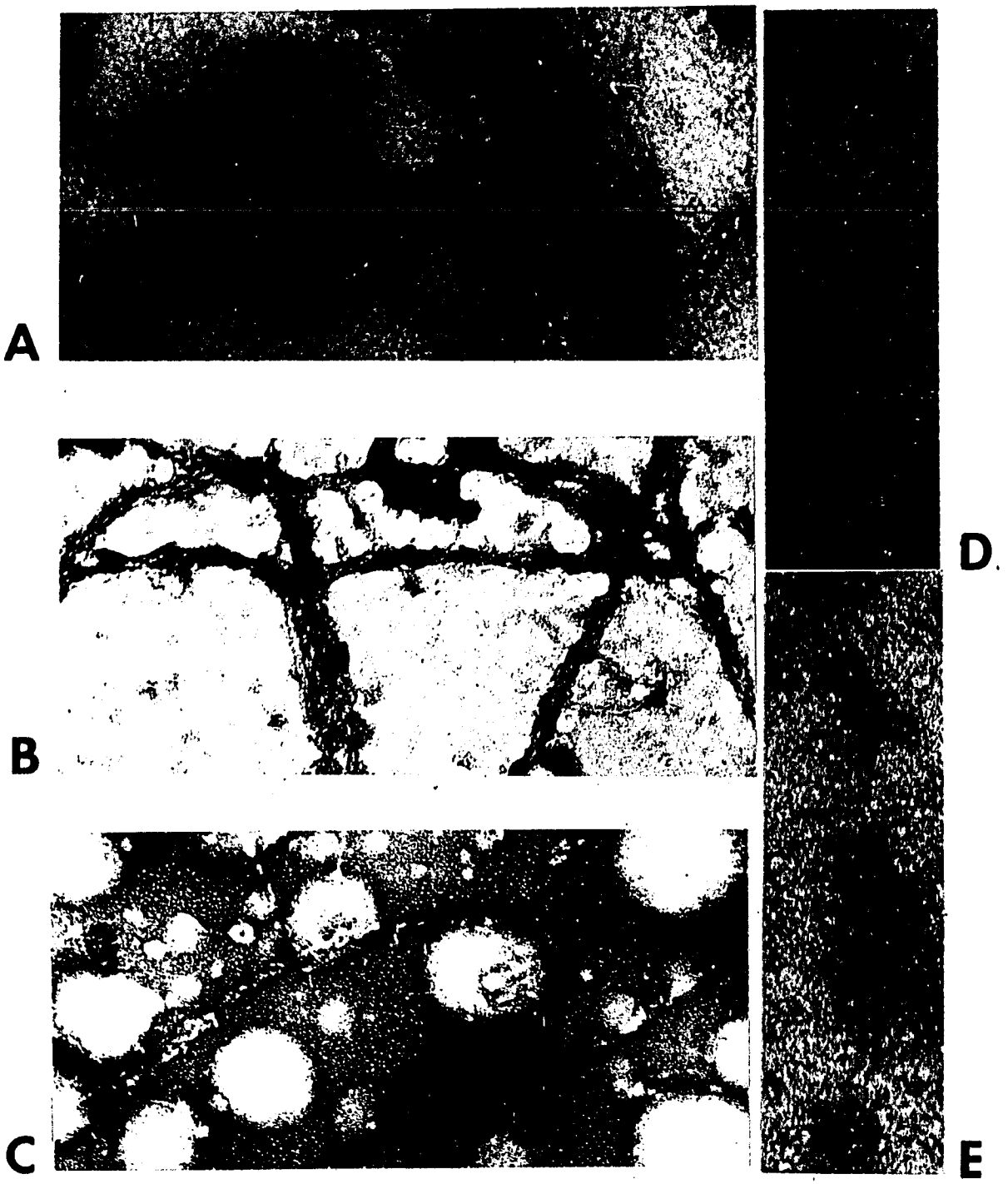

Figure 16

Figure 17:

Electron micrographs of skeletal muscle HMM decorating actin filaments.

a) Skeletal muscle HMM decorating brain actin filaments at 85,000X magnification showing a 398 ± 12 Å periodicity of attachment.

b) Skeletal muscle HMM decorating skeletal muscle actin filaments at 85,000X magnification showing a 398 ± 31 Å periodicity of attachment.

c) Skeletal muscle HMM decorating smooth muscle actin filaments at 85,000X magnification showing a 376 ± 29 Å periodicity of attachment.

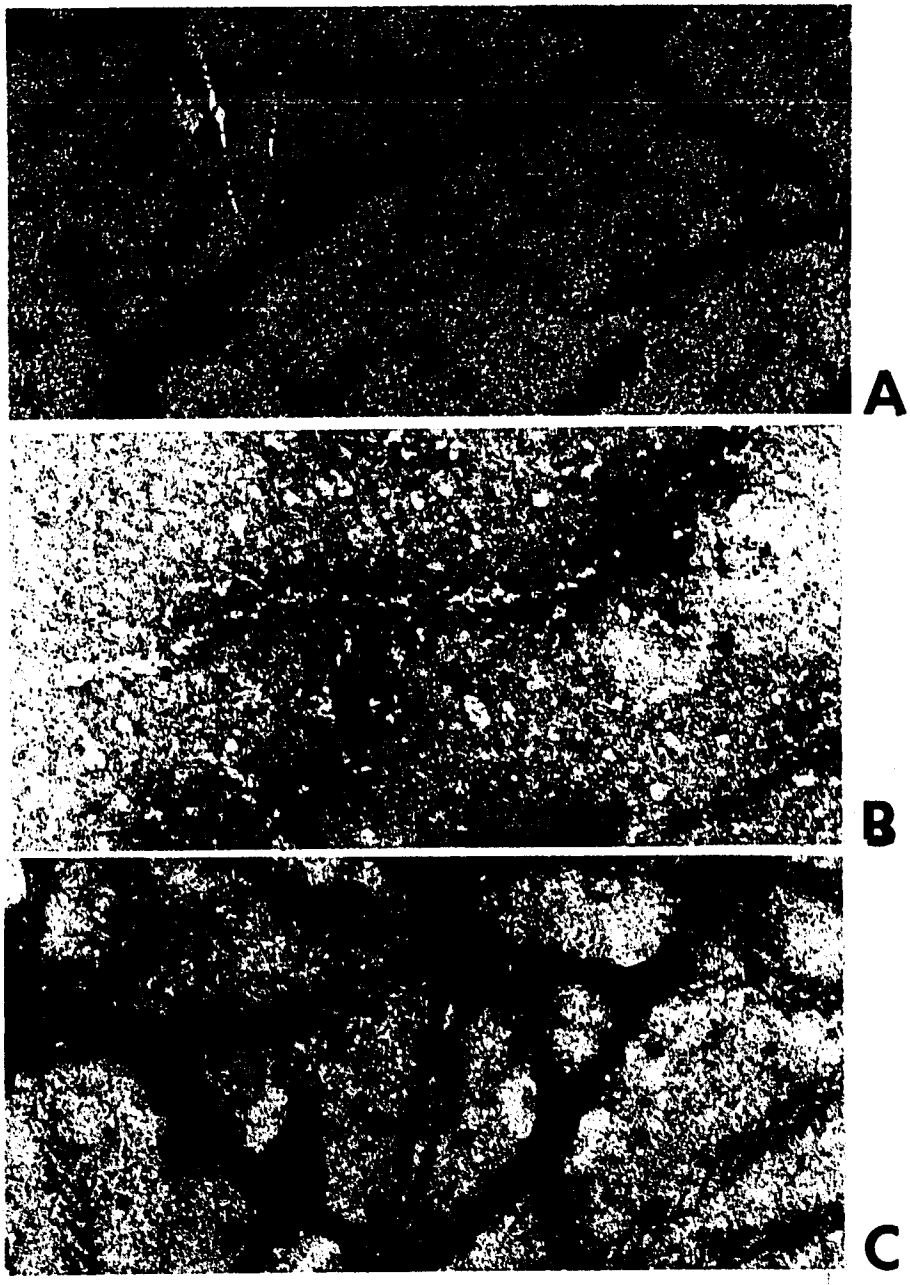

Figure 17

Figure 18:

Electron micrographs of smooth muscle HMM decorating actin filaments.

a) Smooth muscle HMM decorating brain actin filaments at 85,000X magnification showing a 358 ± 22 Å periodicity of attachment.

b) Smooth muscle HMM decorating skeletal muscle actin filaments at 85,000X magnification showing a 372 ± 29 Å periodicity of attachment.

c) Smooth muscle HMM decorating smooth muscle actin filaments at 85,000X magnification showing a 376 ± 29 Å periodicity of attachment.

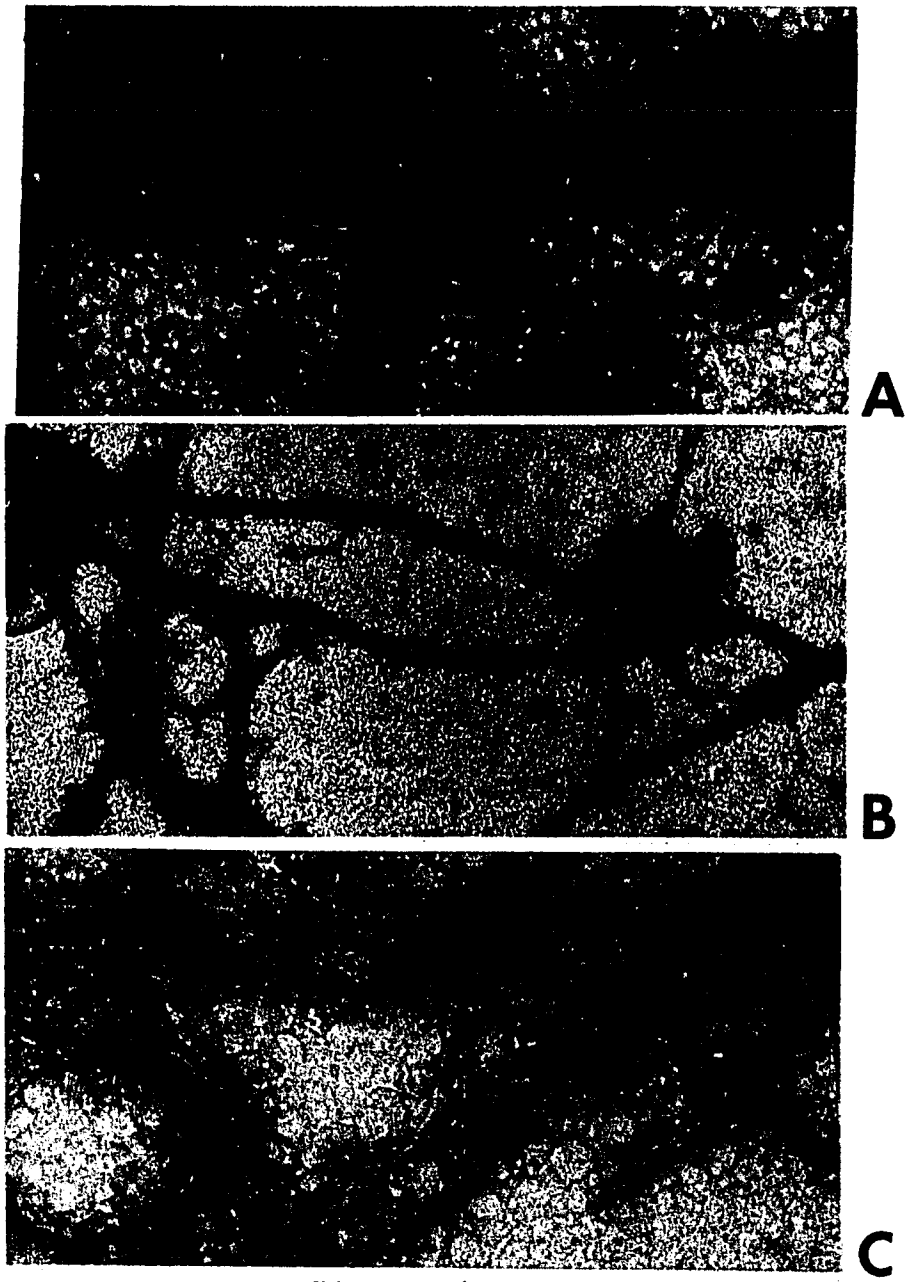

Figure 18

Figure 19:

Time course curves for skeletal muscle myosin Ca^{2+}-ATPase at pH 5.5 (▲-▲) and 9.0 (x-x). The y axis represents micromoles of inorganic phosphorus liberated from ATP per mg of protein and the x axis stands for time in minutes. The plot of Ca^{2+}-ATPase of skeletal muscle myosin at pH 5.5 over a period of 20 minutes incubation time has a linear correlation coefficient value (r^2) of 0.997 and at pH 9.0 an r^2 of 0.998.

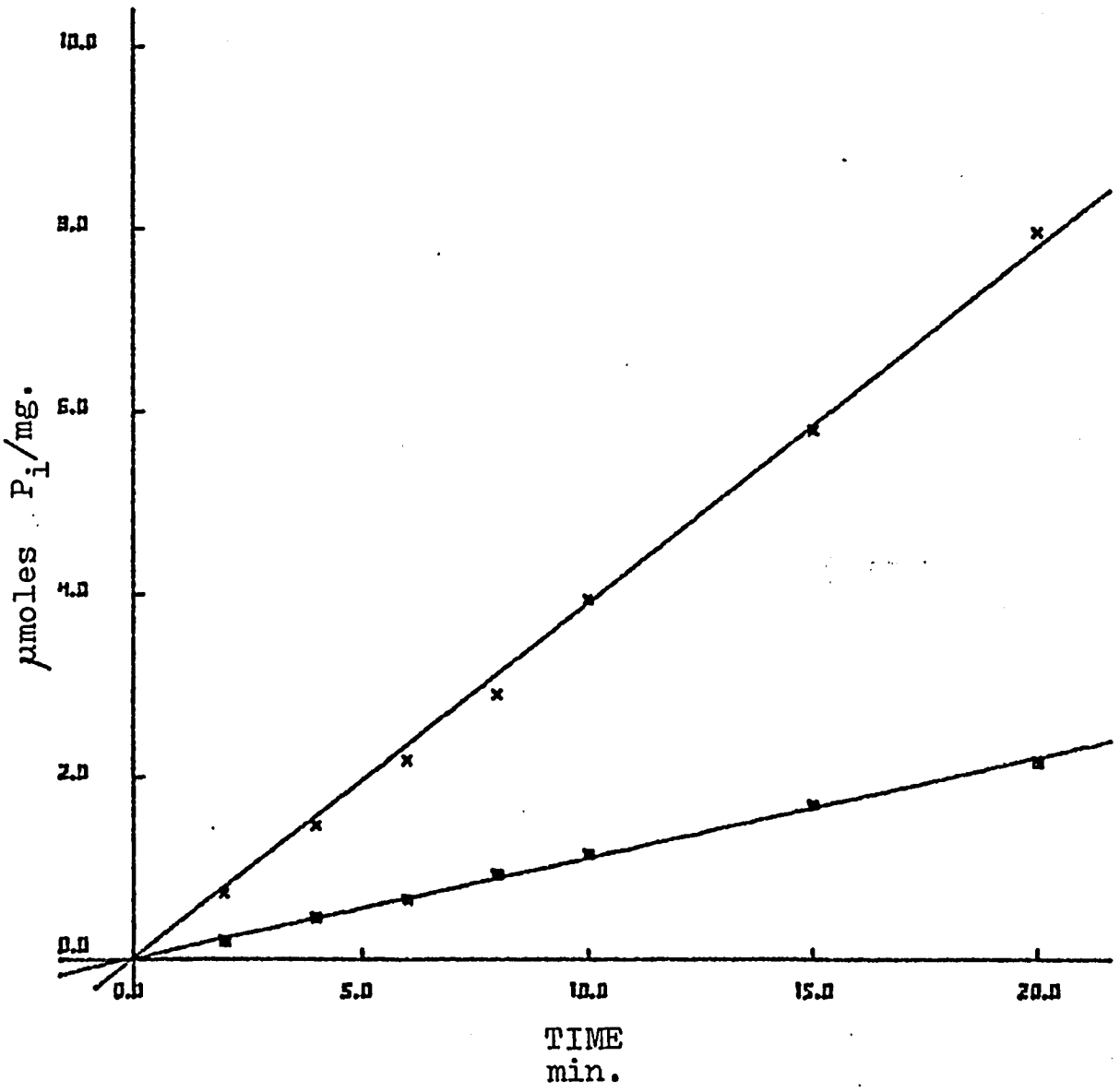

FIGURE 19

Figure 20:

Time course curves for skeletal muscle myosin K^+-EDTA-ATPase at pH 6.5 (■-■) and 9.0 (x-x). The K^+-EDTA-ATPase of skeletal muscle myosin at pH 6.5 over a period of 20 minutes incubation has an r^2 of 0.998 and at pH 9.0 an r^2 of 0.996.

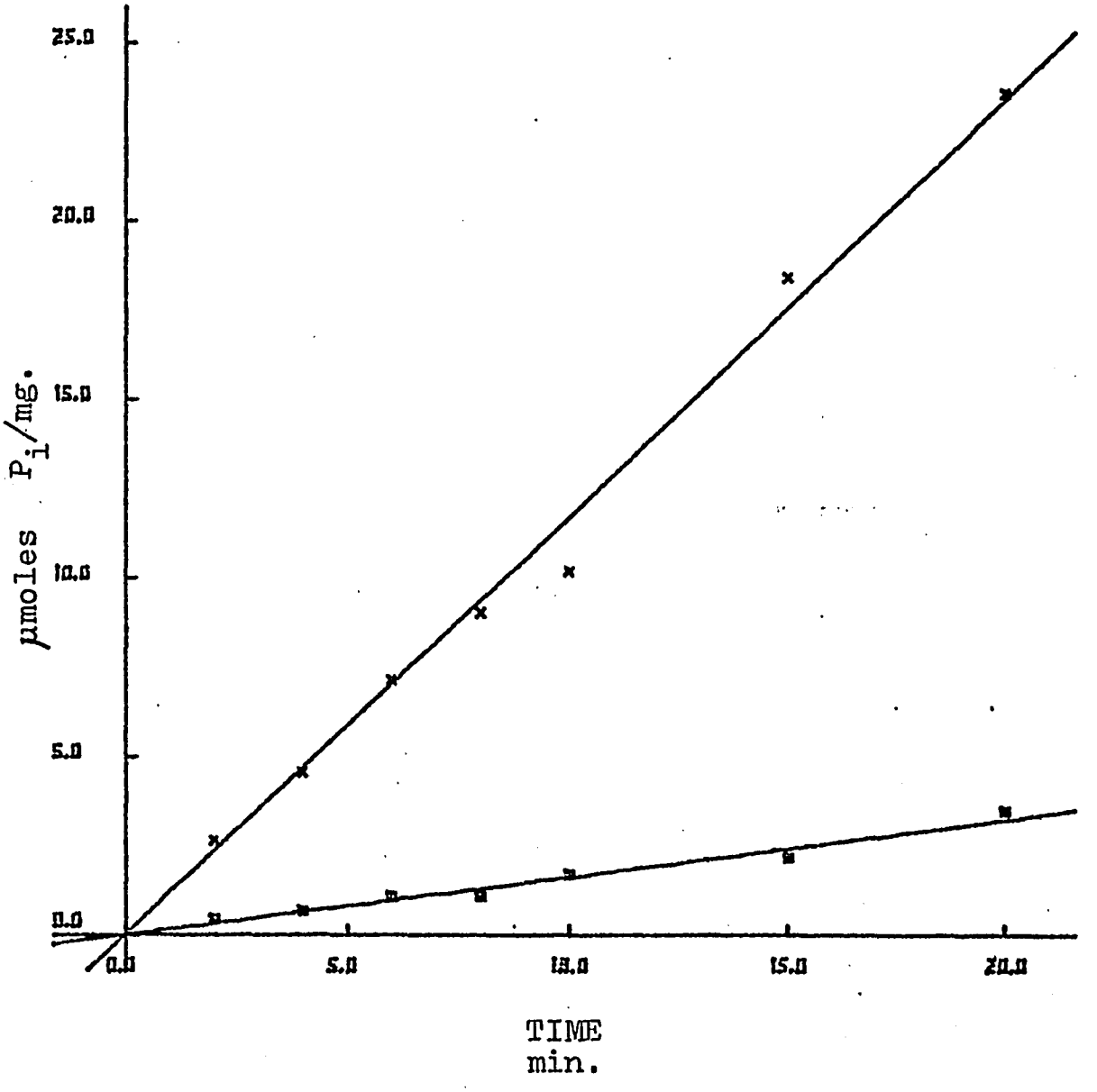

FIGURE 20

Figure 21:

Enzyme concentration curve of skeletal muscle myosin Ca^{2+} and K^{+}-EDTA-ATPase at pH 7.0. The y axis represents micromoles of inorganic phosphorus liberated from ATP per ml of incubation medium, and the x axis stands for micrograms of protein assayed. For the different concentrations of skeletal muscle myosin incubated in the presence of Ca^{2+} there is an r^2 of 0.998 and in the presence of K^{+}-EDTA there is an r^2 of 0.995. Ca^{2+}-ATPase is represented by ▫-▫ and K^{+}-EDTA-ATPase by x-x.

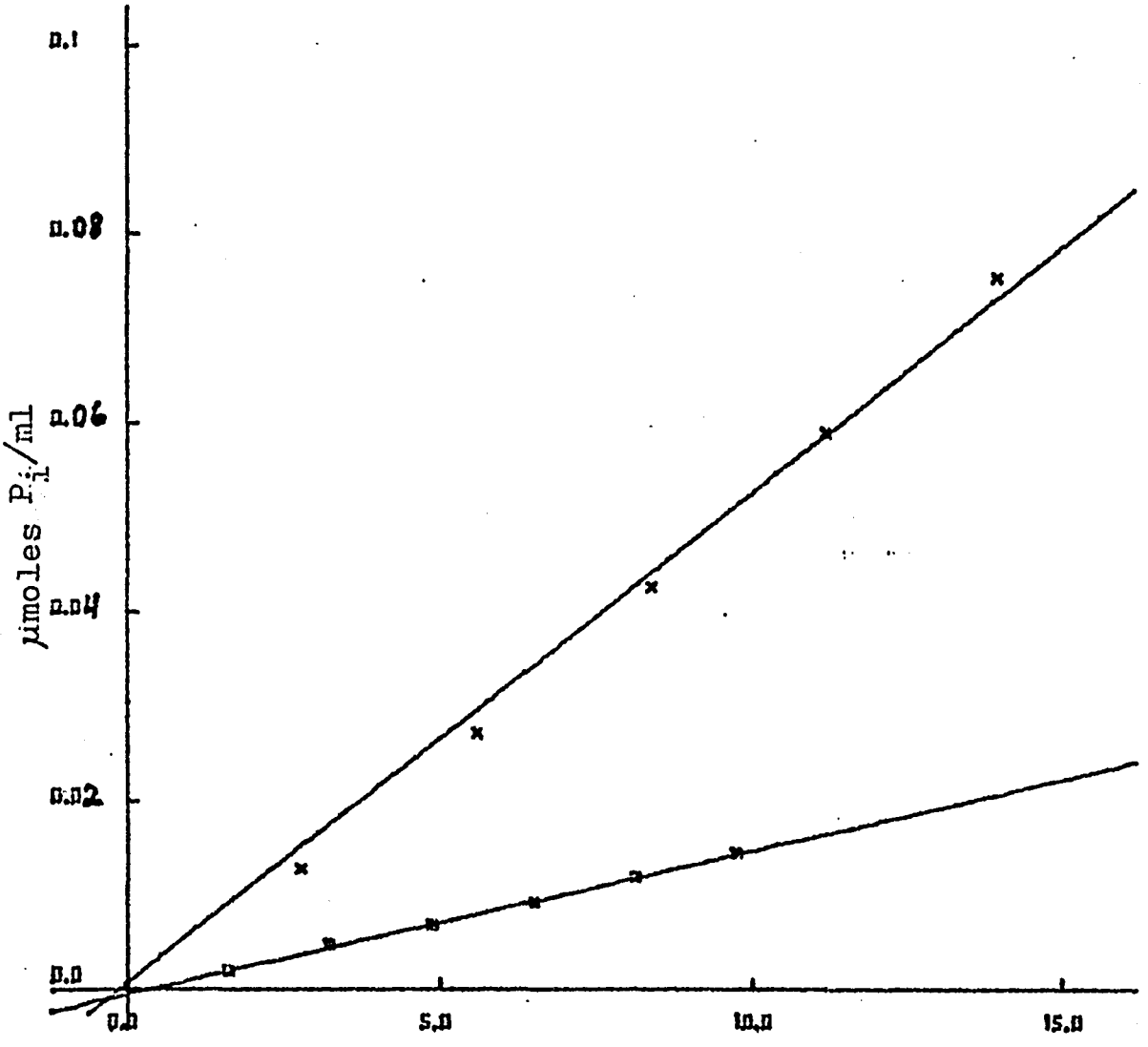

FIGURE 21

Figure 22:

Time course curves for brain myosin K^+-EDTA-ATPase at pH 6.5 (⊡-⊡) and 9.0 (x-x). The y axis represents micromoles of inorganic phosphorus liberated from ATP per mg of protein and the x axis stands for time in minutes. The plot of K^+-EDTA-ATPase of brain myosin at pH 6.5 over a period of 60 minutes has an r^2 of 0.974 and at pH 9.0 an r^2 of 0.992.

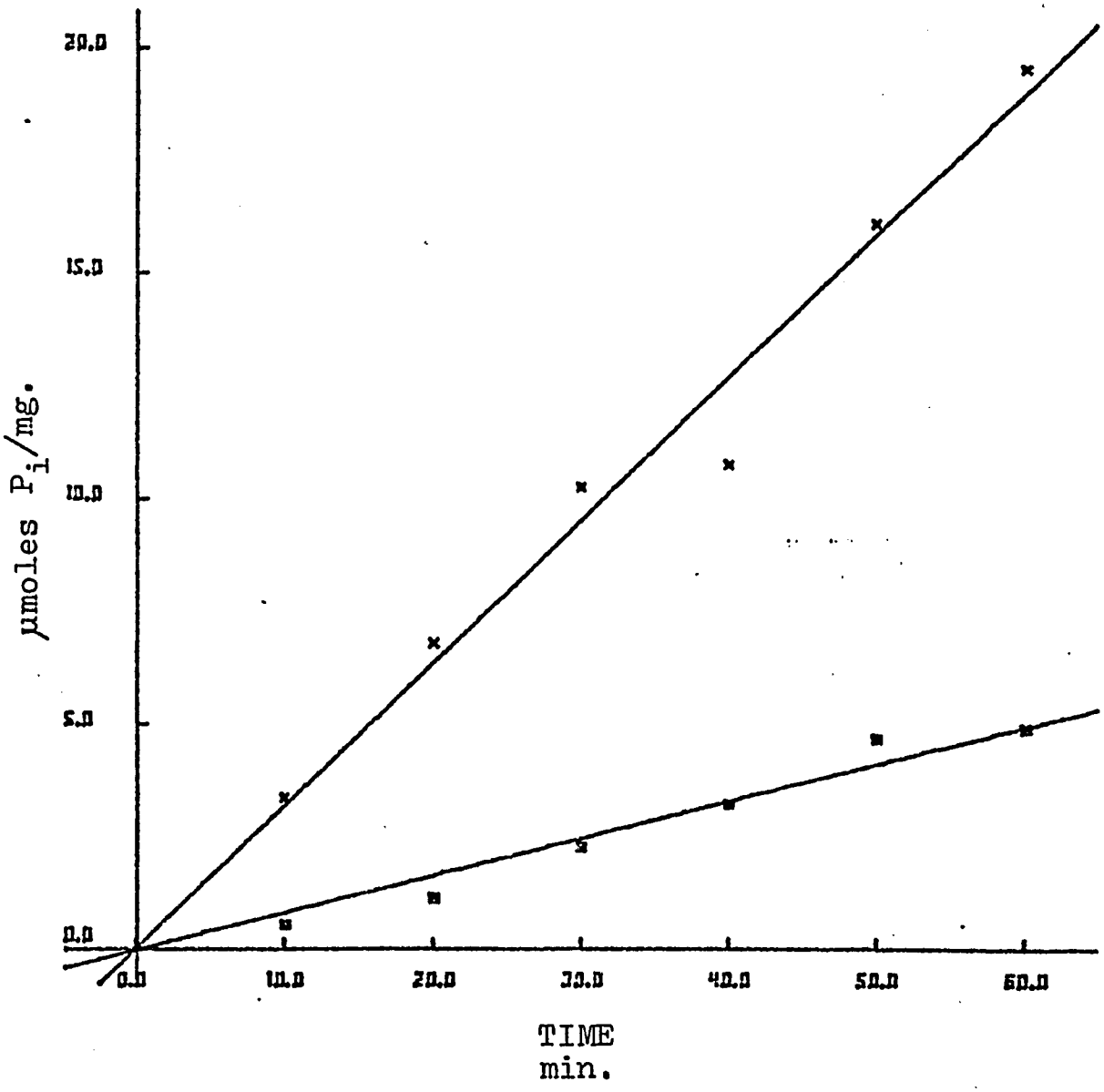
20.0
15.0
10.0
5.0
0.0
µmoles P_i/mg.
0.0
10.0
20.0
30.0
40.0
50.0
60.0
TIME
min.

FIGURE 22

Figure 23:

Enzyme concentration curve of brain myosin K^+-EDTA-ATPase at pH 7.0. The y axis represents micromoles of inorganic phosphorus liberated from ATP per ml of incubation medium and the x axis stands for micrograms of protein assayed. For the different concentrations of brain myosin incubated in the presence of K^+ and EDTA, there is an r^2 of 0.989.

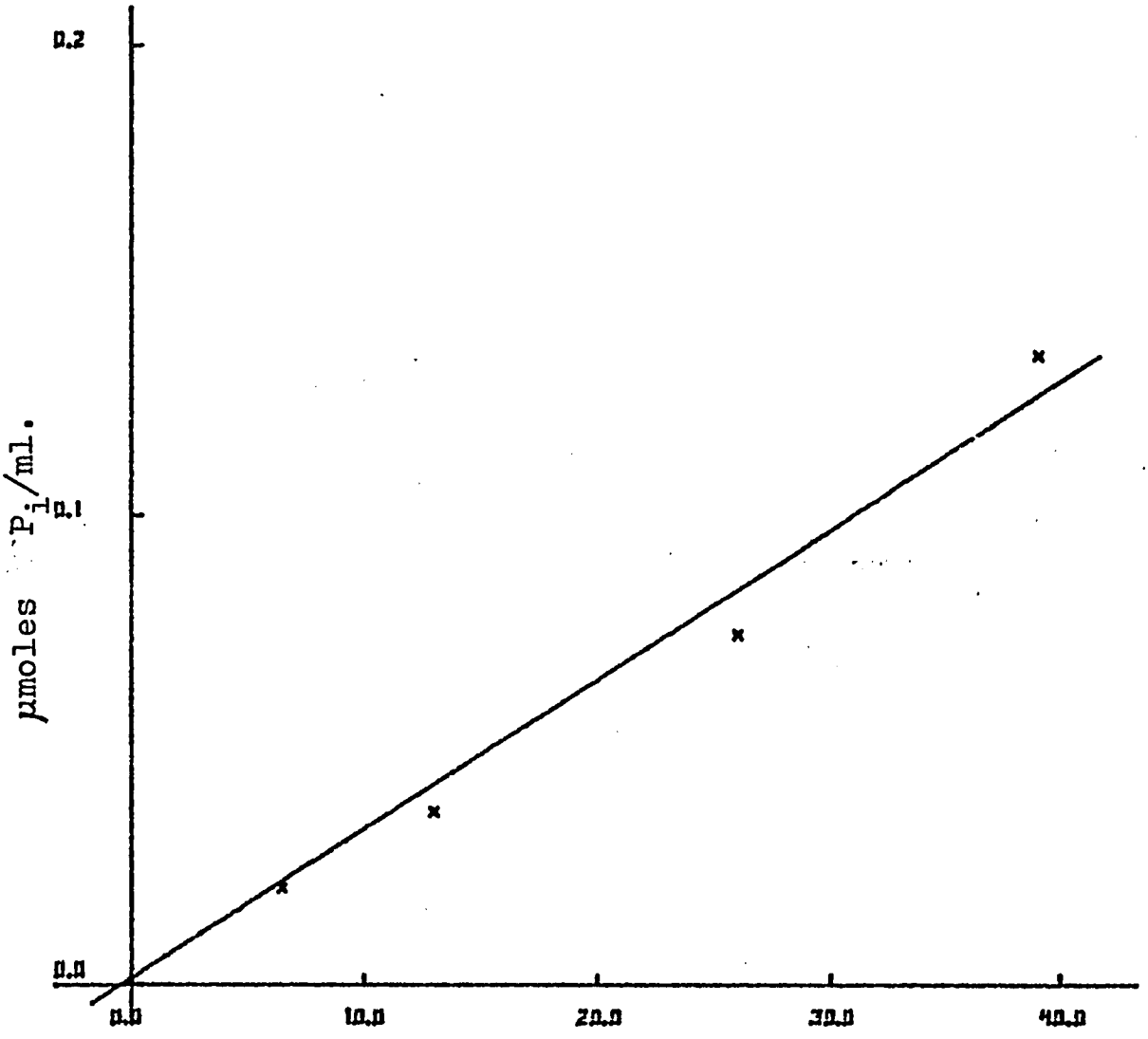

FIGURE 23

Figure 24:

Substrate saturation curves for skeletal muscle myosin Ca^{2+}-ATPase, at different pH values. The y axis represents the specific activity measured as μ moles $P_i \cdot mg^{-1} \cdot min^{-1}$, and the x axis represents the corresponding concentrations of ATP substrate in millimoles.

+ pH 6.0, x pH 6.5, X pH 7.0, ▪ pH 7.5, ◇ pH 8.0, ⊕ pH 8.5, ⊗ pH 9.0.

Figure 25:

Substrate saturation curves for skeletal muscle myosin K^+-EDTA-ATPase at different pH values.

x pH 6.5, X pH 7.0, ▫ pH 7.5, ◇ pH 8.0, + pH 8.5, ⊗ pH 9.0.

Figure 26:

Substrate saturation curves for brain myosin Ca^{2+}-ATPase at different pH values.

+ pH 6.0, x pH 6.5, X pH 7.0, ▫ pH 7.5, ◇ pH 8.0, ⊕ pH 8.5, ⊗ pH 9.0.

Figure 27:

Substrate saturation curves for brain myosin K^+-EDTA-ATPase at different pH values.

x pH 6.5, X pH 7.0, ▪ pH 7.5, ◇ pH 8.0, + pH 8.5, ⊗ pH 9.0.

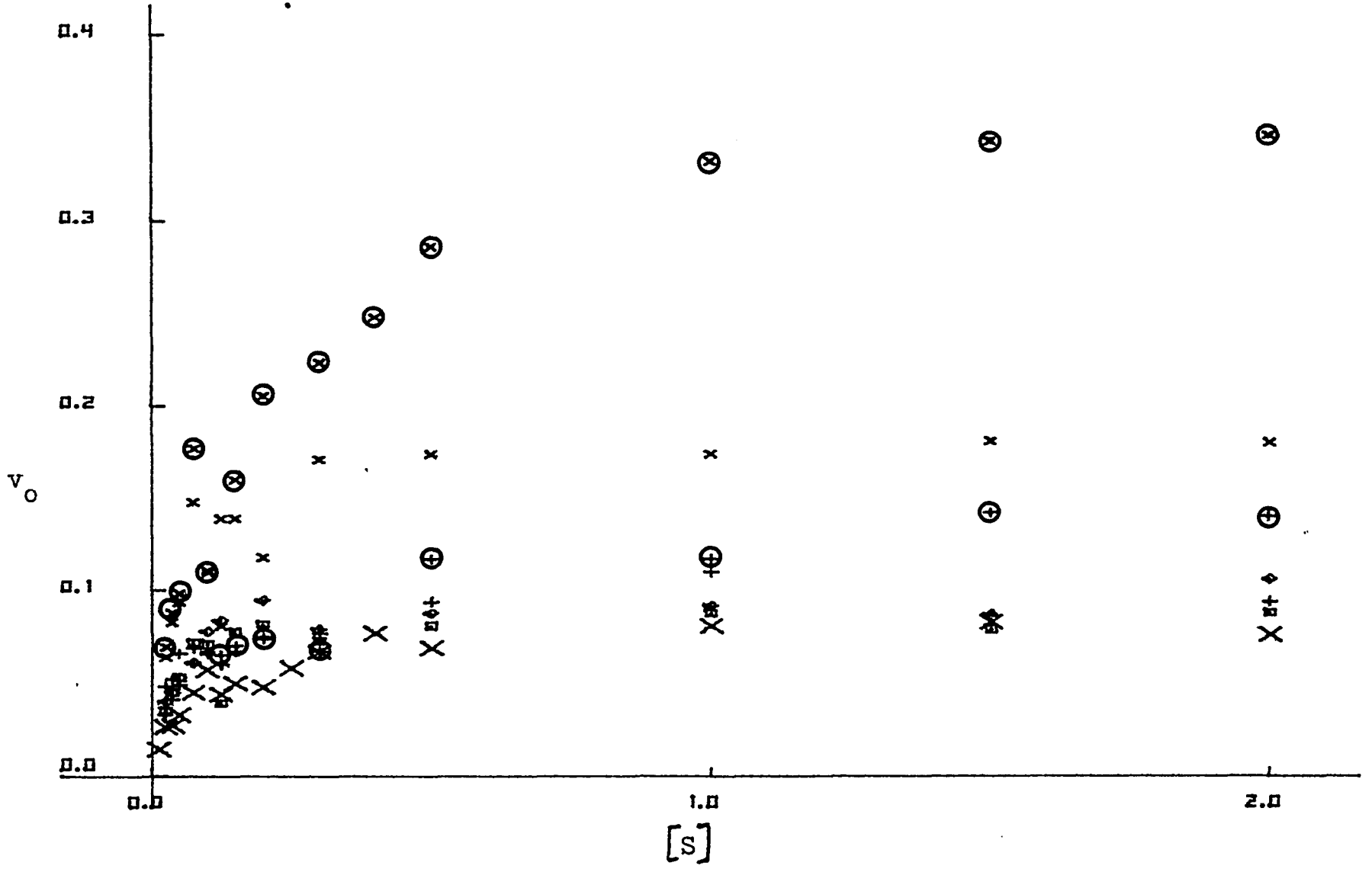

FIGURE 24

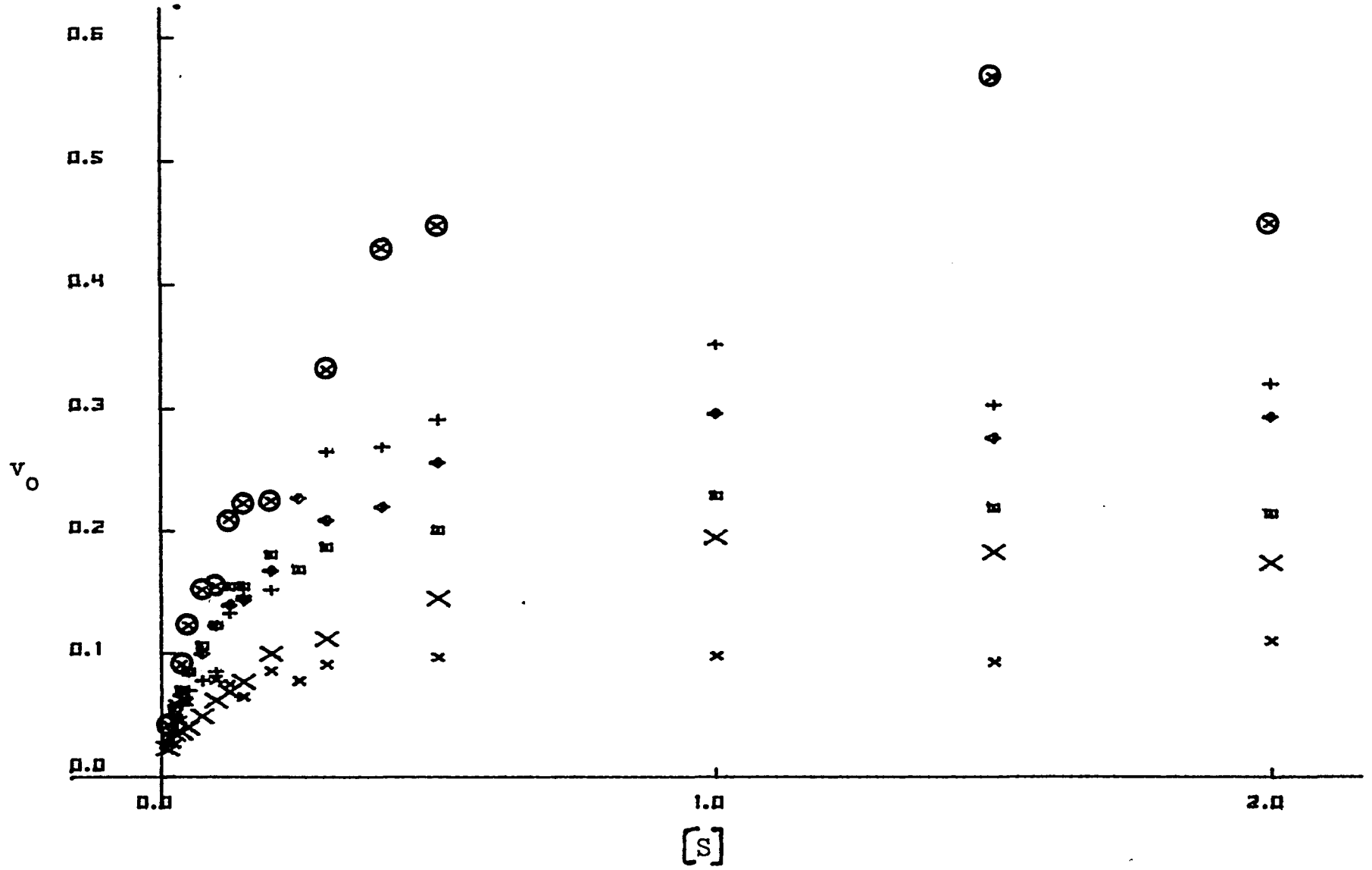

FIGURE 25

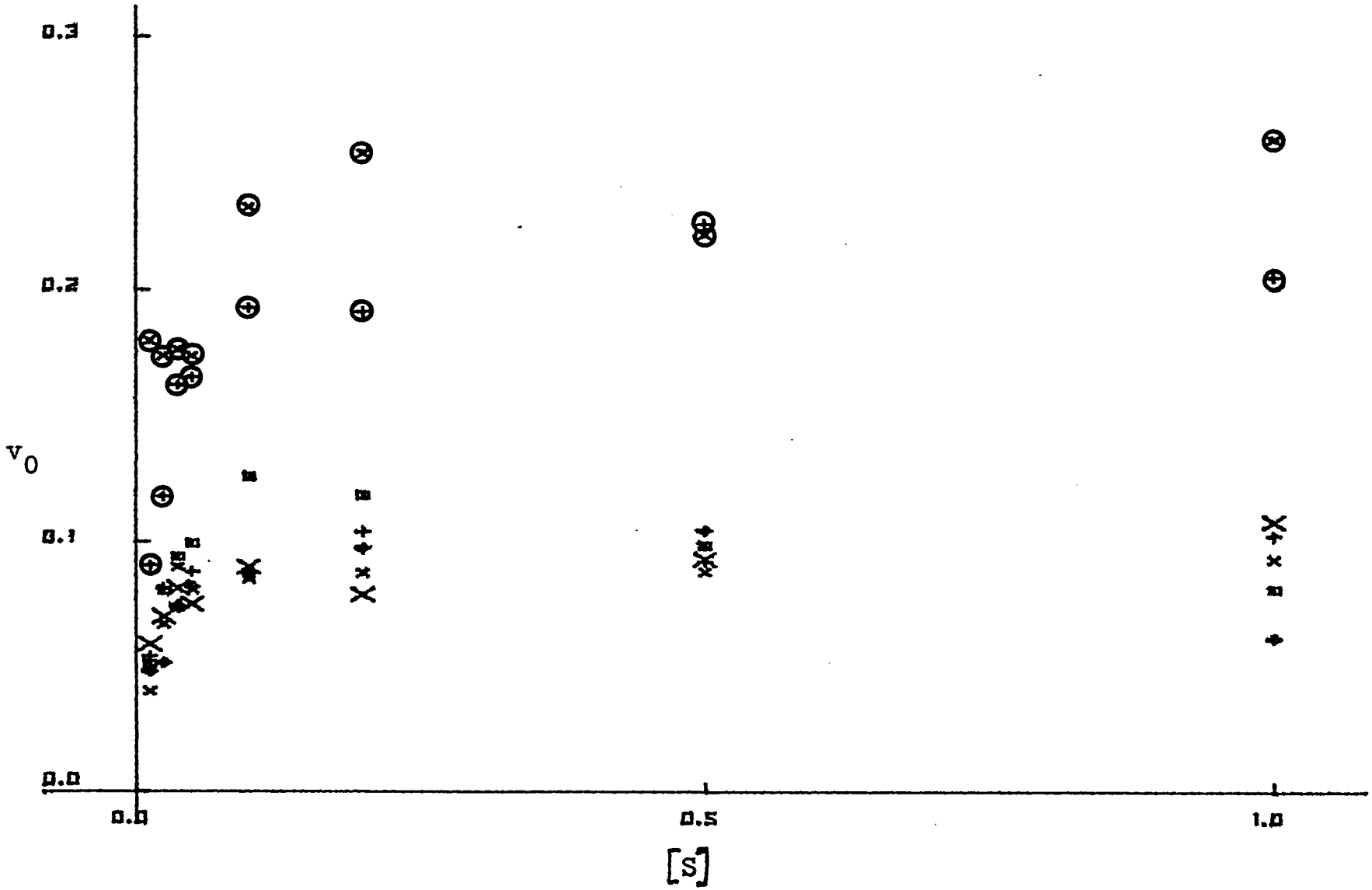

FIGURE 26

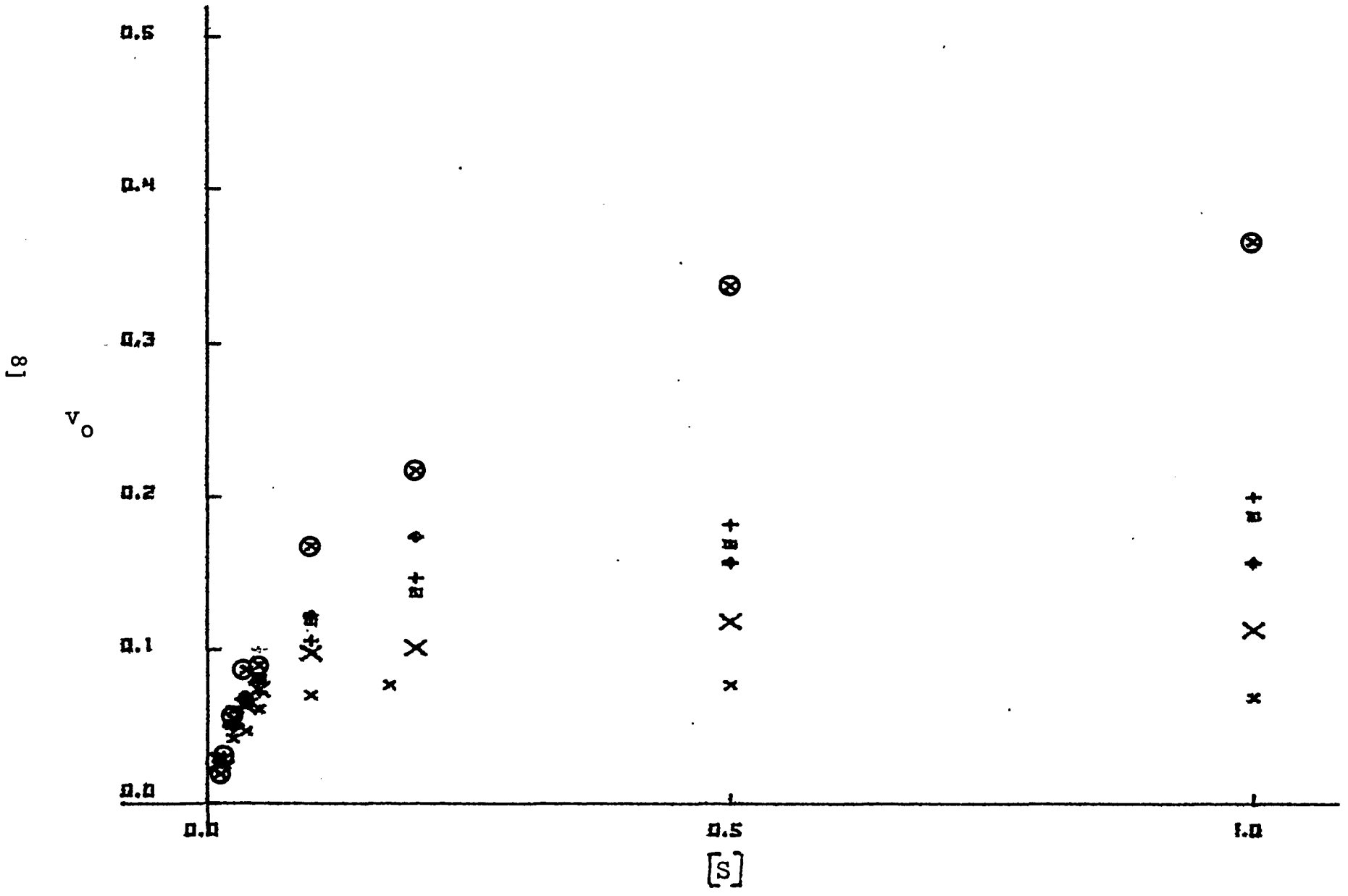

FIGURE 27

Figure 28:

Plot of Vmax versus pH for rabbit skeletal muscle myosin K^+-EDTA-ATPase. X axis represents pH range and y axis represents Vmax values calculated according to the Wilkinson (1961) method, and has the dimensions of micromoles of inorganic phosphorus liberated from ATP per mg of protein per minute of incubation. The middle point stands for the calculated value of Vmax and the points above and below it stand for the calculated error.

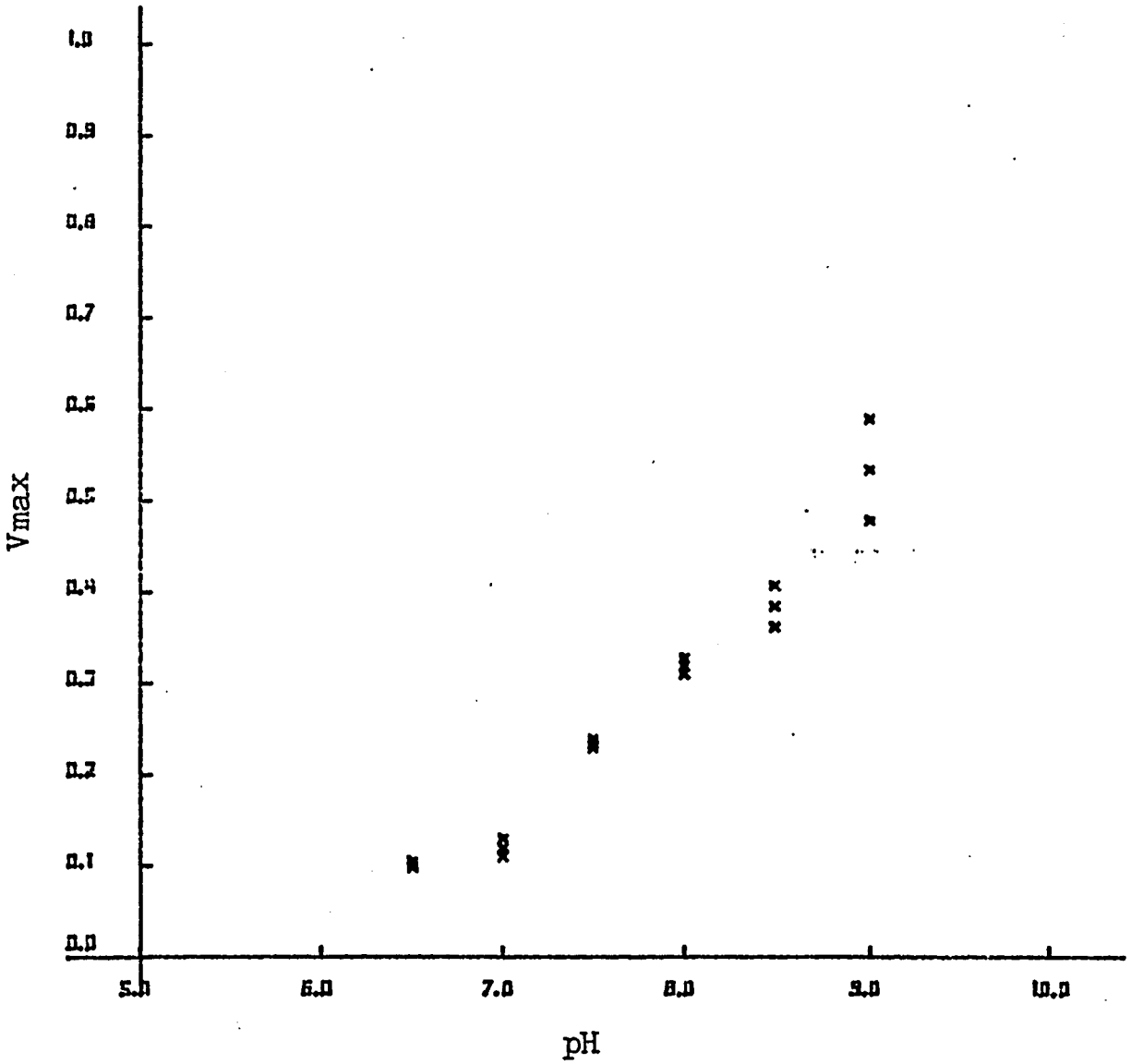

FIGURE 28

Figure 29:

Plot of Km versus pH for rabbit skeletal muscle myosin K^+-EDTA-ATPase. The x axis represents pH range and the y axis represents Km values calculated according to the Wilkinson (1961) method and has the dimensions of millimoles of ATP.

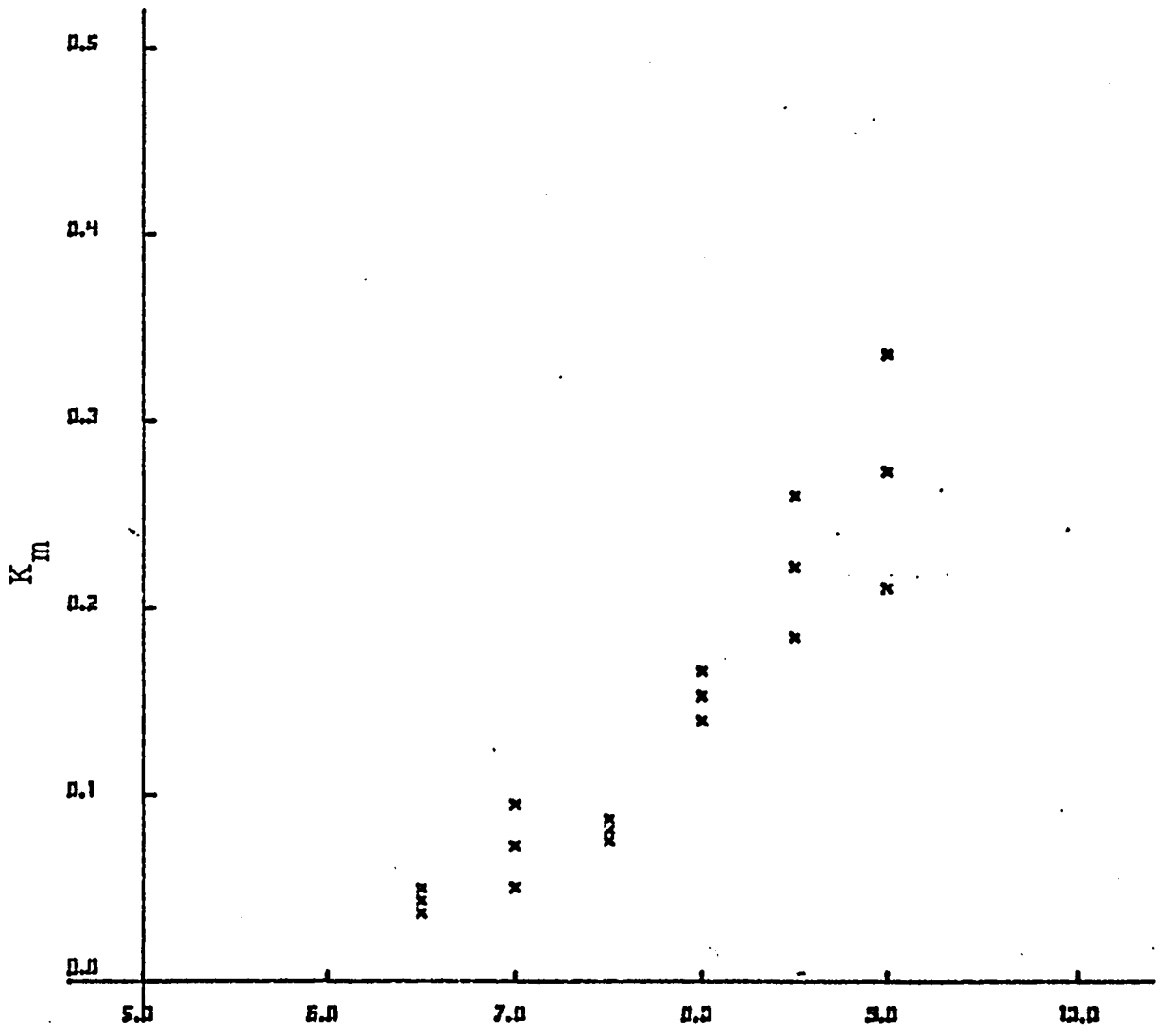

FIGURE 29

Figure 30:

Plot of pKm (-log Km) versus pH for rabbit skeletal muscle myosin K^+-EDTA-ATPase. The x axis represents pH range and the y axis represents the pKm values, with standard errors.

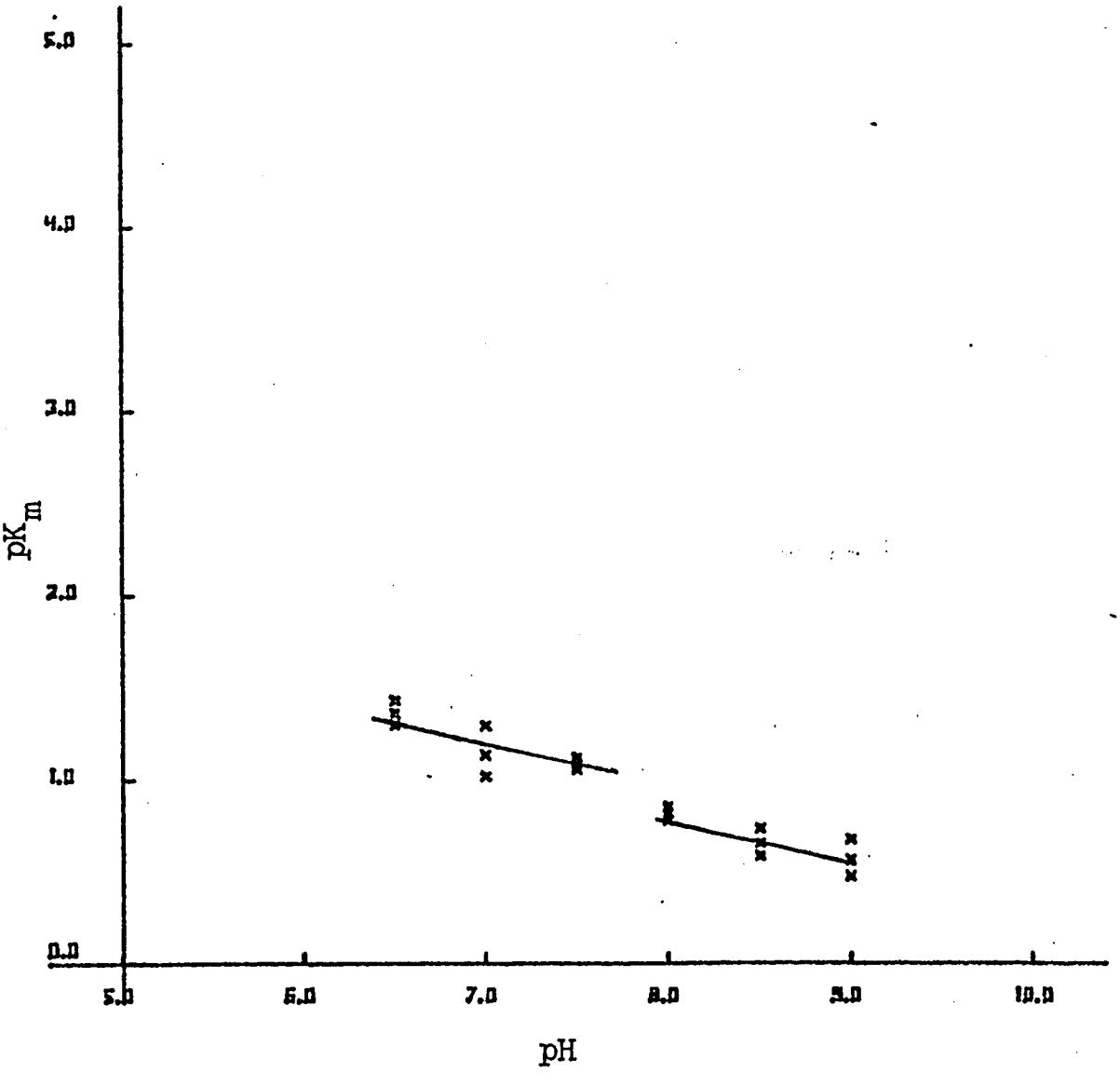

FIGURE 30

Figure 31:

Plot of Vmax versus pH for rabbit skeletal muscle myosin Ca^{2+}-ATPase. The x axis represents pH range and the y axis represents the calculated Vmax values with standard errors.

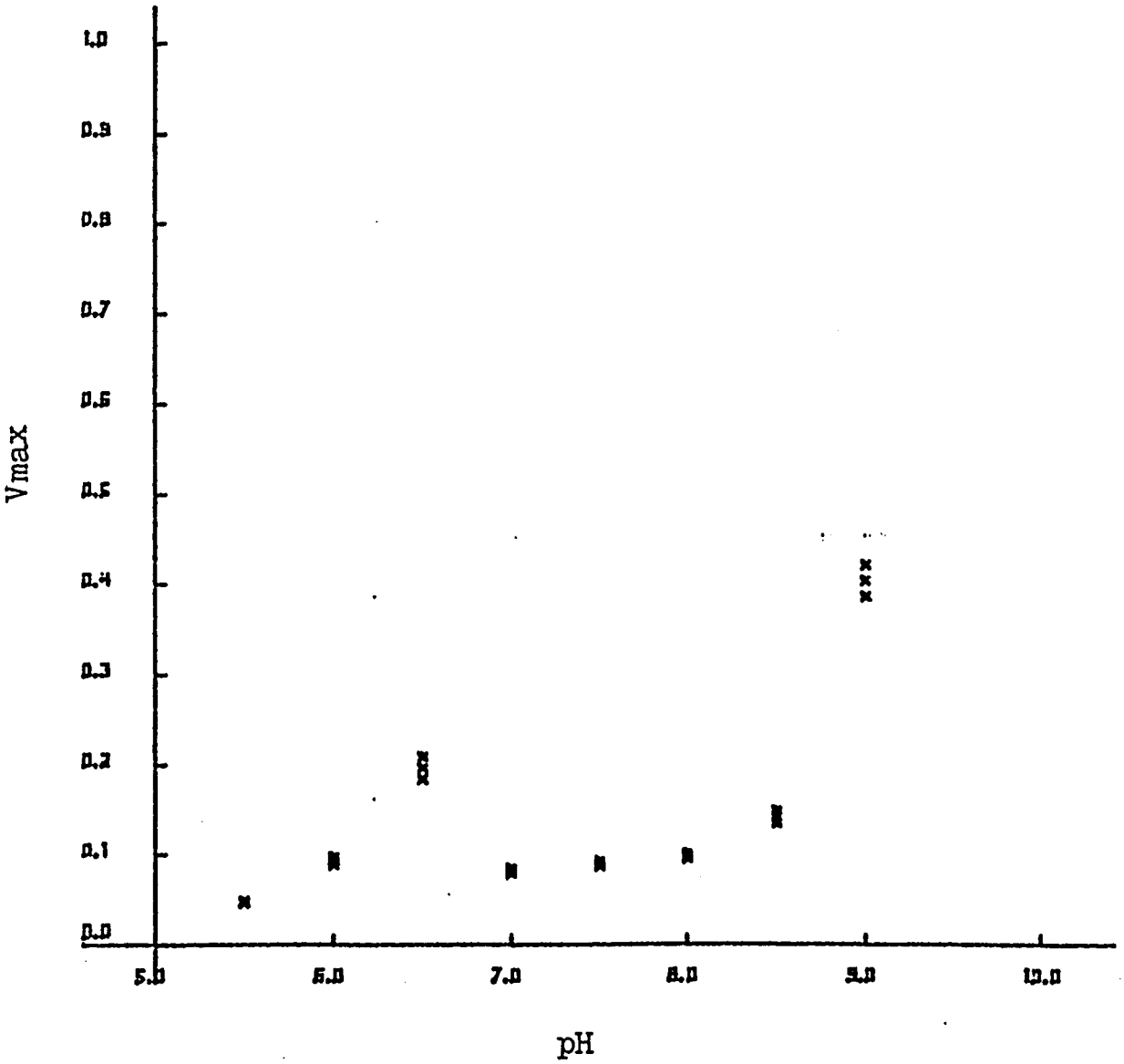

FIGURE 31

Figure 32:

Plot of Km versus pH for rabbit skeletal muscle myosin Ca^{2+}-ATPase. The x axis represents pH range and the y axis represents the calculated Km values with standard errors.

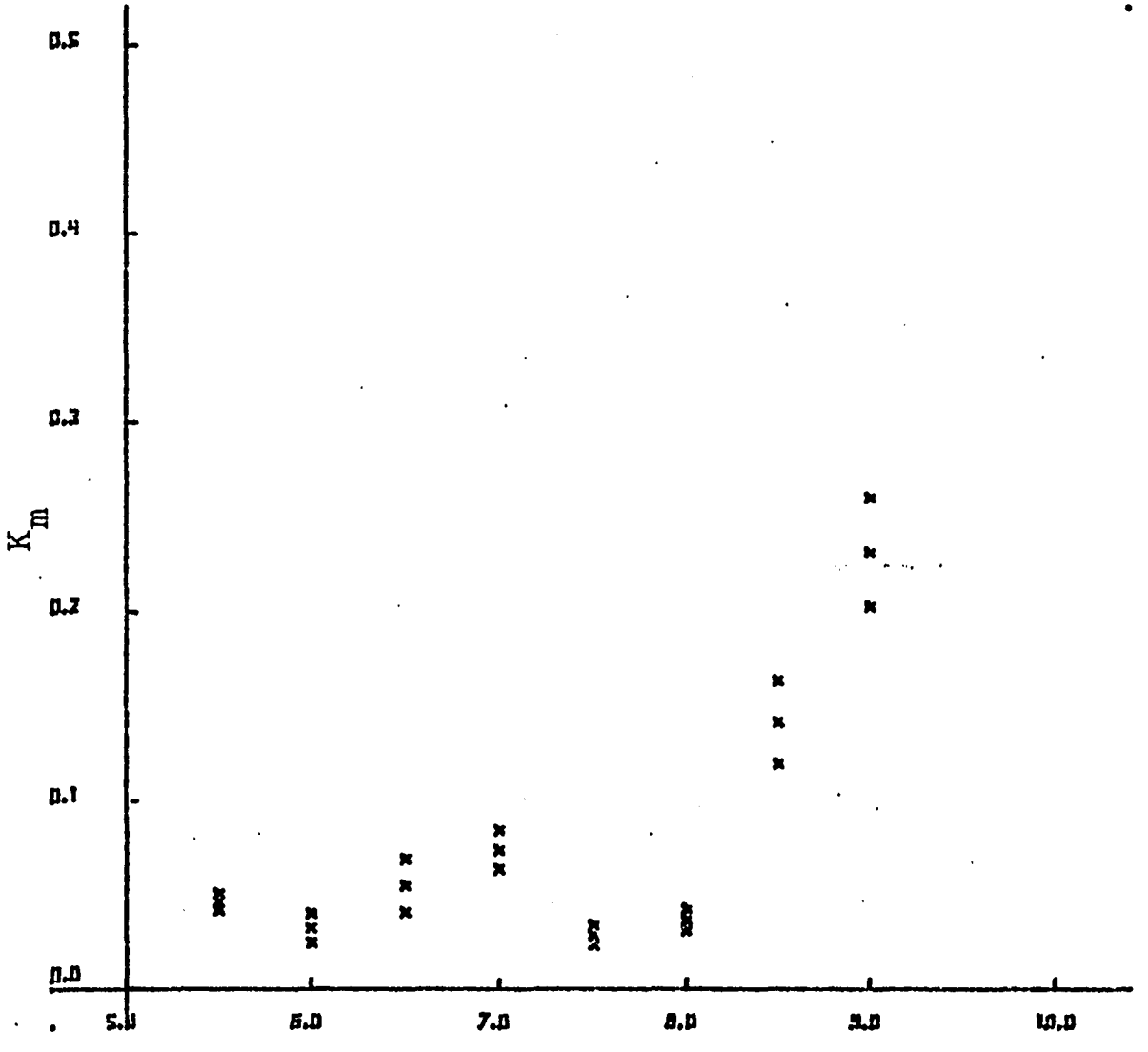

FIGURE 32

Figure 33:

Plot of pKm (-log Km) versus pH for rabbit skeletal muscle myosin Ca^{2+}-ATPase. The x axis represents pH range and the y axis represents the calculated pKm values with standard errors.

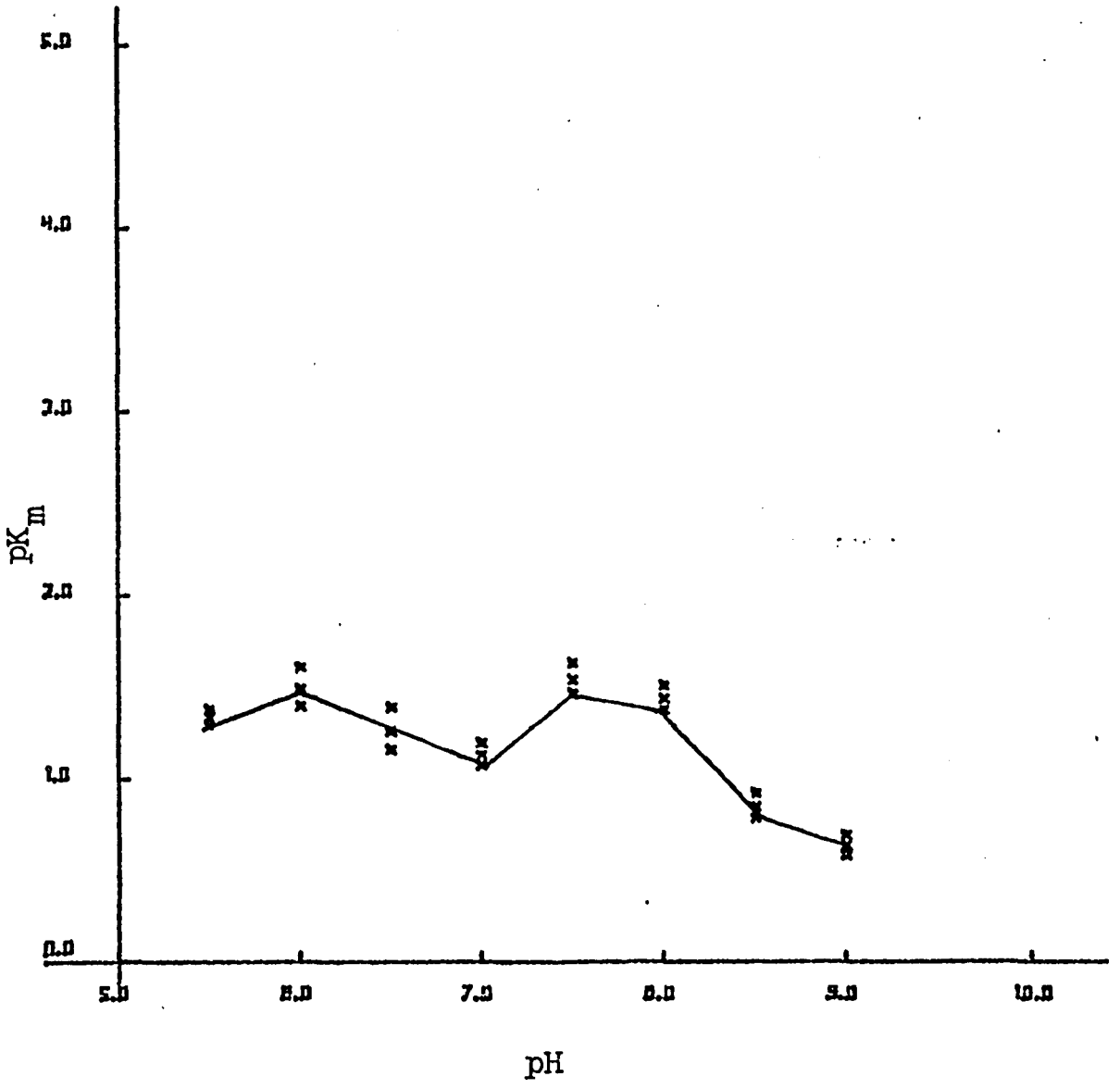

FIGURE 33

Figure 34:

Plot of Vmax versus pH for bovine brain K^+-EDTA-ATPase. The x axis represents pH range and the y axis represents the calculated Vmax values with standard errors.

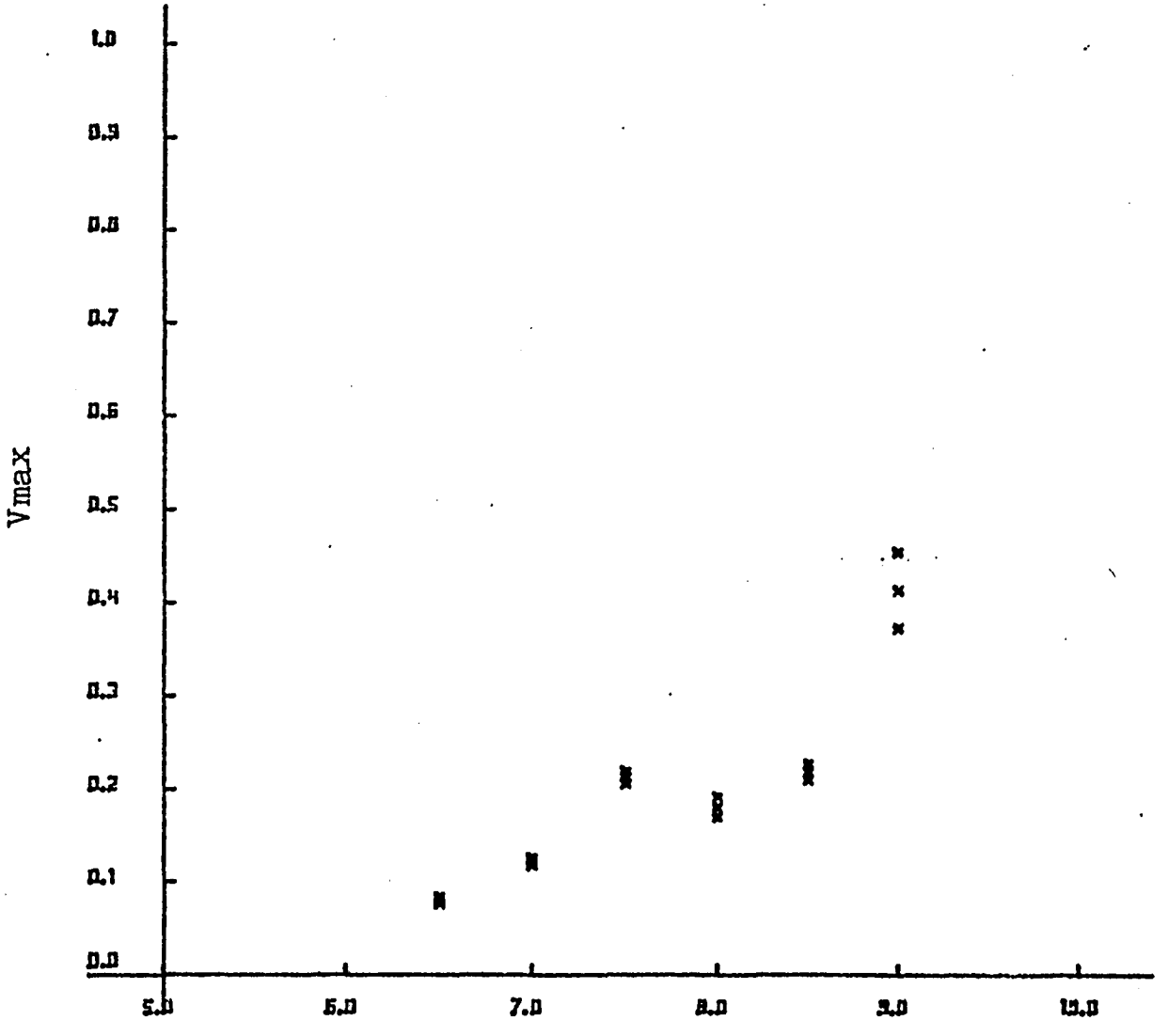

FIGURE 34

Figure 35:

Plot of Km versus pH for bovine brain myosin K^+-EDTA-ATPase. The x axis represents pH and the y axis represents calculated Km values with standard errors.

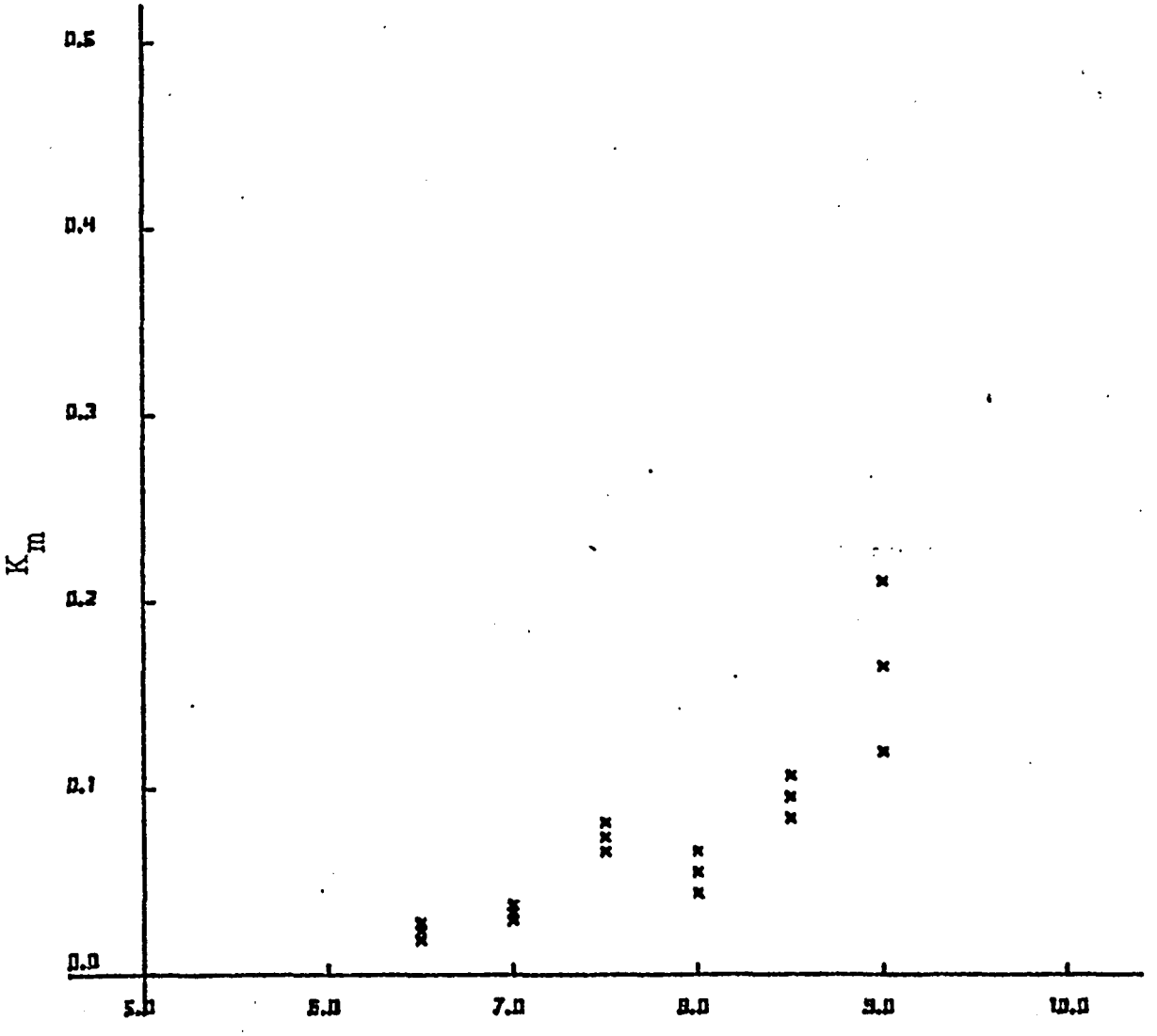

FIGURE 35

Figure 36:

Plot of pKm versus pH for bovine brain myosin K^+-EDTA-ATPase. The x axis represents pH and the y axis represents calculated pKm values with standard errors.

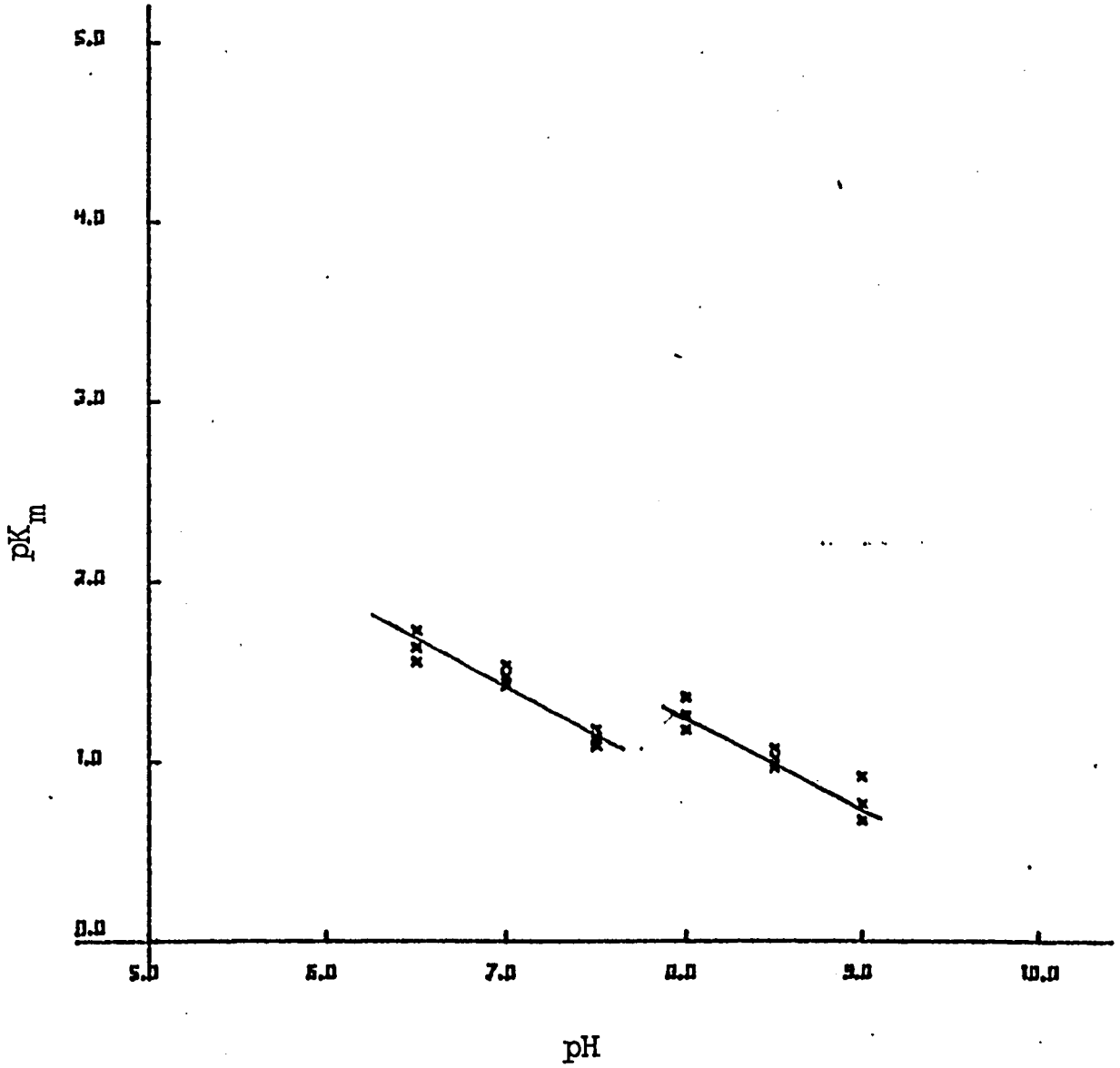

FIGURE 36

Figure 37:

Plot of Vmax versus pH for bovine brain myosin Ca^{2+}-ATPase. The x axis represents pH and the y axis represents calculated Vmax values with standard errors.

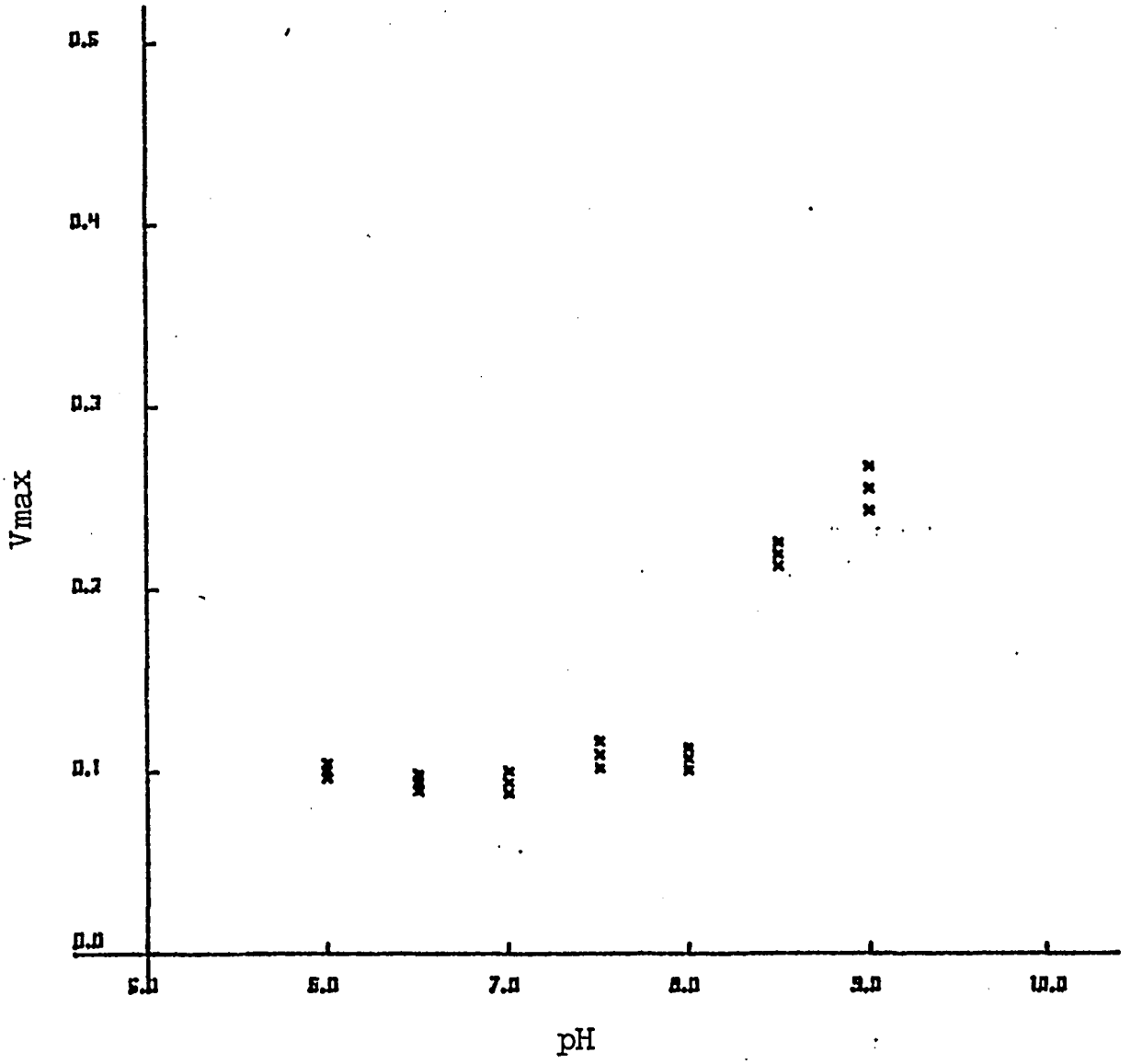

FIGURE 37

Figure 38:

Plot of Km verses pH for bovine brain myosin Ca^{2+}-ATPase. The x axis represents pH and the y axis represents the calculated Km values with standard errors.

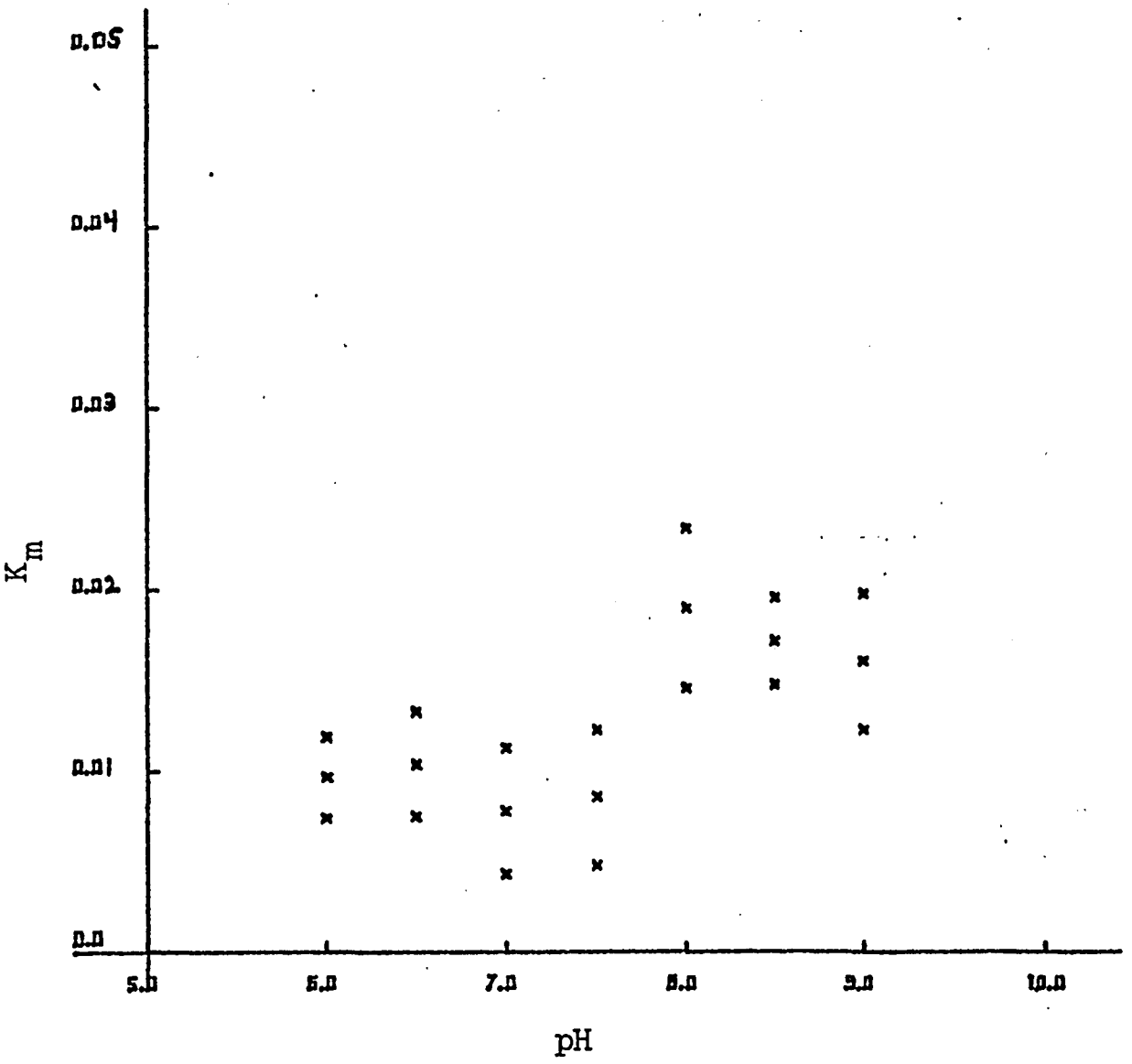

FIGURE 38

Figure 39:

Plot of pKm versus pH for bovine brain myosin Ca^{2+}-ATPase. The x axis represents pH and the y axis represents the calculated pKm values with standard errors.

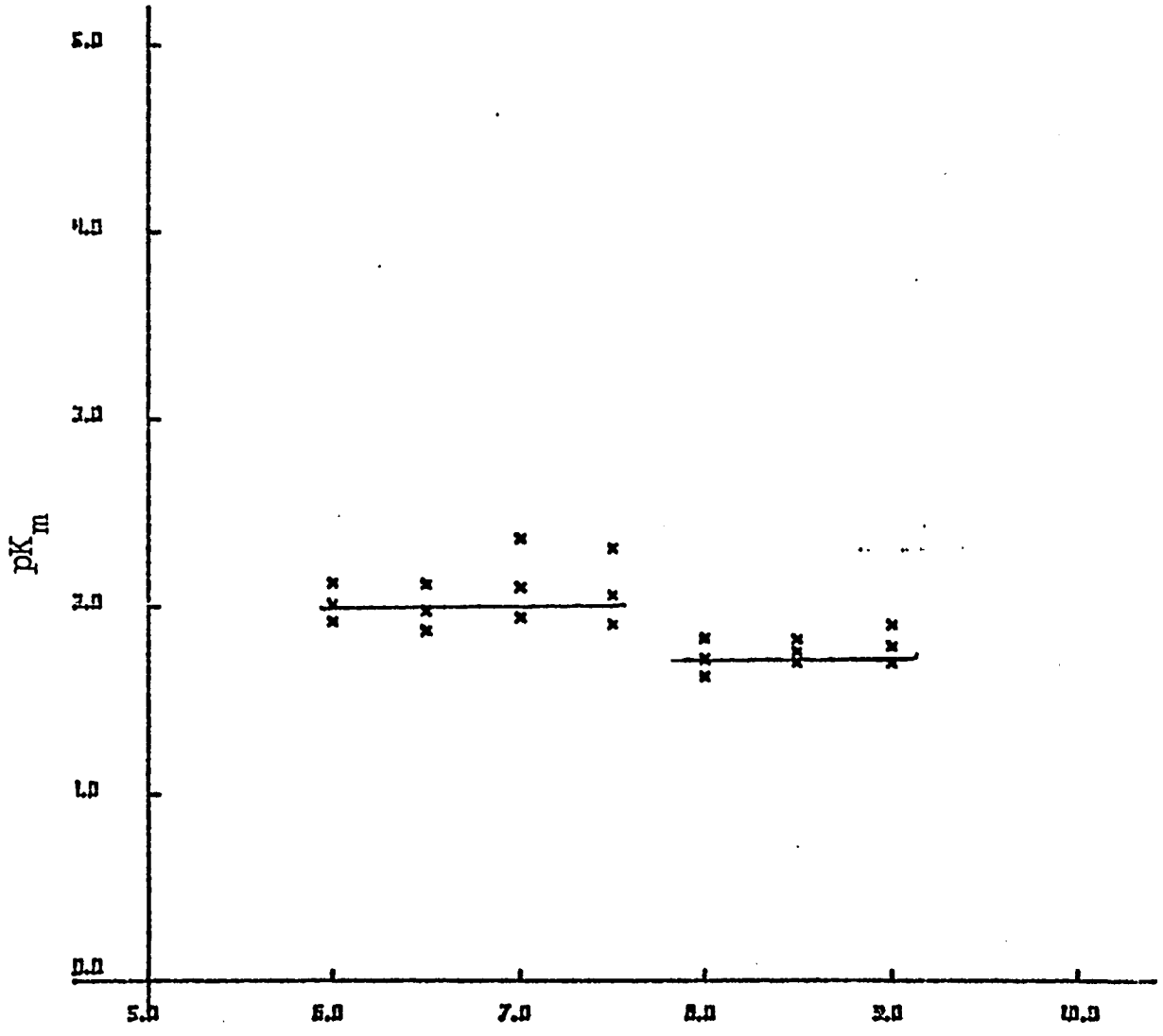

FIGURE 39

Legend for Table 1:

This table shows the specific activity of column eluted brain myosin expressed in μmoles of inorganic phosphorus liberated from ATP per milligram of protein per minute at 37°C. The ATPase activities measured were both the K^+-EDTA-ATPase and the Ca^{2+}-ATPase of brain myosin. The 18mg of protein accumulated in fractions 40-60, after being precipitated twice, shows an increase in enzyme activity and the recovery of 4-6mg of protein.

Table 1:

Fraction	Protein	Specific Activity µmoles/mg/min	
		EDTA	Ca^{2+}
40-60	18 mg	0.409	0.149
Twice Precipitated	4.6	0.994	0.370

Legend for Table 2:

This table contains the Km and Vmax values with appropriate standard erros, calculated by the Wilkinson (1961) method for skeletal muscle myosin K^+-EDTA and Ca^{2+}-ATPase at different pH values. The -log Km is also included.

Table 2:

Rabbit skeletal muscle myosin K^+-EDTA-ATPase

pH	Km	-log Km (pKm)	Vmax
6.5	0.0435 ± 0.0066	1.3615	0.1019 ± 0.0034
7.0	0.0730 ± 0.0223	1.1367	0.1203 ± 0.0096
7.5	0.0815 ± 0.0058	1.0088	0.2349 ± 0.0046
8.0	0.1534 ± 0.01337	0.8142	0.3196 ± 0.0088
8.5	0.2228 ± 0.0379	0.6521	0.3854 ± 0.0228
9.0	0.2738 ± 0.0625	0.5626	0.5344 ± 0.0556
Rabbit skeletal muscle myosin Ca^{2+}-ATPase			
5.5	0.0463 ± 0.0045	1.3344	0.0470 ± 0.0010
6.0	0.0323 ± 0.0078	1.4908	0.0931 ± 0.0045
6.5	0.0550 ± 0.0142	1.2596	0.1972 ± 0.0124
7.0	0.0740 ± 0.0103	1.1308	0.0817 ± 0.0029
7.5	0.0287 ± 0.0054	1.5421	0.0900 ± 0.0031
8.0	0.0367 ± 0.0057	1.4353	0.0981 ± 0.0032
8.5	0.1417 ± 0.0220	0.8486	0.1419 ± 0.0069
9.0	0.2321 ± 0.0288	0.6343	0.4044 ± 0.0175

Legend for Table 3:

This table contains the Km and Vmax values with appropriate standard errors, calculated by the Wilkinson (1961) method for brain myosin K^+-EDTA and Ca^{2+}-ATPase at different pH values. The -log Km is also included.

Table 3:

Bovine brain myosin K^+-EDTA-ATPase

pH	Km	-log Km (pKm)	Vmax
6.5	0.0232 ± 0.0046	1.6349	0.0803 ± 0.0037
7.0	0.0333 ± 0.0043	1.4775	0.1221 ± 0.0041
7.5	0.0738 ± 0.0079	1.1317	0.2132 ± 0.0064
8.0	0.0550 ± 0.0113	1.2614	0.1811 ± 0.0109
8.5	0.0956 ± 0.0115	1.0193	0.2188 ± 0.0084
9.0	0.1657 ± 0.0458	0.7638	0.4144 ± 0.0410

Bovine brain myosin Ca^{2+}-ATPase

6.0	0.0097 ± 0.0023	2.0155	0.1010 ± 0.0039
6.5	0.0104 ± 0.0029	1.9829	0.0946 ± 0.0045
7.0	0.0078 ± 0.0035	2.1090	0.0946 ± 0.0061
7.5	0.0086 ± 0.0038	2.0670	0.1095 ± 0.0073
8.0	0.0190 ± 0.0044	1.7220	0.1073 ± 0.0061
8.5	0.0172 ± 0.0024	1.7641	0.2195 ± 0.0065
9.0	0.0161 ± 0.0037	1.7943	0.2555 ± 0.0121

DISCUSSION

A discussion of the possible physiological role of myosin in terms of some contractile event, depending upon Ca^{2+} as a regulator in skeletal muscle, smooth muscle, neurons and glia, was covered in the Introduction. Important in terms of assembling a theory for the function of myosin in striated muscle, was the structure of the molecule and its chemical nature. The contractile apparatus in muscle relies, in theory, on a structural enzyme which couples the hydrolysis of ATP with a mechanical action that produces work. This system in striated muscle is of a well defined composite nature that is easily accessible to microscopic and x-ray diffraction studies. Coupling the structural and biochemical information of this system has led to a more or less accepted conceptualization of how this system works. However, the similar contractile proteins which are present in smooth muscle and non-muscle cells, do not form such well defined structures as in striated muscle. The intactness of the ultrastructure of smooth muscle, for example, is very difficult to maintain upon chemical fixation, and thus it is difficult to visualize the structure of the contractile mechanism (Small and Squire, 1972).

However, the structure, and chemistry of myosins isolated from each of these cell types, although different in some ways, bear considerable resemblance. Szent-Gyorgyi (1951) has provided an excellent analysis of the basic chemistry of myosin isolated from striated muscle. Striated muscle myosin is readily soluble in 0.6M KCl but insoluble in 0.1M KCl. Thus, extraction of tissue with high salt and dilution of the extract supernatant to low salt concentration results immediately in a partial

separation of this protein from its tissue source and other proteins. The property of high salt solubility also belongs to myosins outside of the striated muscle system, and is utilized in the isolation of myosin from these other sources. Solubilization of the myosin component from striated muscle, smooth muscle and brain in 0.6M KCl and precipitation by reducing the ionic strength to 0.1-0.03M KCl was utilized in this research to purify myosin. However, this was not sufficient to fully purify the myosin component from brain. As mentioned earlier in the Introduction, the purification of brain myosin requires more elaborate manipulation of the proteins solubility properties. These properties are shared by brain and other myosins, and have been utilized in some isolation procedures. Precipitation by $(NH_4)_2SO_4$ is utilized in the purification of myosin from striated muscle (Richards et.al., 1967) and platelets (Pollard et.al., 1974) and in this research from brain. Also, the presence of 0.6M KI which was found to depolymerize striated muscle actin (Szent-Gyorgi, 1951) was utilized in the purification procedure for platelet myosin (Pollard et.al., 1974) and is utilized here for brain. Globular actin (42,000 daltons) can be easily separated from myosin (500,000 daltons) whereas F-actin of high molecular weight cannot.

The solubility properties of myosin are consistent with a model of the striated muscle myosin filament at 0.1M KCl (Figure 3), where the non-soluble tail portions assemble into the backbone of a filament which has its heads projected outside and freely soluble to interact with actin filaments (Huxley, 1963). Striated muscle myosin characteristically forms cigar-shaped structures with tapered ends (Figure 12). The rough surfaces are believed to be the heads of the individual molecules arranged in a

pattern by the stacking of the rod portion of the molecules within the core of the filament. The arrangement of the heads is believed to be apparent as the 140 A periodicity observed in x-ray diffraction patterns and in some electron micrographs. The heads are arranged in opposite directions at either end of the filament due to an anti-parallel stacking arrangement of the molecules. This is considered to be the reason for a bare zone in the middle of the filament, i.e., the bare zone is the area where the tail ends of myosin molecules lie next to each other and butt end to end in an opposite fashion (Huxley, 1963). The 0.15-0.2 μ length (Huxley, 1963) of this region compares to the length range of the myosin molecule determined by shadow casting in the electron microscope, which is 0.126-0.178 μ (Huxley, 1963). Thus, if these molecules lie next to each other in anti-parallel arrangement, the closest the heads on opposite ends could be would be about the length of the molecule.

The brain myosin filament, albeit much smaller than the striated muscle filament, shows a bare zone of the same length as the bare zone for the striated muscle filament. Its dumbell appearance is consistent with bipolar arrangement of molecules with a head and tail portion. In fact, Huxley (1963) occasionally found in his preparation of striated muscle myosin filaments, small dumbell shaped filaments. The smallest of these filaments measures 0.25-0.3 μ in length with a bare zone of 0.15-0.2 μ in length. The formation of such a small striated muscle filament is not as consistently observed as the formation of the cigar-shaped filament, which more closely resemble the electron microscopic appearance of the filaments within the sarcomere itself. In fact, it has been noted (Hinssen et.al.,1978), that the small skeletal myosin

filament has not been observed since Huxley's (1963) report.

The association of other proteins with the striated myosin filament, such as M-line protein (Masaki et.al., 1968) and C protein (Offer, 1972) suggests their possible involvement in the structure of the filament. It is therefore possible that the assembly of these filaments may depend on non-myosin proteins as well as the myosin molecule itself.

In smooth muscle, analysis of the tissue by x-ray diffraction shows a 140 A periodicity (Small and Squire, 1972). Electron microscopic study of smooth muscle shows ribbon-like structures with a 140 Å periodicity (Small and Squire, 1972). 140 Å is the periodicity found in the striated muscle filament and is believed to be the arrangement of the projecting heads of the molecules (Huxley, 1963). Therefore, the 140 Å periodicity along the length of the branching ribbons in smooth muscle was considered a marker for the spacing of the myosin molecules (Small and Squire, 1972). The model proposed by Small and Squire (1972) for the native assembly of myosin in smooth muscle includes a backbone protein that is not myosin, called the lentofilmaent backbone. This model is bipolar in terms of a sided-ness to the ribbon, molecules on one side face in the direction opposite to those of the other side.

Myosin isolated from all sources shows upon SDS polyacrylamide gel electrophoresis numerous small bands lying below the 200,000 dalton heavy chain component of the molecule. Although the identity of these bands is not established, they could represent either fragments of the molecule or a filament-associated protein like M-line or C protein which have molecular weights of 155,000 and 146,000 daltons respectively (Masaki et.al., 1968;

Offer, 1972). The bands lying beneath the 200,000 dalton component may also be contaminants associated with the molecule during the purification due to its solubility properties, and not at all involved in the formation of filaments. It is interesting that the in vitro formed filaments shown in this dissertation for smooth muscle myosin form huge branching structures with a 140 Å periodicity. This could very well represent the ribbon like structures described for smooth muscle by Small and Squire (1972). There are also reports of short-tapered filaments and short bi-polar filaments (Sobieszek and Small, 1972; Hinssen et.al., 1978), for in vitro assembled smooth muscle myosin. These differences could be due to differences in isolation and concomitant levels of associated filament proteins. Perhaps the elaborate structures observed in the electron micrographs in this dissertation are due to such an association.

Brief tryptic digestion of myosin forms two parts, one which is soluble at low ionic strength, and one which is insoluble at low ionic strength (Szent-Gyorgi, 1951; Lowey and Cohen, 1962). The portion which is soluble at low ionic strength possesses the ATPase activity and interacts with actin. This soluble portion is the head or globular region of the myosin molecule, and is called heavy meromyosin (HMM). The HMM is represented by the projections outside the myosin filament which are free to interact with actin and hydrolyze ATP. The HMM portion disintegrates upon negative stain electron microscopy, but shadow casting reveals short tailed globular structures up to 800 Å long (Huxley, 1963). The low ionic strength insoluble portion, called light meromyosin (LMM), when solubilized in 0.6M KCl may be observed by shadow casting in the electron microscope. The length of this rod-like structure is up to 900 Å (Huxley, 1963). The

LMM portion of this tryptic digest when dialyzed to 0.1M KCl at neutral pH, is visible upon negative stain electron microscopy. Striated muscle LMM forms long structures with a periodicity of 430 Å (Huxley, 1963). The light-staining band which occupies 100 Å of the 430 Å period is believed to represent a denser protein area where possibly the LMM molecules overlap upon assembly. This type of structure was reproduced in this research with rabbit striated muscle myosin isolated using the same procedure used for brain myosin isolation. However, the LMM portion of brain myosin and smooth muscle myosin did not form these complex structures. Rather, they formed short structures, somewhat indefinite in length, and had frayed ends. This appeared much like a dumbell shaped filament with its globular head region cut off.

The HMM portion of all three myosins is shown to interact with actin filaments isolated from each of these sources. This interaction is in the form of arrowheads, all possessing similar periodicities along the length of the different actin filaments. The arrowhead configuration bears a certain sophistication in that its periodicity follows the structural repeat of the actin double helix. It is also unidirectional along the length of any one filament, a molecular arrangement required for a pull on the actin filament in a given direction by myosin. The actin filament is a polymer of a 42,000 dalton globular unit. It consists of two chains of units wound around each other in a double helix. The pitch of the helix of each chain is about 700 Å, and the two helices are displaced relative to each other by a half a turn. Thus the resultant structure repeats after 700Å/2 = 350Å. This 350 Å period is the period seen by the attached HMM moiety on the decorated fiber (Huxley, 1963).

The ability of the three myosins to decorate the three different actins shows that all three of the myosins possess similar binding sites for actin. The consistency of the periodicity of the HMM decoration of the actin filaments from the three different sources shows that enough of the structure of the actin is conserved so that they assemble similarly as a double helix with a 350 Å repeat.

The ATP dissociation of the HMM-actin complex is supposedly representative of the dissociation in the association-dissociation scheme that occurs between myosin and actin filaments which occurs during the contraction and relaxation of muscle. This is coupled to the hydrolysis of ATP. In view of this it is interesting to note that although the purified brain myosin Mg^{2+}-ATPase is not activatable by actin, the brain HMM associates with actin and dissociates in the presence of ATP.

Kinetic studies on striated muscle myosin ATPase have been undertaken by several investigators in hopes of better understanding the molecular dynamics of myosins hydrolysis of ATP and interaction with actin. An excellent review on the mechanism of actomyosin ATPase was published by Taylor (1979). Although the exact biochemical mechanism of the actomyosin ATPase activity is not known, an attempt was made by Taylor (1979) to relate a structural model of the actin-myosin interaction to a probable biochemical mechanism.

Most of the kinetic studies were performed on the SF-1 portion of the myosin molecule, which is single headed and freely soluble at low ionic strength. Evidence indicated that ATP dissociates the actomyosin complex by binding at the myosin head, and that the hydrolysis step occurs on free SF-1. Actin then recombines with the myosin product complex.

Taylor fits this biochemical scheme to the structural model of the cross-bridge cycle of Huxley. The structural model is shown in Figure 40. It can be seen that the head of the myosin molecule which may be a myosin product intermediate, associated with the actin filament, undergoes a conformational change whereupon it dissociates from the actin filament. This dissociated stage may be a myosin substrate intermediate. The acto-myosin complex therefore dissociates in the presence of ATP, and hydrolysis occurs on the myosin alone.

Apparently, in the presence of Mg^{2+}-ATP, brain myosin, although it can associate and dissociate from actin, cannot repeat the cycle and produce any turnover of ATP. Perhaps, the brain myosin heads, already present as a myosin product complex were able to associate with actin, undergo configurational change and possibly release inorganic phosphate. Although able to bind ATP and thus dissociate from the actin, the brain myosin was either unable to hydrolyze this freshly bound ATP in the presence of Mg^{2+}, or perhaps, was unable to liberate the end products of hydrolysis and not be able to repeat the cycle of association-dissociation.

In view of the recent observations that myosin from smooth muscle (Chacko and Conti, 1977; Sobieszek, 1977), platelets (Adelstein and Conti, 1975), and macrophages (Trotter and Adelstein, 1979), require phosphorylation of a light chain component in order to demonstrate actin activation of the myosin Mg^{2+}-ATPase, it seems possible that myosin from brain could also require such phosphorylation. Perhaps the phosphorylation effectively permits the hydrolysis and/or product release of ATP on the myosin head in the presence of Mg^{2+} and actin. Further evidence in favor of the phosphorylation of myosin from brain is a report of a phosphorylated

light chain component of myosin from murine astrocytes (Scordilis et.al., 1977). Also, a kinase has been isolated from bovine brain which phosphorylated platelet myosin and thereby rendered it activatable by actin (Dabrowska and Hartshore, 1978).

Further attempts to better understand the nature of the brain myosin molecule as compared to skeletal muscle myosin were done by studying the ATPase activity of enzymes in the presence of Ca^{2+} or K^{+} and EDTA. Mommaerts and Green (1953) studied the effect of pH on skeletal muscle myosin from rabbit. They found that the Ca^{2+}-ATPase had an optimum of activity at pH 6.3-6.5, a minimum at pH 7.0, and a steady increase of activity above pH 7.0. They noticed that the Ca^{2+}-ATPase optimum at pH 6.3-6.5 was very labile and within two days after preparation of the enzyme, decreased four fold and was barely apparent on a graph of specific activity versus pH.

Barany et.al., (1964) studied the effect of pH on both the ATPase activity of rabbit skeletal muscle and cardiac muscle myosins. He also observed for the Ca^{2+}-ATPase of rabbit skeletal muscle myosin a pH optimum at 6.0-6.5, with a sharp increase in activity above pH 7.0 with increasing pH to pH 9.5. The Ca^{2+}-ATPase of cardiac myosin on the other hand showed a slight optimum at pH 6.0-6.5 and either decreased in activity with increasing pH or remained the same. Barany observed that the K^{+}-EDTA-ATPase activity of skeletal muscle myosin was lowest at pH 6.0 and increased with increasing pH to pH 9.5. The K^{+}-EDTA-ATPase activity of the cardiac myosin was also lowest at 6.0 and increased with increasing pH until pH 8.0 was reached whereupon the activity decreased from pH 8.0 to 9.5.

Wikmann-Coffelt et.al., (1975) compared the effect of pH on the Ca^{2+} and K^{+}-EDTA-ATPase activity of canine cardiac myosin to canine skeletal muscle myosin in the presence of a fixed amount of substrate. She also studied the effect of substrate concentration on the specific activity of canine cardiac myosin at different pH values and calculated Km and Vmax values from that data using the Lineweaver-Burke equation. It was observed with canine skeletal muscle and cardiac muscle myosin that the K^{+}-EDTA-ATPase activity increased with pH from pH 6.5 to 7.5 and decreased with increasing pH from 7.5 to 8.5. The specific activity of the Ca^{2+}-ATPase of both of these myosins was measured from pH 5.0-7.5 with an apparent optimum at pH 5.5. In these latter studies, the substrate saturation curves for the canine cardiac myosin were done over an ATP range of 0.125mM-5.0mM ATP. It is apparent by looking at the velocity versus substrate concentration graphs that above 1mM ATP, the v_o values began to drop. This researcher showed a parallel between the calculated Km and Vmax values, i.e., if the Vmax values decreased, the Km value decreased, and if the Vmax value increased, the Km value increased. This is similar to what is observed in this dissertation research. In this dissertation, the effect of substrate concentration on the enzyme activity at different pH values was studied. This was not done by Mommaerts and Green (1953), Barany (1964) or Wikman-Coffelt et.al., (1975) for skeletal muscle myosin. Rather, they studied the effect of pH on velocity at a fixed amount of substrate.

The disadvantage of determining the effect of pH on v_o at a fixed substrate concentration is that the amount of the effective ionic form of the substrate present may vary from pH to pH and thus introduce a

possible effect on the calculated v_o values due to altered amount of the ionic form of biologically active substrate. The advantage to studying the effect of substrate concentration on the enzyme activity resides in the calculation of a Vmax value which represent maximal velocity extrapolated to saturating substrate concentrations, thus annihilating the pH effect on affinity for substrate (Dixon and Webb, 1958).

Another advantage to studying the effect of substrate concentration on enzyme activity at different pH values lies in the determination of the Michaelis constant Km. There exists a relationship between Km and pH, derived from the Michaelis pH functions from which the pK values of the dissociating groups may be calculated (Dixon and Webb, 1958). The relationship is:

$$pKm = p\overline{Km} - pf_{es}^{-} + pf_{e}^{-} + pf_{s}$$

where p stands for the negative $\log_{10}$, Km represents the amount of substrate providing one-half Vmax, $\overline{Km}$ is the Km value when both enzyme and substrate are in the ionic forms that are enzymatically active, and the f values are the Michaelis pH functions for the enzyme-substrate complex(es), enzyme (e) and substrate (s). The Michaelis pH functions apply to a substance which undergoes two successive ionizations with ionization constants K1 and K2 (a symmetric dibasic acid) where for

$$AH_2 \underset{}{\overset{K1}{\rightleftharpoons}} AH^{-} \overset{K2}{\rightleftharpoons} A^{=}$$

there are three pH functions:

$$f = 1 + \frac{K1}{H} + \frac{K1K2}{H}$$

$$f^{-} = 1 + \frac{H}{K1} + \frac{K2}{H}$$

$$f^{=} = 1 + \frac{H}{K2} + \frac{H^2}{K1K2}$$

such that the amount of any ionic form of a substance is obtained by dividing the total amount of the substance by the appropriate pH function. For example:

$$A_{total} = AH_2 + AH^- + A^=$$

$$A_{total} = AH_2(f)$$

$$A_{total} = AH^-(f^-)$$

$$A_{total} = A^=(f^=)$$

The Km is therefore dependent on the ionization of the enzyme, enzyme-substrate complex and substrate (Dixon and Webb, 1958).

A statistical method was used for estimating the Km and Vmax values of the Michaelis-Menten equation and their standard errors (Wilkinson, 1961). This computational method has the advantage of determining the Km and Vamx values from the linear form of the Michaelis-Menten equation:

$$\frac{s}{v} = \frac{Km}{V} + \frac{1}{V} \cdot s$$

rather than the usual Lineweaver-Burke double reciprocal plot, also linear:

$$\frac{1}{v} = \frac{1}{V} + \frac{Km}{V} \cdot \frac{1}{s}$$

which exhibits much greater variation in accuracy over the ranges of substrate concentraion suitable for determination of the Michaelis constants.

As seen in the Results section, the Vmax vales of both bovine brain myosin and rabbit skeletal muscle myosin K^+-EDTA-ATPase increase with pH from pH 6.5-9.0 (Figures 34 and 28). Above pH 9.0, the activity of both myosins is lost. This loss of activity is probably due to a pH effect on the stability of the enzyme. It has been reported that the light chains

of skeletal muscle myosin, which are essential to the activity of the enzyme, are liberated from the molecule at pH 11.0 (Driezen and Gershman, 1972).

Rabbit skeletal muscle myosin is known to have three kinds of light chains, light chain 1 (LC1) which is 25,000 daltons on polyacrylamide gels, light chain two (LC2) at 18,000 daltons, and light chain three (LC3) which is 17,000 daltons (Weeds and Lowey, 1971). The light chains of skeletal muscle myosin are essential for the enzymatic activity of the molecule. Dissociation of the light chains from the myosin molecule by treatment with 4M LiCl destroys the ATPase activity as well as the ability to combine with actin (Stracher, 1969). Reconstitution of the dissociated myosin molecule leads to restoration of 30% of the control ATPase activity as well as restoration of the ability to combine with actin. Stracher (1969) has found that the loss of ATPase activity occuring within 15-20 minutes exposure to pH 11.0 is irreversible.

Driezen and Gershman (1970) were able to restore 70% of the ATPase activity of 4M LiCl-dissociated myosin upon reconstitution. This loss of ATPase activity and actin binding ability is believed to be due to the removal of LC1 and LC3 because papain derived proteolytic subfragment S1 which is practically devoid of the LC2 is fully enzymatically active and can still bind actin. Papain-derived S1 is practically devoid of LC2 because of the susceptibility of this light chain to proteolytic damage, whereas LC1 and LC3 require rather drastic treatment with high pH or 4M LiCl in order to dissociate (Weeds and Lowey, 1971). Although a function for LC2 has not been elucidated, it appears that the presence of LC1 and LC3 are essential for enzymatic activity as well as actin binding.

It is conceivable that isolated brain myosin is not activated by actin because of the loss of an essential light chain during the rigorous

isolation process, or as mentioned before, may require phosphorylation of one of the light chain components. Bray and Thomas (1975) report for chick brain myosin, light chain components of 23,000, 20,000 and 17,000 daltons, whereas Kuczmarski and Rosenbaum (1978) report for chick brain myosin, light chain components of 16,000 and 21,000 daltons and occasionally an 18,000 dalton component. The differences for molecular weight determinations of brain myosin light chains may reside in the fact that SDS-PAGE was used to determine molecular weights (Bray and Thomas, 1975; Kuczmarski and Rosenbaum, 1978) rather than amino acid composition and/or ultracentrifugation.

For both brain and skeletal muscle myosin there is a loss of K^+-EDTA-ATPase activity below pH 6.5 (Figures 34 and 28). However, the Ca^{2+}-ATPase activity extends below pH 6.5. For brain (Figure 37), this activity extends to pH 6.0 and for skeletal muscle (Figure 31) the activity extends down to pH 5.5. The brain myosin Ca^{2+}-ATPase at pH 6.0 is of about the same level of activity as it is at pH 7.0, whereas the K^+-EDTA-ATPase activity at pH 6.5 is lower than that at pH 7.0. The skeletal muscle myosin appears to have a slight optimum of activity at pH 6.5. Although there is no apparent optimum for brain myosin Ca^{2+}-ATPase below pH 7.0, it must be understood that this is known to be a labile property in skeletal muscle myosin (Mommaerts and Green, 1953). It should be noted that in the presence of Ca^{2+}, both brain and skeletal myosins are active below pH 6.5 whereas without the Ca^{2+} they are not. Both the Ca^{2+} and K^+-EDTA-ATPase of both brain and skeletal muscle myosins increased with pH.

The Km values of both proteins show a similar trend in that they tend to increase with increasing pH. The pKm versus pH plots for these enzymes

show a possible ionization for skeletal muscle K^+-EDTA-ATPase (Figure 30), and brain myosin K^+-EDTA-ATPase (Figure 36), and Ca^{2+}-ATPase (Figure 39), between the pH values of 7.5-8.0. This suggests a similarity between the active sites of both of these myosins. However, the pKm veraus pH plot for skeletal muscle myosin Ca^{2+}-ATPase (Figure 33) points in the direction of multiple ionizations at or near the pH values 6.0, 7.0, 7.5, 8.0 and 8.5.

Figure 40:

Schematic diagram of the cross-bridge cycle between actin filaments and myosin heads, from Taylor (1979). The triangles mark the binding sites.

1) Myosin head which is detached from actin (may be a myosin-product intermediate).
2) Myosin head attached to the actin filament.
3) Myosin head having undergone a conformational change after binding to the actin filament.
4) Myosin head detached from the actin filament (may be a myosin-substrate intermediate).

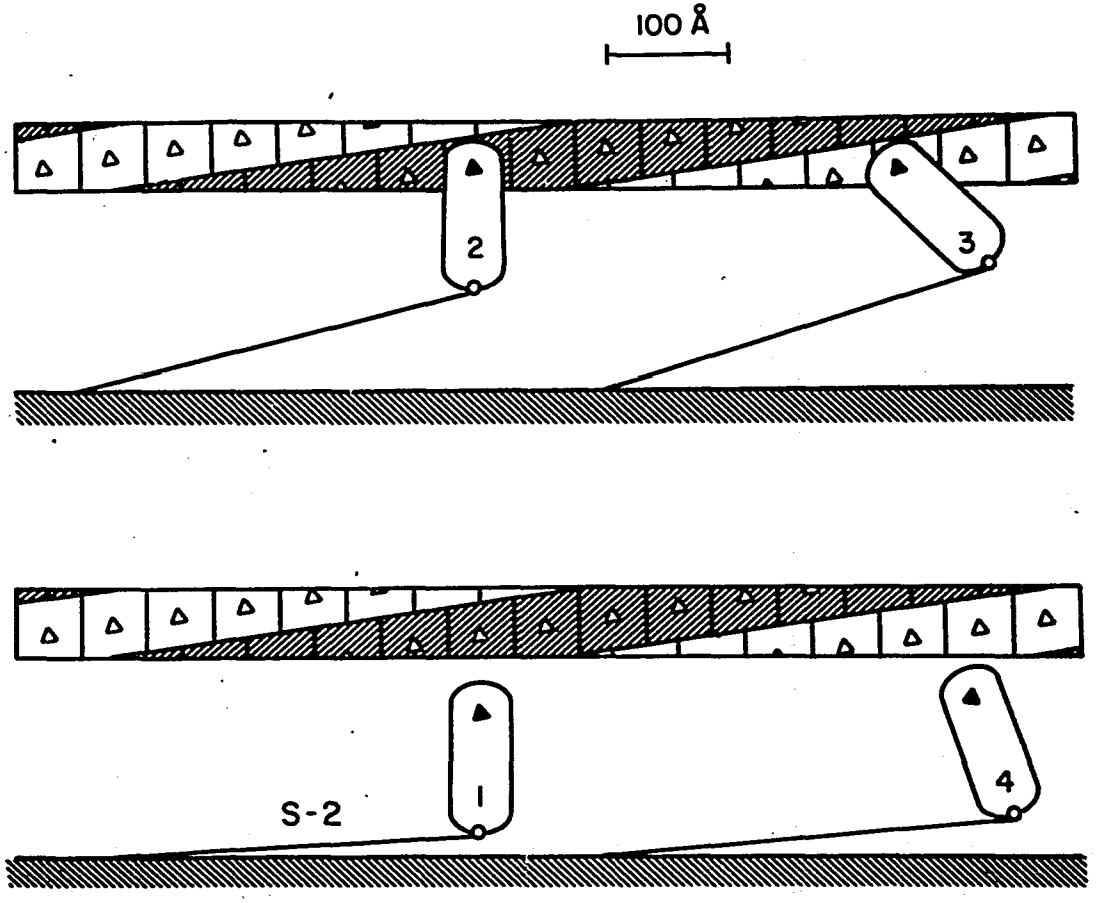

Figure 40

SUMMARY

The isolation of myosin from bovine brain was discussed. Notice was taken that the isolation procedure takes advantage of the solubility properties of the myosin molecule which are similar for skeletal muscle, smooth muscle and brain myosin.

The electrophoretic patterns of each of these proteins show a heavy chain with an apparent molecular weight of about 200,000 daltons and light chains. The light chain components are different for each of these myosins as determined by SDS polyacrylamide gel electrophoresis. Since the light chains of skeletal muscle myosin have been shown to be essential for the enzymatic activity of the molecule as well as actin binding (Driezen and Gershman, 1970; Stracher, 1969), it is possible that variation of this component of the molecule between species and tissue types may very well reflect differences in the type of contractile mechanisms involved.

The structural nature of myosin from bovine brain, rabbit skeletal muscle and chicken smooth muscle were compared electron microscopically both before and after brief treatment with trypsin. The three myosins all possess the ability to form thick filaments in vitro. This is important because the thick filament in skeletal muscle is believed to participate mechanically in the contraction of muscle through the hydrolysis of ATP and interaction with actin.

Brief treatment with trypsin cleaves all three myosins into a light meromyosin portion which is insoluble at low ionic strength and a heavy meromyosin which is soluble at low ionic strength. The light meromyosin portion is believed to form the backbone of the myosin filament and thus

participate in its assembly. The structure of all three myosins appears to be similar enough such that all three myosins possess an LMM portion and form filaments at low ionic strength. Differences in the size and shape of the filaments formed by each of the myosins may very well reflect differences in the amino acid composition of the light meromyosin portions which are believed to form the backbone of the filament structure. In fact, the LMM of skeletal muscle myosin, upon examination by electron microscopy, reveals an assembly quite different from that of smooth muscle and brain LMM's.

All three myosins were shown to have an HMM portion which interacts with actins from brain, skeletal muscle or smooth muscle. This suggests that the structure of this portion of the molecule is sufficiently conserved to enable it to bind actin from the different sources. These results also indicate that the actin structure is conserved sufficiently to bind to myosin from the different sources. The periodicity of attachment of HMM to actin, is believed to follow the period of the helical arrangement of the actin filament. The consistency of the periodicity of attachment of HMM from all three sources to the actins from all three different tissues suggests that enough of the actin structure is conserved to form filaments with a period of about 350Å.

The association of brain myosin with actin is reversible upon addition of ATP which is consistent with a molecular mechanism proposed by Taylor (1979) for the actin and myosin interaction in skeletal muscle. Although the actin and brain myosin do interact, as shown by EM studies there is no stimulation of Mg^{2+}-ATPase activity by actin from brain or skeletal muscle. In view of the recent reports of a Ca^{2+}-dependent

phosphorylation of a light chain as essential to this activity for smooth muscle (Sobieszeck, 1977), platelet (Adelstein and Conti, 1975) and macrophage myosin (Trotter and Adelstein, 1979), it is conceivable that phosphorylation could play a role in the Mg^{2+}-ATPase activity of brain myosin. Recent reports as to the presence of a kinase and phosphorylation of a light chain of murine astrocyte myosin (Scordilis et.al., 1977), and the isolation of a Ca^{2+}-dependent kinase from bovine brain which phosphorylates the light chain of platelet myosin (Dabrowska and Hartshorne, 1978) also supports this notion. It is also consistent with a physiologic Ca^{2+}-requiring contractile event.

Kinetic data which points in the direction of an ionization within the pH range of 7.5-8.0 for both skeletal muscle and brain myosins suggests that there is a similarity in the active sites of both of these proteins. Enzymatic differences between skeletal myosin and brain myosin do exist. As well as the lack of activation of brain myosin Mg^{2+}-ATPase by actin, pKm versus pH plots show a possible ionization occuring between pH 7.5 and 8.0 for brain myosin Ca^{2+}-ATPase in contrast to what may be multiple ionizations for skeletal muscle Ca^{2+}-ATPase.

BIBLIOGRAPHY

Adelstein, R.S., and M.A. Conti, Phosphorylation of platelet myosin increased actin-activated myosin ATPase activity, Nature, 256: 597, 1975.

Ash, J.F.: Purification and characterization of myosin from the clonal rat glial cell strain C-6, Jour. Biol. Chem., 250: 3560, 1975.

Barany, J., E. Gaetjens, K. Barany, and E. Karp: Comparative studies of rabbit cardiac and skeletal myosin, Arch Biochem Biophys., 106: 280, 1964.

Begg, D.A., Rodenwald, R., and L.I. Rebhin: The visualization of actin filament polarity in thin section, evidence for the uniform polarity of membrane associated filaments, J. Cell Biol., 79: 846. 1978.

Berl, S.: Actomyosin-Like Protein in Brain, p.157 in: B.W. Agranoff and M.H. Aprison (eds.), Advances in Neurochemistry, Vol. 1. Plenum New York, 1975.

Berl, S., and S. Puszkin: Mg^{2+} - Ca^{2+} Activated adenosine triphosphatase system isolated from mammalian brain, Biochemistry, 9: 2058, 1970.

Berl, S., S. Puszkin, and W.J. Nicklas: Actomyosin-like protein in brain, Science, 1979: 441, 1973.

Bloom, W., and D.W. Fawcett: A Textbook of Histology, W.B. Saunders Co., Philadelphia, 1975.

Bray, D.: Branching patterns of individual sympathetic neurons in culture, Jour. Cell Biol. 56: 702, 1973.

Bray, D: Model for membrane movements in the neural growth cone, Nature, 244: 93, 1973.

Bray, D., and C. Thomas: Unpolymerized actin in fibroblasts and brain. Jour. Mol. Biol., 105: 527, 1976.

Bunge, M.B.: Fine structure of nerve fibers and growth cones of isolated sympathetic neurons in culture, Jour. Cell Biol., 56: 713, 1973.

Bunge, M.B., R.P. Bunge, and G.D. Pappas: Electron microscopic demonstration of connections between glia and myelin sheaths in the developing mammalian central nervous system, Jour. Cell Biol., 12: 448, 1962.

Bunge, R.P., and P.M. Glass: Some observations on myelin-glial relationships and on the etiology of the cerebrospinal fluid exchange lesion. Ann. New York Acad. Sci., 122: 15, 1965.

Burridge, K., and D. Bray: Purification and structural analysis of myosins from brain and other non-muscle tissues. Jour. Mol. Biol., 99: 1, 1975.

Carter, S.B.: Effects of cytochalasins on mammalian cells, Nature, 213: 261, 1967.

Carsten, M.E., and W.F.H.M. Mommaerts: A study of actin by means of starch gel electrophoresis, Biochemistry, 2: 28, 1963.

Chacko, S., M. Conti, and R.S. Adelstein: Effect of phosphorylation of smooth muscle myosin on actin activation and Ca^{2+} regulation, Proc. Nat. Acad. Sci, 74: 129, 1977.

Clark, J.B., and W.J. Nicklas: The metabolism of rat brain mitochondria, J. Biol. Chem., 245: 4724, 1970.

Craig, S.W., and J.V. Pardo: Alpha-actinin localization in the junctional complex of intestinal epithelial cells, J. Cell Biol., 80: 203, 1979.

Dabrowska, R., D. Aromatorio, J.M.F. Sherry, and D.J. Hartshorne: Composition of the myosin light chain kinase from chicken gizzard, Biochem. Biophys. Res. Comm., 78: 1263, 1977.

Dabrowska, R., and D.J. Hartshorne: A Ca^{2+}-and modulator dependent myosin light chain kinase from non-muscle cells, Bioch. Biophys. Res. Comm., 85: 1352, 1978.

Dixon, M., and E.C. Webb: Enzymes, Longmans, Green and Co., Ltd., London, 1958.

Dreizen, P., and L.C. Gershman: Molecular basis of muscular contraction. Myosin Trans. N.Y. Acad. Sci., 32: 170, 1970.

Dreizen, P., and L.C . Gershman: Relationship of structure to function in myosin II. Salt denaturation and recombination experiments, Biochem., 9: 1688, 1970.

Dreizen, P., and D.H. Richards: Studies on the role of light and heavy chains in myosin adenosine triphosphate, Cold Spring Harbor Symp. Quant. Biol., 37: 29, 1972.

Fine, R.E., and D. Bray: Actin in growing nerve cells, Nature, 234: 115, 1971.

Frearson, N., and S.V. Perry: Phsophyrlation of the light chain components of myosin from cardiac and red skeletal muscles, Biochem. J., 151: 99, 1975.

Geiger, B., Tokuyasu, K.T., and S.J. Singer: Immunocytochemical localization of -actinin in the intestinal epithelial cells, PNAS, 76: 2833, 1979.

Godfrey, J.E., and W.F. Harrington: Self association in myosin system in high ionic strength. II. Evidence for the presence of a monomer dimer equilibrium, Biochem., 9: 894, 1970.

Hathaway, D.R., and R.S. Adelstein: Human platelet myosin light chain kinase requires the calcium binding protein calmodulin for activity, Proc. Natl. Acad. Sci. USA, 76: 1653, 1979.

Herman, I., and T.D. Pollard: Comparison of purified anti-actin and fluorescent-heavy meromyosin staining patterns in dividing cells, J. Cell Biol., 80: 509, 1979.

Hinssen, H., J.D. Haese, J.V. Small, and A. Sobieszek: Mode of filament assembly of myosins from muscle and non-muscle cells, J. Ultrastruct. Res., 64: 282, 1978.

Huxley, H.E.: Electron microscope studies on the structure of natural and synthetic protein filaments from striated muscles, Jour. Mol. Biol., 7: 281, 1963.

Huxley, H.E.: The mechanism of muscular contraction, Science, 164: 1356, 1969.

Huxley, H.E.: Muscular contraction and cell motility, Nature, 243: 445, 1973.

Kendrick-Jones J.: The subunit structure of gizzard myosin, Phil. Trans. R. Soc. Lond. B., 265: 183, 1973.

Korn, E.D.: Biochemistry of actomyosin cell motility (A review), Proc. Natl. Acad. Sci. USA, 75: 588, 1978.

Kuczmarsky, E.R. and J.L Rosenbaum: Chick brain actin and myosin isolation and characterization, J. Cell Biol., 80: 341, 1979.

Langman, J.: Medical Embryology, Ed. Williams and Wilkins Company, Baltimore, 1969.

Lowey, S. and C. Cohen: Studies on the structure of myosin, J. Mol. Biol., 4: 293, 1962.

Lowry, O.H., N.J. Rosebrough, A.L. Farr, and R.J. Randall: Protein measurement with the folin phenol reagent, J. Biol. Chem., 193: 265, 1951.

Mahendran, C., and S. Berl: Tropomyosin and troponin-like complex from bovine brain p.284 in: R.H. Wasserman et. al., (eds.), Calcium Binding Proteins and Calcium Function, Elsevier North-Holland, Inc. New York, 1977a.

Mahendran, C., and S. Berl: Isolation of troponin-like comples from bovine brain cortex, Proc. Natl. Acad. Sci. USA, 74: 2273, 1977b.

Marsh, B.B.: The estimation of inorganic phosphate in the presence of adenosine triphosphate, Biochim. Biophys. Acta, 32: 357, 1959.

Masaki, T., O. Takaiti, S. Ebashi: "M-Substance", a new protein constituting the M-line of myofibrils, J. Biochem., 64: 909, 1968.

Mammaerts, W.F.H.M., and I. Green: Adenosine-triphosphatase systems of muscle III. A survey of the adenosine-triphosphatase activity of myosin, J. Biol. Chem., 208: 833, 1954.

Mooseker, M.S., and L.G. Tilney: Organization of an actin filament-membrane complex, Jour. Cell Biol., 67: 725, 1975.

Needham, D.M.: Machina Carnis: The biochemistry of muscular contraction in its historical development, Cambridge University Press, London, 1971.

Nicklas, W.J., and S. Berl: Effects of cytochalasin B on uptake and release of putative transmitters by synaptosomes and on brain acto-myosin-like protein, Nature, 247: 471, 1974.

Nicklas, W.J., S. Puszkin, and S. Berl: Effect vinblastine and colchicine on uptake and release of putative transmitters by synaptosomes and on brain actomyosin-like protein. Jour. Neurochem., 20, 109, 1973.

O'Farrell, P.H.: High resolution two-dimensional electrophoresis of proteins, Jour. Biol. Chem. 250: 4007, 1975.

Palay, S.L.: The role of neuroglia in the organization of the central nervous system, p. 3 in : K. Rodahl and B. Issekutz, Jr. (eds.), Nerve as a Tissue. Hoeber Med. Div. Harper and Row, New York, 1966.

Pepe, F.A., and B. Drucker: The myosin filament VI. Myosin content, J. Mol. Biol., 130: 379, 1979.

Peters, A., and S.L. Palay: An electron microscopic study of the distributions and patterns of astroglial processes in the central nervous system, Jour. Anat. 99: 419, 1965.

Pires, E.M.V., and S.V. Perry: Purification and properties of myosin light-chain kinase from fast skeletal muscle, Biochem. J., 167: 137, 1977.

Pollard, T.D.: Electron microscopy of synthetic myosin filaments, J. Cell Biol., 67: 93, 1975.

Pollard, T.D.: Functional implications of the biochemical and structural properties of cytoplasmic contractile proteins, p. 259 in: S. Inoue and R.E. Stephens (eds.), Molecules in Cell Movement, Raven Press, New York, 1975.

Pollard, T.D., S.M. Thomas, and R. Niederman: Human platelet myosin. I. Purification by a rapid method applicable to other non-muscle cells, Anal. Biochem., 60: 258, 1974.

Pollard, T.D. and R.R. Weihing: Actin and myosin and cell movement. CRC Crit. Rev. Biochem. 2: 1, 1974.

Puszkin, S., and S. Berl: Actomyosin-like protein from brain: Separation and characterization of the actin-like component, Biochim-Biophys. Acta., 256: 695, 1972.

Puszkin, S., S. Berl, E. Puszkin, and D.D. Clarke: Actomyosin-like protein isolated from mammalian brain, Science, 161: 170, 1968.

Puskin, S., W.J. Nicklas, and S. Berl: Actomyosin-like protein in brain: Subcellular distribution, Jour. Neurochem. 19: 1319, 1972.

Richards, E.G., C.S. Chung, D.B. Menzel, and H.S. Olcott: Chromatography of myosin on diethylaminoehtylsephadex A-50, Biochem., 6: 528, 1967.

Rosenbluth, J.: Functions of glial cells p.21 in : O.T. Bailey and D.E. Smith (eds.), The Central Nervous System. Williams and Wilkins Company, Baltimore, 1968.

Schook, W., Ores, C., and S. Puszkin: Isolation and properties of brain α-actinin, Biochem. J., 175: 63, 1978.

Schroeder, T.E.: Dynamics of contractile ring, p.305 in: S. Inoue and R.E. Stephens (eds.), Molecules in Cell Movement, Raven Press, New York, 1975.

Schwartz, J., S. Berl, W.J. Nicklas, C. Mahendran, W.O. Whetsell, Jr., and T.S. Elizan: Further characterization of brain actin by electron microscopy. Jour. Neuropath. and Exp. Neurol., 36: 398, 1977.

Scordilis, S.P., L. Anderson, R. Pollack, and R.S. Adelstein: Characterization of the myosin phosphorylating system in normal murine astrocytes and derivative SV40 wild-type and A-type mutant transformants, J. Cell Biol., 74: 940, 1977.

Small, J.V., and J.M. Squire: Structural basis of contraction in vertebrate smooth muscle, J. Mol. Biol., 67: 117, 1972.

Sobieszek A., and J.V. Small: Filaments from purified smooth muscle myosin, Cold Spring Harbor Symp. Quant. Biol., 109, 1972.

Sobieszek, A., and D. Bremel: Preparation and properties of vertebrate smooth muscle myofibrils and actomyosin, Eur. J. Biochem., 55: 49, 1975.

Sobieszek, A.: Ca-linked phopphorylation of a light chain of vertebrate smooth muscle myosin, Eur. J. Biochem., 73: 477, 1977.

Spudich, J. and S. Lin: Cytochalasin B, its interaction with actin and actomyosin from muscle, Proc. Nat. Acad. Sci., U.S.A., 69: 442, 1972.

Stracher, A.: Evidence for the involvement of light chains in the biological functioning of myosin, Biochem. Biophys. Res. Comm., 35: 519, 1969.

Stromer, M.H., and D.E. Goll: Studies on purified α-actinin, J. Mol. Biol., 67: 489, 1972.

Szent-Gyorgi, A.: Chemistry of Muscular Contraction, Academic Press, N.Y., 1951.

Taylor, E.W.: Mechanism of actomyosin ATPase and the problem of muscle contraction, CRC Crit. Rev. Biochem., 6: 103, 1979.

Thoa, N., G.F. Wooten, J. Axelrod and I. Kopin: Inhibition of release of dopamine-B hydroxylase and norepinephrine from sympathetic nerves by colchicine, vinblastine, or cytochalasin B, Proc. Natl. Acad. Sci., U.S.A., 69: 520, 1972.

Tilney, L.G.: The role of actin in non-muscle cell motility, p.339 in: S. Inuoue and R.E. Stephens (eds), Molecules in Cell Movement, Raven Press, New York, 1975.

Trotter, J.A., and R.S. Adelstein: Macrophage myosin, J. Biol. Chem., 254, 8781, 1979.

Vandekerckhove, J., and K. Weber: At least six different actins are expressed in a higher mammal: an analysis based on the amino acid sequence of the amino-terminal tryptic peptide, J. Mol. Biol, 126: 783, 1978.

Wang, J.H., and R. Desai: Modulator binding protein, J. Biol. Chem., 252: 4175, 1977.

Weber, A., and J.M. Murray: Molecular control mechanisms in muscle contraction, Physiological Reviews, 53: 612, 1973.

Weber, K., and M. Osborn: The reliability of molecular weigh determination by dodecyl sulfate-polyacrylamide gel electrophoresis, J. Biol. Chem., 244: 4406, 1969.

Weeds, A., and S. Lowey: Substructure of the myosin molecule II. The light chains of myosin, J. Mol. Biol., 61: 701, 1971.

Wessels, N.K., B.S. Spooner, J.F. Ash, M.O. Bradley, M.A. Luduna, E.L. Taylor, J.T. Wrenn, and K.M. Yamada: Microfilaments in cellular and developmental processes: Contractile microfilament machinery of many cell types is reversibly inhibited by cytochalasin B, Science, 171: 135, 1971.

Wikman-Coffelt, J., C. Fenner, R. Zelis, and D.T. Mason: Effects of variation in pH on kinetics of myosin, p.47 in P. Roy and P. Harris eds., Recent advances in studies on cardiac structure and metabolism Vol. 8. The cardiac sarcoplasm, Univ. Park Press, Baltimore, 1975.

Woodrum, D.T., S.A. Rich, and T.D. Pollard: Evidence for biased bi-directional polymerization of actin filaments using heavy meromyosin prepared by an improved method. Jour. Cell Biol., 67: 231, 1975.

Wilkinsion, G.N.: Statistical estimations in enzyme kinetics, Biochem. J., 80: 324, 1961.

Yamoda, K.M., B.S. Spooner, and N.K. Wessells: Ultrastructure and function of growth cones and axons of cultured nerve cells, Jour. Cell Biol., 49: 614, 1971.